Elucidating the roles of secretory immunoglobulins in asthma under homeostatic and infectious conditions

Thesis

for the degree of

doctor rerum naturalium (Dr. rer. nat.)

approved by the Faculty of Natural Sciences of Otto von Guericke University Magdeburg

by: M. Sc. Alexander Pausder

born on: 30.10.1989 in Magdeburg

Examiner: Prof. Dr. rer. nat. Dunja Bruder

Prof. Dr. rer. nat. Astrid Westendorf

submitted on: 20.04.2022

defended on: 14.10.2022

This thesis was prepared at the Medical Faculty, Otto-von-Guericke-University Magdeburg, Institute of Medical Microbiology and Hospital Hygiene, Research Group Infection Immunology & at the Helmholtz Centre for Infection Research Braunschweig, Research Group Immune Regulation.

The project was funded by the ESF Graduate School on Analysis, Imaging and Modelling of Neuronal and Inflammatory Processes (ABINEP).

Results of the present work were published in:

A Pausder, J Fricke, K Schughart, J Schreiber, T Strowig, D Bruder and JD Boehme. Exogenous and endogenous triggers differentially stimulate Pigr expression and antibacterial secretory immunity in the murine respiratory tract. *Lung*, 200(1):119–128, 2022. DOI: 10.1007/s00408-021-00498-8.

A Pausder, **P Mras**, L Hoenicke, N Waldburg, TR Lesker, J Schreiber, T Strowig, JD Boehme, D Bruder. Altered nasal microbiota in asthmatic patients is not related to changes in secretory immunity in the nasopharynx. *Clin Exp Allergy*, 52(10):1213–1218, 2022. DOI: 10.1111/cea.14200.

Contents

List of Tables

List of Figures

List of Acronyms

Table 1: List of acronyms

Acronym	Meaning
Acc.	According
ACK buffer	Ammonium-chloride-potassium buffer
Actβ	β-Actin
ADONIS	Analysis of dissimilarities
AEC	Airway epithelial cell
AF700	Alexa Fluor® 700
AHR	Airway hyperresponsiveness test
ANOVA	Analysis of variance
APC	Allophycocyanin
APC/Cy7	Allophycocyanin-Cyanin 7
APS	Ammonium persulfate
BAL	Bronchoalveolar lavage
BALF	Bronchoalveolar lavage fluid
BCA	Bicinchonic acid
BHI	Brain-heart infusion
bp	Base pair
BSA	Bovine serum albumin
BV	Brilliant violet
C	Celsius
cAMP	Cyclic adenosine monophosphate
Cat. No.	Catalogue number
Cbp A	Choline-binding protein A
CD	Cluster of differentiation
cDNA	Complementary deoxyribonucleic acid

Continued on next page

Acronym	Meaning
CFU	Colony forming units
Cldn	Claudin
cm	Centimeter
Comb	All asthmatics combined
COPD	Chronic obstructive pulmonary disease
Cp	Crossing point
CRP	C-reactive protein
d	Day
DCs	Dendritic cells
ddH_2O	Double-distilled water
DEPC	Diethyl pyrocarbonate
dIgA	Dimeric immunoglobulin A
DMEM	Dulbecco's Modified Eagle Medium
DNA	Deoxyribonucleic acid
DNAH11	Dynein axonemal heavy chain 11
DNase I	Deoxyribonuclease I
DPBS	Dulbecco's phosphate buffered saline
D. pteronyssinus	*Dermatophagoides pteronyssinus*
DTT	Dithiothreit
ECL	Enhanced chemiluminescence
E. coli	*Escherichia coli*
EDTA	Ethylenediaminetetraacetic acid
e.g.	*exempli gratia*
ELISA	Enzyme-linked immunosorbent assay
Endo	Endogenous asthmatics
EpCAM	Epithelial cell adhesion molecule
et al.	*et alii*
Exo	Exogenous asthmatics

Continued on next page

Acronym	Meaning
FACS	Fluorescence-activated cell sorting
FCS	Fetal calf serum
FEV	Forced expiratory volume
Fig.	Figure
FITC	Fluorescein isothiocyanate
FSC	Forward scatter
FVC	Forced vital lung capacity
g	Gram
gDNA	Genomic deoxyribonucleic acid
GF	Germ-free
GM-CSF	Granulocyte-macrophage colony-stimulating factor
Gpt	Gigaparticles
H	Healthy
h	Hours
HDM	House dust mite
H&E	Hemalum eosin
HEPES	4-(2-hydroxyethyl)-1-piperazineethanesulfonic acid
HRP	Horseradish peroxidase
HZI	Helmholtz Centre for Infection Research
ICS	Inhaled corticosteroid
i.e.	*id est*
IFN	Interferon
Ig	Immunoglobulin
IL	Interleukin
IMDM	Iscove's Modified Dulbecco Medium
i.n.	Intranasally
i.p.	Intraperitoneally
IU	International unit

Continued on next page

Acronym	**Meaning**
IVC	Individually ventilated cage
J chain	Joining chain
K	Kilo
kU	Kilo unit
l	Liter
LABA	Long-acting β_2-agonist
LAMA	Long-acting muscarinic antagonist
LCF	Lymphocyte chemoattractant factor
LDA	Linear discriminant analysis
L/D	LIVE/DEATH
LEfSe	Linear discriminant analysis effect size
LPS	Lipopolysaccharide
LRT	Lower respiratory tract
Lyz	Lysozyme
M	Molar
MCh	Methacholine chloride
mg	Milligram
MHC	Major histocompatibility complex
min	Minutes
Mix	Subjects with mixed asthma phenotypes
ml	Milliliter
MLE	Immortalized mouse lung epithelial cells
mM	Millimolar
mRNA	Messenger ribonucleic acid
N	Total number
n	Number
NA	Not assigned
NAL	Nasal lavage

Continued on next page

Acronym	Meaning
NALF	Nasal lavage fluid
NALT	Nasal-associated lymphoid tissue
NEC	Nasal epithelial cell
ng	Nanogram
nm	Nanometer
n.s.	Not significant
NTC	No template control
OD	Optical density
OTU	Operational taxonomic units
OvGU	Otto-von-Guericke-University
PAMP	Pathogen-associated molecular pattern
Pbp	Penicillin–binding protein
PBS	Phosphate buffered saline
PC	Phosphorylcholine
PCoA	Principle coordinates analysis
PCR	Polymerase chain reaction
PC1	Principle coordinate 1
PC2	Principle coordinate 2
PE	Phycoerythrin
PerCP/Cy5.5	Peridinin Chlorophyll Protein Cyanin 5.5
PFA	Paraformaldehyde
pg	Picogram
pH	Potential of hydrogen
pIgM	Pentameric immunoglobulin M
PIGR	Polymeric immunoglobulin receptor (human, protein)
PIGR	Polymeric immunoglobulin receptor (human, gene)
Pigr	Polymeric immunoglobulin receptor (murine, gene)
pIgR	Polymeric immunoglobulin receptor (murine, protein)

Continued on next page

Acronym	Meaning
PMSF	Phenylmethylsulfonyl fluoride
PVDF	Polyvinylidene difluoride
qPCR, qRT-PCR	Quantitative real-time reverse transcription polymerase chain reaction
RDP	Ribosomal database project
RFU	Relative fluorescence units
RI	Airway resistance
RNA	Ribonucleic acid
RPLP0	Ribosomal protein lateral stalk subunit P0
rpm	Revolutions per minute
rRNA	Ribosomal ribonucleic acid
RT	Room temperature
s	Seconds
SC	Secretory component
SD	Standard deviation
SDS	Sodium dodecyl sulfate
SDS-PAGE	Sodium dodecyl sulfate polyacrylamide gel electrophoresis
SIgA	Secretory immunoglobulin A
SIgM	Secretory immunoglobulin M
SIgs	Secretory immunoglobulins
Spec.	Specific
SPF	Specific pathogen-free
S. pneumoniae	*Streptococcus pneumoniae*
SSC	Sideward scatter
TBS	Tris-buffered saline
TBST	Tris-buffered saline and TWEEN 20
TEMED	Tetramethyl ethylenediamine
TGF	Transforming growth factor

Continued on next page

Acronym	**Meaning**
THY medium	Todd Hewitt broth yeast medium
TLR	Toll-like receptor
TMB	3,3',5,5'-tetramethylbenzidine
TNF	Tumor necrosis factor
TRIS	Tris(hydroxymethyl)aminomethane
URT	Upper respiratory tract
vs.	*versus*
v/v	Volume per volume
w/v	Weight per volume
β_2AR	β_2-adrenergic receptor
µg	Microgram
µl	Microliter
µM	Micromolar
µm	Micrometer

1 Abstract

Secretory immunoglobulin A (SIgA) as well as its exclusive epithelial transport molecule, the polymeric immunoglobulin receptor (pIgR), are crucial elements of respiratory mucosal immunity whose absence or downregulation are linked to an increased susceptibility to bacterial infections. While the crucial role of pIgR and SIgA for mucosal antibacterial defense as well as their relevance for intestinal immunity are well understood, little is known so far regarding their regulation throughout the entire respiratory tract and related possible implications for airway mucosal immunity. Thus, the overarching goal of this thesis was to dissect airway secretory immunity during homeostatic, inflammatory and infectious conditions. In the first part of this study, the impact of different endogenous *vs.* exogenous (environmental) factors on airway associated antibacterial and secretory immunity was assessed using different murine models. These initial analyses revealed that site-specific differences regarding basal *Pigr* gene expression are depending on microbial colonization as well as on yet unknown intrinsic effects. Moreover, secretory immunity in the upper respiratory tract (URT) and lower respiratory tract (LRT) can be partly modulated by exogenous (microbial-derived) as well as endogenous (host-derived) stimuli.

Allergic asthma was previously shown to reduce PIGR-mediated secretory immunity in the LRT and to increase the susceptibility to bacterial pneumonia. The URT, *e.g.* the nasal cavities, represents both entry site and natural reservoir of several pathogenic bacteria, as well as site of allergic sensitization to aeroallergens during asthma development. It is conceivable, that allergic asthma is associated with altered secretory immunity in the URT, which in turn might affect infection with respiratory bacterial pathogens as well as microbial composition in general. Following this hypothesis, the second part of this thesis focused on analysing secretory immunity as well as pneumococcal colonization of the respiratory tract of asthmatic and non-asthmatic mice under homeostatic conditions and in reaction to intranasal treatment with an endogenous molecule (IFN-γ). To this end, two different murine models of house dust mite (HDM)-induced allergic asthma were established and characterized in detail. High-dose, mid-term HDM treatment led to a stable phenotype of allergic asthma. IFN-γ treatment improved antipneumococcal immunity in the URT of non-asthmatic mice. This effect was not reproducible in asthmatic mice, indicating that IFN-γ stimulation exerts no effect on host antibacterial defense in the astmathic URT and shows that this

cytokine has a context-dependent role on antipneumococcal immunity in healthy *vs.* pre-diseased individuals.

Ultimately, the third and final part of this thesis addressed the impact of allergic asthma on secretory immunity and microbiota composition in the human URT in frame of a clinical cohort study. These analyses revealed, that neither asthma nor the presence of allergy affects PIGR-mediated secretory immunity in the URT. Yet, asthma was partly associated with elevated nasal IgG2 levels and increased microbial diversity. However, there was no correlation between these two parameters. Thus, asthma-associated alterations in nasal microbiota composition seem to be independent of secretory and antibacterial immunity.

2 Introduction

2.1 Respiratory tract and airway epithelial cells

The surface of the human respiratory tract has a size of about 100 m^2 in adults and consists of nose, nasopharynx, oropharynx, trachea, and lung – including bronchi, bronchioles, alveolar ducts and alveoli [1, 2]. Functionally, it can be distinguished into two zones. The conducting zone reaches from nose to bronchioles and conducts the inhaled gases (large airways). The respiratory zone contains alveolar ducts and alveoli, which facilitate gas exchange with the blood (small airways). Anatomically, it can be differentiated into the upper respiratory tract (URT) and lower respiratory tract (LRT). The URT consists of nose, nasopharynx and oropharynx whereas the LRT includes trachea, bronchi, bronchioles, alveolar duct and alveoli (Fig. 1) [2]. The alveolar epithelium consists of type I and type II pneumocytes [3]. Type I pneumocytes cover about 90-95 % of the alveolar surface and facilitate gas exchange between airways and blood. Moreover, they maintain the barrier function of the alveolar epithelium thus preventing intra-alveolar fluid leakage. Type II pneumocytes produce surfactant protein which causes a low surface tension during expiration and therefore prevents collapse of the alveoli. Moreover, type II pneumocytes are able to differentiate into type I pneumocytes in reaction to lung injury which is crucial for alveolar repair and regeneration [4]. The whole respiratory tract is lined with multiple airway epithelial cell (AEC) subtypes, which are vital constituents of the airway mucosa. AECs represent the first cellular line of defense against respiratory pathogens. The airway epithelium in the large and small airways consists of goblet cells, ciliated cells and basal cells. Goblet cells secrete mucus into the mucosal lumen where it immobilizes pathogens, toxins and debris [5]. Ciliated cells are located on the apical mucosal surface and mediate transport of mucus and mucus-entrapped particles up the respiratory tract through continuous cilia movement [6]. Upon epithelial damage, basal cells are able to differentiate into other epithelial cell types, which is important for the maintenance of epithelial integrity [7]. AECs express transmembrane proteins like claudins, junctional adhesion molecules, occludins and tricellulins, which facilitate the formation of tight junctions between neighboring cells [8]. These structures allow only small ions or water to pass through the cell and therefore constitute a strong mechanical barrier [9]. In this context, it was shown that claudins and occludins are crucial for epithelial integrity [10] and that altered claudin expression affects airway epithelial barrier

function [11, 12]. Next to their key roles in forming a mechanical barrier, AECs also represent an immunological barrier. They constitutively secrete complement factors, antimicrobial peptides and cytokines [13–16]. The complement system includes a series of proteins whose antimicrobial functions are triggered either directly by pathogens or indirectly by pathogen-bound antibodies. This initiates a reaction cascade which leads to the binding of special complement components to the pathogen surface, their recognition by complement receptors on phagocytic cells and ultimately to their phagocytosis [17]. AECs furthermore produce and secrete antimicrobial peptides like defensin, cathelicidin and histatin [18–20]. AEC-derived cytokines have pleiotropic immunological functions. For instance, chemotactic cytokines like LCF (lymphocyte chemoattractant factor) are released upon injury and lead to the migration of leukocytes towards the inflammatory area. Colony-stimulating factors such as GM-CSF (granulocyte-macrophage colony-stimulating factor) support the differentiation and survival of migrated inflammatory cells. Moreover, multifunctional cytokines, like IL-1β, IL-6, IL-11 and TNF-α have pleiotropic proinflammatory effects on a multitude of target cells, *e.g.* the activation of monocytes and B cells and initiation of acute phase protein synthesis. Growth factors like TGF-β are secreted by bronchial epithelial cells and mediate cell differentiation, repair and signalling [16].

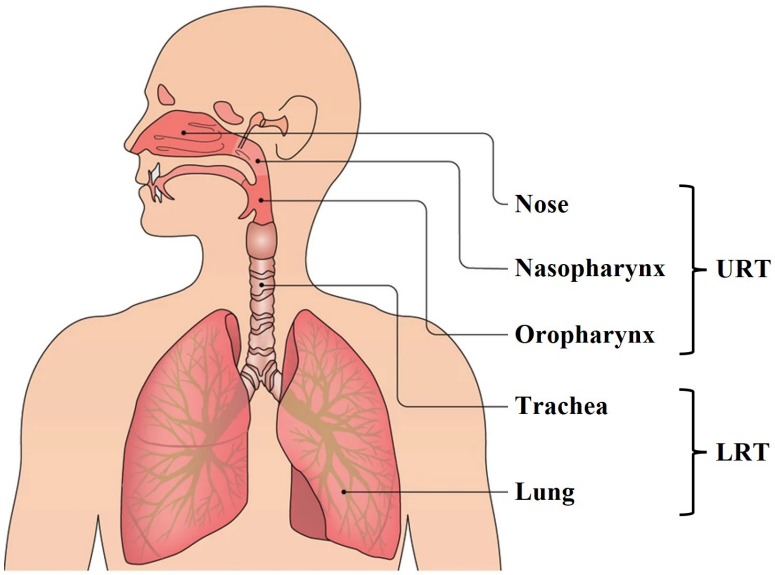

Figure 1: Schematic representation of the human respiratory tract. URT: upper respiratory tract; LRT: lower respiratory tract (modified figure from [21]).

2.2 Immunoglobulins and secretory immunity

Next to their critical functions in forming a physical and mechanical barrier, AECs critically contribute to the airway mucosal immunity by transcellular transport of immunoglobulins. There are five immunoglobulin subclasses: IgG, IgD, IgE, IgM and IgA. IgG is the most abundant immunoglobulin in the body (75 % in serum), exhibits the longest half-life of all subclasses and has a monomeric structure. It activates the complement cascade and directly neutralizes toxins and viruses. Moreover, it specifically binds to antigens which facilitates their phagocytosis by monocytes or macrophages (opsonophagocytosis) [22]. Circulating IgD (< 0.5 % in serum) occurs as a monomer and binds to specific bacterial proteins which activates and stimulates Ig-producing B cells [23]. IgE (< 0.01 % in serum) is found as a monomer and has the shortest half-life of all subclasses. It plays an important role during allergic reactions and is associated with antigen-hypersensitivity as it is typically observed in asthmatic patients. IgE binds Fcε receptors that are expressed on proinflammatory cells like basophils, eosinophils and mast cells with a very high affinity. At the same time, it facilitates the upregulation of Fcε receptor expression. This combination leads to the high potency of IgE [22]. Monomeric IgM is expressed on the surface of naïve B cells where it facilitates cell signalling. After maturation and antigen contact, monomeric IgM molecules form pentameric structures. Pentameric IgM (10 % in serum) binds antigens with a low affinity to facilitate their opsonophagocytosis. This serves as a quick primary response to a broad range of antigens and is therefore counted as part of innate immunity [22, 24]. IgA makes up about 15 % of all immunoglobulins in the serum where it is mainly found as a monomer [22]. However, it has the ability to polymerize into dimers by forming a covalent bond with the J chain [25]. IgA is vital to protect mucosal surfaces against toxins, viruses and bacteria either by directly neutralizing them or preventing their adhesion. IgA production is mainly initiated by T cell-dependent mechanisms (adaptive immunity). Upon antigen contact, dendritic cells, B cells and macrophages activate T cells by presenting fragments of the antigen to them. Activated CD4+ T cells release cytokines that stimulate B cells, which in turn produce and release antigen-specific immunoglobulins like IgA [22, 26–28]. Dimeric IgA and pentameric IgM are actively transported from the blood trough AECs via the polymeric immunoglobulin receptor (PIGR) and secreted into the mucosal lumen as secretory immunoglobulins (SIgs) [29, 30]. PIGR is localized on the basolateral site

of mucosal epithelial cells. It consists of an extracellular domain that facilitates the binding of ligands, a short hydrophobic region that is associated with the cell membrane and a relatively long cytoplasmic domain [31, 32]. After binding of dimeric IgA or pentameric IgM to the extracellular component of PIGR, the complex is internalized and transported through the epithelial cell in vesicular compartments. Upon reaching the apical side of the cell, the extracellular component of PIGR is proteolytically cleaved which leads to the formation of the secretory component (SC). SC covalently binds to the transcytosed immunoglobulin by forming a disulfide bridge which leads to its secretion into the mucosal lumen (Fig. 2). The complex of dimeric IgA or pentameric IgM and SC is called secretory IgA (SIgA) or secretory IgM (SIgM) [33]. It is known that SC increases the protection of SIgA against proteolytic degradation [34, 35]. Moreover, carbohydrate residues found on SC facilitate the binding of SIgA to the mucus layer of the epithelium which assures an effective secretory immunity [36]. Especially SIgA is known to prevent the adhesion of pathogens to the epithelium, thus preventing microbial infiltration [37]. Patients with IgA deficiency exhibited an increased susceptibility to respiratory tract infections [38]. Moreover, it was shown that SIgA is crucial for the protection against nasal colonization of mice with the bacterium Streptococcus pneumoniae [39]. *Pigr* knockout mice exhibited an increased susceptibility to mycobacterial infections of the respiratory tract [40] and developed a chronic obstructive pulmonary disease (COPD)-like phenotype caused by an altered lung microbiome and bacterial infiltration of the airway epithelium [41]. Moreover, COPD patients displayed SIgA deficiency in the small airways associated with persistent inflammation and airway wall remodelling, which highlights the importance of SIgA for airway homeostasis [42]. Furthermore, it was shown that chronic airway diseases lead to a decreased PIGR-expression in the bronchial epithelium, which is associated with increased disease severity in COPD patients and diminished SIgA-mediated mucosal defense in asthmatic patients [43, 44]. It was shown that *PIGR* gene expression in human intestinal epithelial cells increases upon stimulation with toll like receptor 4 (TLR4) ligands like double stranded viral RNA or lipopolysaccharides [45, 46]. Moreover, recombinant interferon-γ (IFN-γ), tumor necrosis factor-α (TNF-α) and interleukin-4 (IL-4) synergistically enhance *PIGR* gene expression in a human colon adenocarcinoma cell line [47–51].

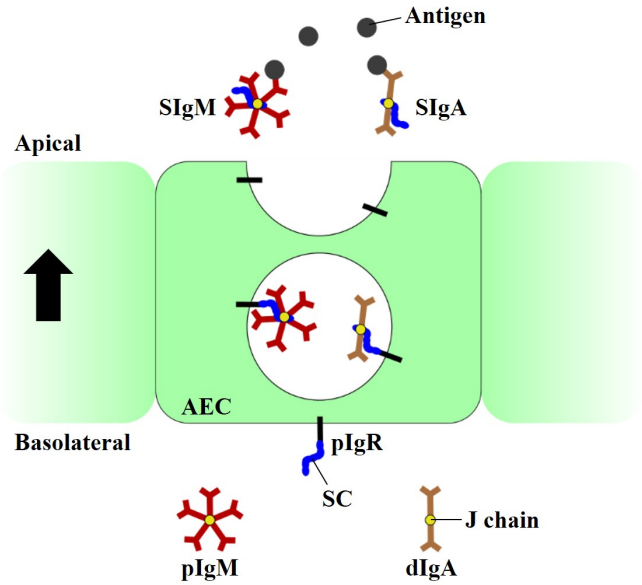

Figure 2: Schematic representation of pIgR-mediated Ig transport through AECs. AEC: airway epithelial cell; dIgA: dimeric IgA; pIgM: pentameric IgM; pIgR: polymeric immunoglobulin receptor; SC: secretory component; SIgA: secretory IgA; SIgM: secretory IgM.

2.3 Asthma

Asthma is a chronic respiratory disease, which affects more than 300-350 million people and causes approximately 250,000 deaths per year worldwide. Asthma-associated deaths mostly occur in individuals older than 45 years and are often accompanied by inadequate long-term medical care or delayed medical aid during an asthma exacerbation. There is also an increase in asthma-associated hospital admissions which are most prominent amongst young children. Despite its rapidly increasing prevalence - 50 % per decade - asthma still remains an underdiagnosed and undertreated disease [52–54]. Asthma commonly manifests in several respiratory symptoms including dyspnoea, coughing, wheezing and chest tightness [55, 56]. Generally, asthmatic disease includes mild to symptom-free episodes as well as acute episodes that are characterized by an increased symptom severity [57]. It was shown that variations regarding disease severity depend on the seasonal changes in prevalence of allergens like grass-pollen and house dust mites (HDM) [58]. In this context, HDM are the main source of asthma-inducing allergens found in house dust [59]. *Dermatophagoides farinae* and *Dermatophagoides pteronyssinus* are the most prevalent HDM species worldwide. HDM-associated allergens are mostly enzymes that originate from the mite digestive system, *i.e.* from feces [60]. The cysteine proteinase *Der p1*, which is derived from *D.*

pteronyssinus, is known to increase respiratory tract permeability and IgE synthesis which promotes asthma pathogenesis [61–64]. Moreover, the microbial cell wall component lipopolysaccharide (LPS) was detected in mite feces and is known to further trigger the allergic immune reaction [65]. Next to their prominent roles for asthma development, allergen exposure as well as bacterial and viral respiratory tract infections are major factors that drive acute asthma exacerbations [66–68]. Asthma exacerbations are potentially life-threatening disease stages that are characterized by bronchial hyperresponsiveness, enhanced airway inflammation and excessive sputum secretion resulting in a tightening of the airways and extreme dyspnoea [69, 70]. Furthermore, asthma exacerbations can promote an imbalance in the levels of type 1 and type 2 cytokines [71]. Type 1 cytokines (IFN-γ, IL-2, IL-12, IL-18, TNF-α) are crucial for opsonization, macrophage activation and immunoglobulin-mediated cytotoxicity. Type 2 cytokines (IL-4, IL-5, IL-6, IL-9, IL-10, IL-13) promote the humoral immune response which includes IgE, IgG and IgA production and secretion by B lymphocytes [72–75]. In line with this, evidence from animal models as well as clinical studies revealed that asthmatic individuals exhibited increased type 2 cytokine levels (IL-4, IL-5, IL-13) in bronchoalveolar lavage (BAL) fluid and lung tissue [76–78]. In this context, it was shown that IL-4 knockout mice lacked allergen-induced airway inflammation and bronchial hyperresponsiveness [79]. Moreover, IL-13 knockout mice were unable to develop airway hyperresponsiveness, goblet cell hyperplasia and mucus hypersecretion in reaction to allergen challenge [80]. Furthermore, IL-5 knockout mice exhibited attenuated aeroallergen-induced eosinophilia. Extensive airway eosinophilia is associated with bronchial hyperresponsiveness, lung damage and pulmonary mucus accumulation [81, 82]. It is also known that IL-10, IL-13 and the type 3 cytokine IL-17A are crucial during the induction of airway hyperreactivity and allergic inflammation [83–85]. Altogether, these findings clearly highlight the contribution of type 2 cytokines (and IL-17A) as drivers of the asthma-typical phenotype and the occurrence of exacerbations. Pathophysiologically, asthma is characterized by airway remodelling, *i.e.* pulmonary epithelial wall thickening, subepithelial fibrosis, goblet cell hyperplasia, mucus hypersecretion and epithelial cell hypertrophy. The remodelling process in asthma is the result of chronic airway inflammation which ultimately leads to a cycle of tissue injury and repair [86]. As asthma is a heterogenous disease that can have a multitude of different causes and characteristics, it is subdivided into three main phenotypes: exogenous, endogenous and mixed asthma. Exogenous (allergic)

asthmatics exhibit a specific sensitization to allergens like pollen, spores, animal hair, house dust mite or food, which trigger the asthma-typical symptoms. Moreover, they show eosinophilic airway inflammation, increased total and allergen-specific IgE levels in serum and increased prevalence of allergic rhinoconjunctivitis and atopic dermatitis. Endogenous (non-allergic) asthmatics show no signs of an allergic sensitization to aeroallergens. The pathogenesis is linked to a preceding bacterial or viral infection. It is mostly found in adults and characterized by a higher disease severity, while exogenous asthma is more prevalent in children and often exhibits a less severe phenotype. Mixed asthmatics exhibit characteristics of both allergic and non-allergic asthma [87–92]. Common among all three forms of asthma is that the symptoms can be triggered by cold air, cigarette smoke or exercise [91]. Clinical diagnosis of asthma is commonly performed by combining several tests. Spirometry (also known as lung function test) is applied to determine the ratio between the forced expiratory volume at 1 second and the forced vital lung capacity (FEV1/FVC). Defined ratio abnormalities are an indicator for the presence of airflow obstruction which is a typical characteristic of asthmatics [93]. Moreover, asthmatic patients exhibit an increased level of exhaled nitric oxide which is proportional to bronchial wall inflammation and induced-sputum eosinophilia and is therefore used as an asthma marker [94, 95]. The airway hyperresponsiveness test (AHR) is another method to validate an asthma diagnosis. Here, patients inhale increasing concentrations of methacholine chloride (MCh) which induces bronchoconstriction and a measurable, concentration-dependent increase in airway resistance. Bronchoconstriction at low MCh concentrations indicates an increased airway hyperresponsiveness which is prevalent in asthmatics [96]. There are common therapeutical approaches that target different characteristics of the disease. The application of β_2-adrenergic receptor (β_2AR) agonists causes a local increase in cAMP concentration, which leads to the opening of Ca^{2+} channels, consequent relaxation of airway smooth muscle and bronchodilation. Glucocorticoids dampen the expression of a multitude of pro-inflammatory genes and activate anti-inflammatory genes through recruitment of histone deacetylase-2, which makes them very effective in alleviating chronic inflammatory stress in the airways of asthmatics [97]. Omalizumab is a humanized, multiclonal anti-IgE antibody. It binds to circulating IgE thus preventing IgE-mediated activation of inflammatory cells. It reduces the risk of exacerbations and enhances the lung function in patients with severe persistent asthma [98]. Next to its detrimental effects on the respiratory system itself, asthma is also associated with a deteriorated antimicrobial immunity in the airways.

It was shown that asthmatic patients exhibit decreased PIGR expression in the bronchial epithelium which is associated with diminished SIgA-mediated mucosal defense [44] and an increased risk for severe pneumococcal infections [99, 100].

2.4 *Streptococcus pneumoniae*

Streptococcus (*S.*) *pneumoniae* is a gram-positive, spherical, aerotolerant, facultatively anaerobic bacterium with more than 90 known serotypes. It is able to lyse red blood cells either via α-hemolysis by producing hydrogen peroxide (aerobic conditions) or via β-hemolysis by producing the exotoxin streptolysin (anaerobic conditions). When the bacterium grows on blood agar medium, its hemolytic activity leads to the formation of smooth yellow colonies, which can be used for its microbiological identification [101]. *S. pneumoniae* is a common colonizer of the human nasopharynx and persists asymptomatically in healthy individuals. However, in immunosuppressed or very young/very old individuals it might spread locally and lead to infections of the upper or lower respiratory tract as well as pneumococcal meningitis [102, 103]. Moreover, the pathogen is considered the most common cause of community acquired pneumonia [104]. Pathogenesis is initiated by the attachment of the pneumococci to the mucus and cells of the nasopharynx [105–107]. The likelihood of a spread of the bacterium beyond the nasopharynx depends on the immune state of the host and the virulence of the pathogen, which is defined by different factors. The presence of a polysaccharide capsule is crucial for pneumococcal virulence as it protects the bacterium to a certain degree from phagocytosis [108]. The bacterial cell wall polysaccharide contains phosphorylcholine, which promotes the attachment of the organism to endothelial cells of the host during the course of an invasive infection [109, 110]. Besides surface polysaccharides, *S. pneumoniae* also contains a multitude of other virulence factors. Intracellular autolysin lyses the bacterial cell wall which leads to the release of pneumolysin. Pneumolysin is an intracytoplasmic toxin that activates the complement system, lyses cholesterol-containing cell membranes, disrupts pulmonary tissue barriers and has inhibitory effects on immune cells [111–113]. Transcarboxypeptidases are cell wall associated proteins which bind the antibiotic penicillin (penicillin-binding proteins). The stepwise alteration of these proteins by gene transfer between streptococcal species leads to the development of a resistance to penicillin and other beta-lactam antibiotics. Many penicillin-resistant *S. pneumoniae* strains are also multidrug resistant which highlights the necessity of performing susceptibility tests

before administering antibiotics to diseased patients [114]. Vaccination against *S. pneumoniae* is an effective measure to protect from multidrug resistant pneumococci and prevent their development. Conjugate vaccines employ a combination between a capsular polysaccharide antigen which directly stimulates B lymphocytes and a carrier protein that initiates a T lymphocyte dependent immune reaction. The deployment of a pneumococcal protein has the advantage of granting species-specific immunity [115]. A crucial protective mechanism against *S. pneumoniae* infections is the secretion of IgA by airway epithelial cells. As previously described (2.2), SIgA counteracts nasal pneumococcal colonization of mice [39]. On the other hand, *S. pneumoniae* binds to the extracellular domain of PIGR on the apical side of epithelial cells via its choline-binding protein A. It was shown that this process is crucial for the invasion of human nasopharyngeal cells *in vitro* and is discussed to play a central role regarding the progress of pneumococcal infections [116–119] (Fig. 3).

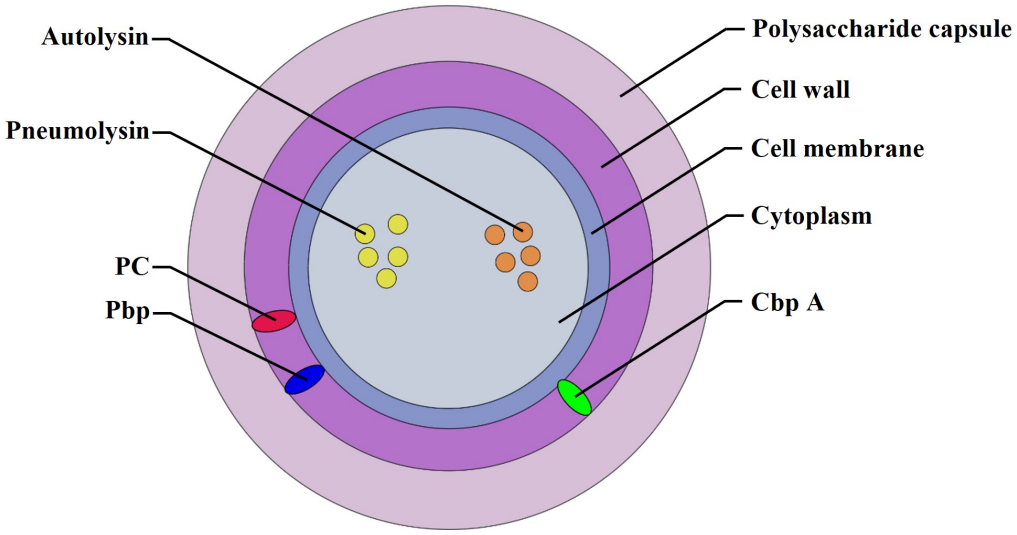

Figure 3: Schematic representation of *Streptococcus pneumoniae* and its virulence factors. Cbp A: choline-binding protein A; Pbp: penicillin–binding protein; PC: phosphorylcholine.

2.5 The human airway microbiota in homeostasis and asthma

The human respiratory tract is colonized by a broad variety of microorganisms. The entirety of these commensal, symbiotic and pathogenic microorganisms is summarized as airway microbiota. The presence of a 'healthy' microbiota is considered to be crucial for defence against airborne pathogens as well as immuneregulation and thus is key to the maintenance of airway homeostasis [120–123]. The microbial flora in healthy lungs resembles that of the oropharynx with a relatively high abundance of *Prevotella*, *Veillonella* and *Streptococcus* [124–127]. It was shown that spatial variation of a healthy lung microbiome is rather impacted by the balance between microbial immigration and elimination, than by local growth conditions. The degree of microbial variation as well as the amount of microorganisms generally decreases from URT to LRT [128]. The highest microbial density in the respiratory system is present in the URT. Here, *Staphylococcus*, *Propionibacterium*, *Corynebacterium*, *Moraxella* and *Streptococcus* are the most abundant bacterial species in healthy individuals. Microbial communities in the URT play an important role in preventing pathogens from colonizing the respiratory mucosal surface and spreading to the LRT [21]. It is known that chronic airway diseases like COPD, chronic rhinosinusitis and asthma are associated with alterations of the respiratory microbiota composition [129, 130]. Asthmatic patients exhibited an elevated diversity of microbial communities, decreased abundance of the Bacteroidetes phylum (*Prevotella*) and increased abundance of Proteobacteria, especially *Haemophilus*, in the lower airways [131]. In the upper airways, increased abundance of Firmicutes (*Streptococcus*), Bacteroidetes (*Prevotella buccalis*), Proteobacteria (*Burkholderia*) and decreased abundance of Actinobacteria (*Corynebacteriales*) was observed [130]. Moreover, it was found that airway hyperresponsiveness – a hallmark symptom of allergic asthma – correlates with the abundance of different families of Proteobacteria (*e.g.* Pseudomonadaceae, Enterobacteriaceae, Burkholderiaceae, Neisseriaceae) [131–133].

In summary, functional airway epithelial integrity and secretory immunity as well as a 'healthy' microbiota composition are crucial for maintaining airway homeostasis and protection against respiratory pathogens. Asthma has detrimental effects on all of these parameters and is associated with an increased susceptibility to respiratory tract infections, which is a major cause of morbidity and hospitalization in asthmatic individuals.

3 Materials and methods

3.1 Materials

3.1.1 Instruments

Table 2: Used instruments

Instrument	Model	Company
Automatic sample preparation system	Tissue-Tek® VIP® 6	Sakura Finetek Germany GmbH
Aspiration system	VACUSAFE	Integra Biosciences
Anesthesia chamber	Posi-Seal induction chamber	Rothacher Medical GmbH
Anesthesia machine	combi-vet®	Rothacher Medical GmbH
Blotting chamber	REL-SD20	Carl Roth
Counting chamber	Neubauer	Marienfeld Superior
CO_2 incubator	NU-8500E	Integra Biosciences
Cryoconsole	EC350-1	Intertek
Flow cytometer	Attune™ NxT	Thermo Fisher Scientific
Gel electrophoresis chamber	Mini-PROTEAN	BIORAD
Gene sequencing platform	MiSeq™ PE250	illumina®
Glass coverslipper	Leica CV5030	Leica Biosystems
Hand dispenser	POLYTRON® PT 3100 D	KINEMATICA AG
Ice machine	AF 80	Scotsman
Imaging system	ChemoCam Tetra Cell	Intas Science Imaging
Incubation shaker	Ecotron	INFORS HAT
Laboratory balance	Pioneer®	Ohaus
Laboratory centrifuge	Allegra® X-15R	Beckman Coulter

Continued on next page

Instrument	**Model**	**Company**
Laboratory shaker	DOS-10L	Neolab
Magnetic stirrer	C-MAG HS7	IKA
Microcentrifuge	5417R	Eppendorf
Microplate reader	Synergy HT	BioTek Instruments
Microscope	CX21	Olympus
Microtome	HM 325	Microm GmbH
pH meter	EL20	Mettler Toledo
Resistance and compliance system	Buxco® FinePointe™	Harvard Bioscience, Inc.
Roller mixer	SRT9	Stuart
Safety cabinet	HERAsafe® KS	Heraeus
Sample scanner	Aperio CS2	Leica Biosystems
Spectrophotometer	GeneQuant™ pro	Amersham Biosciences
Spectrophotometer	ND-1000	NanoDrop Technologies
Real-time PCR Thermocycler	LightCycler® 480 II	Roche
Thermocycler	peqSTAR 2X	Peqlab
Thermomixer	Thermomixer comfort	Eppendorf
Universal centrifuge	Multifuge® 1 S-R	Heraeus
Vortexer	Vortex Genie 2	Scientific Industries
Water bath	WNE 7	Memmert

3.1.2 Consumables

Table 3: Used consumables

Name	Type	Company
BD Falcon™ cell strainer	70 µm, 100 µm Nylon	BD Biosciences
Blood collection tube	S-Monovette® Serum	Sarstedt
Blood collection tube (EDTA)	S-Monovette® K3 EDTA	Sarstedt
Disposable syringes	Discardit™ II 5 ml, 10 ml	BD Biosciences
Disposable syringes	Omnifix®-F 10 µl – 1 ml	B Braun Melsungen AG
Embedding cassettes	Macrosette™	Carl Roth
FACS tubes	1.4 ml PP round bottom	Thermo Scientific
Falcon™ tubes	15 ml, 50 ml	Greiner bio-one
Homogenization tubes	10 ml PP round bottom	Sarstedt
Injection cannulas	Sterican® 0.45 x 12 mm	B Braun Melsungen AG
Microscope slides	SuperFrost®	Engelbrecht
Nasal curettes	Rhino-Pro®	Arlington Scientific
Reaction vessels	Eppendorf Tubes® 3810X 1.5 ml, 2 ml	Eppendorf
Semi-micro cuvette	Polystyrol, 10 x 4 x 45 mm	Sarstedt
Serological pipettes	5 ml, 10 ml, 25 ml	Greiner bio-one
Tracheostomy tubes	4252098B	Introcan®
Transfer pipettes	LD-PE 3.5 ml	Sarstedt
Venipuncture cannula	Venofix®	B Braun Melsungen AG
Western Blot transfer-membrane	Immobilon®, PVDF, 0.45 µm	Merck Millipore
12-well plates	Cellstar®	Greiner bio-one
6-well plates	Cellstar®	Greiner bio-one
96-well plates (ELISA)	Nunc MaxiSorp™	Thermo Fisher Scientific
96-well plates	Cellstar®	Greiner bio-one

Continued on next page

Name	Type	Company
(flat or round bottom)		
96-well plates (qRT-PCR)	LightCycler® 480	Roche

3.1.3 Chemicals

Table 4: Used chemicals

Substance	Cat. No.	Company
Acrylamide/bis solution (30 %)	161-0156	BIORAD
Ammonium chloride	K298.1	Carl Roth
Ammonium persulfate	9592.2	Carl Roth
Attune™ focusing fluid	4449791	Thermo Fisher Scientific
Attune™ shutdown solution	A24975	Thermo Fisher Scientific
Attune™ wash solution	A24974	Thermo Fisher Scientific
Bacto™ yeast extract	210941	BD Biosciences
Bromphenol blue	A512.1	Carl Roth
BSA	K45-001	GE Healthcare
Collagenase D	11088858001	Roche
cOmplete™ ULTRA tablets, EDTA free	5892791001	Roche
DEPC-treated water	AM9920	invitrogen™
DNaseI	D4527-40KUI	Sigma-Aldrich
DPBS	14190-094	gibco®
EDTA	E6758-500G	Sigma-Aldrich
Eosin Y solution (1 %)	3137.1	Carl Roth
Ethanol, absolute	2246.1000	CHEMSOLUTE®
FCS	P4047500	PAN Biotech

Continued on next page

Substance	**Cat. No.**	**Company**
Glycerol	-	Pharmacy
Glycine	HN07.3	Carl Roth
Glucose	-	Pharmacy
HDM extract (*D. pteronyssinus*)	XPB70D3A25	Stallergenes Greer
Hemalum, acc. to Mayer	T865.1	Carl Roth
Heparin sodium	PZN3029843	ratiopharm®
IFN-γ (recombinant, murine)	315-05	PeproTech
IL-4 (recombinant, murine)	214-14	PeproTech
IMDM (GlutaMAX™-1)	31980-022	gibco®
Isoflurane	-	Pharmacy
Isopropanol	CP41.3	Carl Roth
Ketamine (10%)	-	Pharmacy
LPS (*E. coli* O111:B4)	L2630	Sigma-Aldrich
Methacholine chloride	A2251	Sigma-Aldrich
Methanol, 'BAKER ANALYZED'	8045	J. T. Baker®
Paraformaldehyde	252549-1L	Sigma-Aldrich
PBS tablets	18912-014	gibco®
PCR-grade water	17000-11	MO BIO Laboratories
Penicillin/Streptomycin	11548876	gibco®
Percoll™	17-0891-01	GE Healthcare
PMSF	8553	Cell Signaling
Potassium bicarbonate	X887.1	Carl Roth
RNAlater	76106	QIAGEN®
SDS	2326.1	Carl Roth
Sodium bicarbonate	6885.2	Carl Roth
Sodium carbonate	A135.1	Carl Roth
Sodium chloride	S5886-1KG	Sigma-Aldrich
Sodium chloride solution	14IH20	Fresenius Kabi

Continued on next page

Substance	Cat. No.	Company
		Deutschland GmbH
Sulfuric acid (2N)	X873	Carl Roth
TEMED	2367.3	Carl Roth
Todd Hewitt broth	T1438	Sigma-Aldrich
Tris base	4855.2	Carl Roth
Tris HCl	9090.3	Carl Roth
Triton X-100	3051.2	Carl Roth
Trypan blue	15250-061	gibco®
TWEEN 20	A1379-100ML	Sigma-Aldrich
Xylazine (2%)	-	Pharmacy
Xylene	CN80	Carl Roth
β-mercaptoethanol	1001090202	Sigma-Aldrich

3.1.4 Kits and ancillary reagents

Table 5: Used kits and ancillary reagents

Kit/Reagent	Cat. No.	Company
BD™ CompBeads Anti-Rat and Anti-Hamster Ig, κ	51-90-9000949	BD Biosciences
BD™ CompBeads Negative Control	51-90-9001291	BD Biosciences
DNA/RNA Shield™ collection tube with swab	R1107-E	Zymo Research
LEGENDplex™ MU Th Cytokine Panel	741043	BioLegend
LEGENDplex™ HU Immunoglobulin Isotyping Panel (1-plex)	740642	BioLegend
LEGENDplex™ HU	740640	BioLegend

Continued on next page

Kit/Reagent	Cat. No.	Company
Immunoglobulin Isotyping Panel (6-plex)		
Microbank™ vials with cryopreservative	PL.170/M	Pro-Lab Diagnostics
MiSeq™ Reagent Kit v2	MS-102-2001	illumina®
Oligo dT(20) Primer	18418020	invitrogen™
Pierce™ BCA Protein Assay Kit	23227	Thermo Fisher Scientific
Pierce™ ECL Plus	32132	Thermo Fisher Scientific
Western Blotting Substrate		
Random Primers	48190011	invitrogen™
RNeasy® Plus Mini Kit	74136	QIAGEN
SensiFAST™ SYBR® No-ROX Kit	BIO-98005	Bioline
SuperScript™ III Reverse Transcriptase	18080093	Thermo Fisher Scientific
TMB Substrate Set	421101	BioLegend
UltraClean®-htp 96 Well PCR Clean-Up Kit	12596-3	MO BIO Laboratories
UltraComp eBeads™	01-2222-42	invitrogen™
ZymoBIOMICS DNA Miniprep Kit	D4300	Zymo Research
5Prime HotMasterMix®	2200400	QIAGEN

3.1.5 Buffers and media

Table 6: Used buffers and media

Name	Composition/Company
ACK buffer	10 mM $KHCO_3$ in H_2O
	0.15 mM NH_4Cl
	0.1 mM 0.5 M EDTA
	(pH = 8)
Assay diluent	1 % (w/v) BSA

Continued on next page

Name	**Composition/Company**
	1 ml TWEEN 20
	ad 100 ml PBS
Coating buffer	100 mM $NaHCO_3$ in H_2O
	33.6 mM Na_2CO_3
	(pH = 9.5)
Columbia blood agar plates	BD Biosciences
(5 % sheep blood)	
Dulbecco's Modified Eagle Medium	Thermo Fisher Scientific
FACS buffer	2 mM EDTA in PBS
	2 % (v/v) FCS
Gel running buffer	25 mM tris base in H_2O
	192 mM glycine
	0.1 % (w/v) SDS
	(pH = 8.3)
Lung digestion medium	IMDM (GlutaMAX^{TM}-1)
	0.2 mg/ml Collagenase D
	0.01 mg/ml DNAseI
	5 % (v/v) FCS
Percoll/NaCl solution	27.6 ml Percoll
	3.1 ml 1.5 M NaCl
	69.3 ml 0.15 M NaCl
TBS	0.14 M NaCl in H_2O
	20 mM tris base
	(pH = 7.4)
TBST	0.1 % (v/v) TWEEN 20 in TBS
THY medium	3.7 g Todd Hewitt broth
	1 g Bacto^{TM} yeast extract
	ad 100 ml H_20

Continued on next page

Name	Composition/Company
TPNE buffer	300 mM NaCl in PBS
	1 mM EDTA
	1 % (v/v) Triton X-100
	10 µm PMSF
	1 cOmplete^{TM} ULTRA tablet per 10 ml
Transfer buffer	25 mM tris base in H_2O
	192 mM glycine
	20 % (v/v) methanol
	10 % (v/v) SDS
	(pH = 8.4)
Wash buffer	0.05 % (v/v) TWEEN 20 in PBS
	(pH = 7.4)
2x SDS buffer	125 mM tris HCl in H_2O
	4 % (w/v) SDS
	0.02 % (v/v) bromphenol blue
	20 % (v/v) glycerol
	100 mM DTT
	(pH = 6.8)

3.1.6 Antibodies and ancillary reagents

Table 7: Used antibodies and ancillary reagents for flow cytometry

Antibody	Fluorochrome	Clone	Company
Anti-CD11b	APC-Cy7	M1/70	BioLegend
Anti-CD11c	APC	N418	BioLegend
Anti-CD16/CD32	-	93	BioLegend

Continued on next page

Antibody	**Fluorochrome**	**Clone**	**Company**
Anti-CD170	PE	E50-2440	BD Biosciences
Anti-CD19	PerCP-Cy5.5	1D3/CD19	BioLegend
Anti-CD4	FITC	RM4-4	BioLegend
Anti-CD4	APC	RM4-5	BioLegend
Anti-CD8a	PE-Cy7	53-6.7	BioLegend
Anti-CX3CR1	BV421	SA011F11	BioLegend
Anti-I-A/I-E	BV711	M5/114.15.2	BioLegend
Anti-Ly6G	AlexaFluor 700	1A8	BioLegend
eBioscience™ fixable viability dye	eFluor™ 506	-	invitrogen™

Table 8: Used antibodies for ELISA

Antibody	**Type**	**Species**	**Cat. No.**	**Company**
Anti-goat	Polyclonal detection, HRP conjugated	Rabbit	5220-0362	SeraCare
Anti-human IgA	Monoclonal capture	Mouse	9140-01	SouthernBiotech
Anti-human pIgR (SC)	Polyclonal secondary	Goat	AF2717	R&D Systems
Anti-mouse IgA	Monoclonal capture	Rat	1165-01	SouthernBiotech
Anti-mouse IgA	Polyclonal secondary	Rabbit	SA5-10308	Thermo Fisher Scientific
Anti-mouse IgE	Monoclonal capture	Rat	1130-01	SouthernBiotech
Anti-mouse IgE	Polyclonal detection, HRP conjugated	Goat	PA1-84764	Thermo Fisher Scientific
Anti-rabbit	Polyclonal detection, HRP conjugated	Swine	P021702-2	Agilent

Table 9: Used antibodies for Western Blot

Antibody	Type	Species	Cat. No.	Company
Anti-goat	Polyclonal detection, HRP conjugated	Rabbit	5220-0362	SeraCare
Anti-human pIgR (SC)	Polyclonal primary	Goat	AF2717	R&D Systems
Anti-human RPLP0	Polyclonal primary	Rabbit	PA5-30158	Thermo Fisher Scientific
Anti-rabbit	Polyclonal detection, HRP conjugated	Swine	P021702-2	Agilent

3.1.7 Primer

Table 10: Primer for qRT-PCR

Primer	Orientation	Sequence
Actb 5‘	Forward	ACACCCGCCACCAGTTCG
Actb 3‘	Reverse	GTCACCCACATAGGAGTCCTTC
CD19 5‘	Forward	CCTGGGCATCTTGCTAGTGA
CD19 3‘	Reverse	CGGAACATCTCCCCACTATCC
Cldn-18 5‘	Forward	GACACCAGATGACAGCAACTTC
Cldn-18 3‘	Reverse	TTCATCGTCTTCTGTGCGGG
Cldn-7 5‘	Forward	AGCGAAGAAGGCCCGAATAG
Cldn-7 3‘	Reverse	AGGTCCAAACTCGTACTTAACG
DNAH11 5‘	Forward	GGGGTTCACGGAGGAGAAAT
DNAH11 3‘	Reverse	TGCATCTCTTGGAATCTCCTGG
EpCAM 5‘	Forward	TTGCTCCAAACTGGCGTCT
EpCAM 3‘	Reverse	GTTGTTCTGGATCGCCCCTT

Continued on next page

Primer	Orientation	Sequence
IgJ 5‘	Forward	GCATGTGTACCCGAGTTACC
IgJ 3‘	Reverse	TTCAAAGGGACAACAATTCGG
Lyz2 5‘	Forward	AAGGCATTCGAGCATGGGTG
Lyz2 3‘	Reverse	TCGAGGGAATGTGACCTCTCT
Muc5ac 5‘	Forward	TCTACTGACTGCACCAACACA
Muc5ac 3‘	Reverse	AGGCTTGCTCAGCACATAGG
PIGR 5‘	Forward	CAAGAAGGCAAAAAGGTCATCCAA
PIGR 3‘	Reverse	AGGTGATTGTCATGGGTGCAG
Pigr 5‘	Forward	GTGCCCGAAACTGGATCACC
Pigr 3‘	Reverse	TGGAGACCCCTGAAAAGACAGT

Table 11: Primer for amplification of genomic DNA

Primer	Type	Sequence	Company
515F	Forward	AATGATACGGCGACCACCGAGAT CTACACGCT XXXXXXXXXXXX TATGGTAATT GT GTGYCAGC MGCCGCGGTAA	illumina®
806R	Reverse	CAAGCAGAAGACGGCATACGAGAT AGTCAGCCAG CC GGACTACNVGG GTWTCTAAT	illumina®

Table 12: Primer for 16S rRNA gene sequencing

Primer	Type	Sequence
Read 1 sequencing	Forward	TATGGTAATT GT GTGYCAGCMGCCGCGGTAA
Read 2 sequencing	Reverse	AGTCAGCCAG CC GGACTACNVGGGTWTCTAAT
Index sequencing	-	AATGATACGGCGACCACCGAGATCTACACGCT

3.1.8 Software

Table 13: Used software

Software	Version	Company
Aperio ImageScope	12.3.2	Leica Biosystems
FinePointe™ Review software	2.9.0	Harvard Bioscience, Inc.
FlowJo™	10	BD Biosciences
Gen5™	2.04	BioTek
GraphPadPrism	5.04	GraphPad Software Inc.
ImageJ	1.8	Wayne Rasband
LightCycler® 480	1.5	Roche
PowerPoint	2203	Microsoft
RStudio	2021.09.2+382	RStudio PBC

3.1.9 Bacteria

Streptococcus pneumoniae serotype 19F (strain BHN100) [134] was provided by Birgitta Henriques-Normark (Karolinska Institutet, Stockholm).

3.1.10 Mice

BALB/c and C57BL/6J mice were maintained in individually ventilated cages (IVCs) under specific pathogen-free (SPF) conditions at the Helmholtz Centre for Infection Research (HZI), Braunschweig. Germ-free mice (C57BL/6N) were bred and maintained in isolators in a germ-free (GF) facility (HZI). C57BL/6J mice with an undefined microbiome (maintained in open cages) were provided by Dirk Schlüter (Otto-von-Guericke-University [OvGU], Magdeburg). Female C57BL/6JRj mice were purchased from Janvier Labs (France) and maintained in IVCs under SPF conditions (OvGU). All conducted animal experiments were carried out at the OvGU, Magdeburg, in accordance with the guidelines of the Saxony-Anhalt State Administration Office (file number: 42502-2-1495 Uni MD; 42502-2-1637 Uni MD) and at the HZI, Braunschweig, in accordance with the guidelines of the Lower Saxony State Office for Consumer Protection and Food Safety (file number: 42502-04-14/1715; 42502-04-16/2319).

3.1.11 Patients

A total of 112 male and female patients (30 control subjects, 33 exogenous asthma, 24 endogenous asthma, 25 mixed asthma) at the age of 18-82 years were included in this study (Table 22). All conducted experiments involving the acquisition and further processing of human material were carried out by Paula Mras at the practice of Dr. med. Nadine Waldburg and at the OvGU, Magdeburg, in accordance with the Ethics Committee of the OvGU, Magdeburg (file number: 51/19).

3.1.12 Cell lines

Immortalized mouse lung epithelial cells (MLE-15) [135] were used for *in vitro* stimulation experiments (3.2.6).

3.2 Methods

3.2.1 Induction of allergic asthma

Isoflurane was vaporized using an anesthesia machine, enriched with oxygen and directed into an anesthesia chamber. The mice were put into the chamber, monitored until the onset of anesthesia and were taken out for subsequent intranasal (i.n.) treatments. The animals were held upright for all i.n. administrations. All inocula were administered dropwise onto both nostrils.

Two different murine allergic asthma models were applied and characterized in frame of this thesis:

Model 1: 20 µg HDM extract in 30 µl PBS or PBS alone (control group) were intranasally (i.n.) administered three times a week over a timespan of 5 weeks.

Model 2: 100 µg HDM extract in 50 µl PBS or PBS alone (control group) were intranasally administered once a week over a timespan of 3 weeks.

For immune modulation experiments mice were treated i.n. with 10 µg LPS in 25 µl PBS or solvent alone or 1 µg recombinant murine IFN-γ in 20 µl ddH_2O with 5 % BSA or solvent alone. After i.n. administration mice were monitored until the end of anesthesia.

3.2.2 Intranasal infection of mice with *Streptococcus pneumoniae* 19F

Cultures of *S. pneumoniae* serotype 19F were stored at -80°C in Microbank™ vials containing cryopreservative and polystyrene beads. Three beads were taken out and plated onto three columbia blood agar plates using sterile inoculation loops. The plates were incubated over night at 37°C, 5 % CO_2. Single bacterial colonies were recovered by rinsing the plates with 2 ml sterile THY medium per plate. The bacterial suspension optical density (OD) was measured photometrically at a wavelength of 600 nm. The suspension was accordingly diluted in THY medium to reach an OD of 0.05 and incubated at 37°C, 5 % CO_2 for approximately 3 h. After reaching an OD of 0.5 the bacterial culture was spun down (3 min, 20.000 x g, 4°C) and the cells were washed twice in sterile, ice-cold PBS. The cell pellet was resuspended and diluted 1:10 in sterile, ice-cold PBS and the OD of the bacterial suspension was determined. Using this value and a previously created growth curve, a dilution factor was determined to attain a cell concentration of 10^{10} CFU/ml. Mice were anesthetized by intraperitoneal (i.p.) injection of ketamine/xylazine (1 mg/ml ketamine, 0.1 mg/ml xylazine, 10

µl/g body weight). After the onset of anesthesia the animals were held upright and 10 µl of bacterial suspension (containing 10^8 CFU) was i.n. administered. Bacterial infection doses were restrospectively verified by plating serial dilutions of the infectious inocula onto blood agar plates (equation (1)).

$$\text{CFU} = \text{Formed colonies} \times \text{Dilution factor} \tag{1}$$

3.2.3 *In vivo* airway hyperresponsiveness test

Assessment of airway hyperresponsiveness was carried out using a resistance and compliance system and FinePointe^{TM} Review software (version 2.9.0, Harvard Bioscience, Inc.). Mice were anesthetized by i.p. injection of ketamine/xylazine (1 mg/ml ketamine, 0.1 mg/ml xylazine, 10 µl/g body weight). After the onset of anesthesia the trachea was carefully exposed without damaging any of the surrounding vessels and a thread was loosely tied around it. After inserting a tracheostomy tube into the trachea the thread was tightened to hold the tube in place. Immediately afterwards, the mouse was put into the body chamber and the tracheostomy tube was connected to the ventilation system to actively respirate the animal. Electrodes were attached on both front legs and the left hind leg to monitor the heart rate during the experiment. The body chamber was tightly closed. Increasing concentrations (0, 6.25, 12.5, 25, 50, 100 mg/ml in PBS) of methacholine chloride solution were instilled in the nebulizer head, vaporized and directed trough the tracheostomy tube into the murine respiratory tract. The instrument constantly measured airflow, pressure and breathing volume and these parameters were used for calculation of airway resistance. After the procedure the mouse was taken out of the body chamber and euthanized by cervical dislocation.

3.2.4 Preparation of murine organs

Mice were euthanized by i.p. injection of ketamine/xylazine (2 mg/ml ketamine, 0.2 mg/ml xylazine, 10 µl/g body weight). Afterwards, the mice were processed further depending on the subsequent

experimental procedure:

Procedure with subsequent quantitative real-time PCR (qRT-PCR), enzyme-linked immunosorbent assay (ELISA) and bead-based immunoassay. Lung, trachea, nasal-associated lymphoid tissue (NALT), heart blood, bronchoalveolar lavage fluid (BALF) and nasal lavage fluid (NALF) was taken from the mice. RNA was isolated from lung, trachea and NALT using the RNeasy® Plus Mini Kit (QIAGEN) according to the manufacturer's instructions and used for cDNA synthesis (3.2.9). Heart blood was incubated for 20 min at 37°C, 5 min at 4°C and spun down (10 min, 10.600 x g, 4°C). BALF and NALF were centrifuged as well (10 min, 1.700 x g, 4°C). Supernatants were used for ELISA (3.2.11) and bead-based immunoassay analysis (3.2.7).

Procedure with subsequent flow cytometric analysis. Mice were transcardially perfused with 10 ml PBS to remove intravascular erythrocytes. Lung, spleen, NALT and BALF were excised and obtained, respectively. Lung tissue was cut into small pieces in a 6-well plate using surgical scissors, suspended in 3 ml enzymatic lung digestion medium, transferred into a 15 ml Falcon™ tube and incubated for 30 min, 37°C, 150 rpm on a plate shaker. After the incubation time 2 ml fresh lung digestion medium was added and incubated for another 15 min, 37°C, 150 rpm. After the second incubation step the enzymatic reaction was stopped by adding 60 µl 0.5 M EDTA. Tissue suspensions were put on ice for 5 min and subsequently passaged trough a 100 µm cell strainer into a 50 ml Falcon™ tube. The strainer was flushed with 20 ml PBS. The cell suspension was spun down (10 min, 350 x g, 4°C) and supernatant was discarded. Erythrocyte lysis was performed by resuspending the cell pellet in 1 ml ACK buffer and cell suspension was transferred into a 15 ml Falcon™ tube. Remaining cells in the 50 ml Falcon™ tube were resuspended in 1 ml ACK buffer, added to the other cells and incubated for a total of 2 min. 8 ml FACS buffer was added to stop erythrocyte cell lysis. The cell suspension was spun down (10 min, 350 x g, 4°C), supernatant was discarded and the cell pellet was resuspended in 1 ml Percoll/NaCl solution (composition see table 6). Another 9 ml of Percoll/NaCl solution was added and spun down (20 min, 750 x g, 25°C, centrifuge deceleration inactivated). The supernatant was discarded and the cell pellet was resuspended in 200 µl PBS. Spleen and NALT were each passed through a 100 µm cell strainer into a 6-well plate filled with 4 ml PBS. The strainer was flushed with 10 ml PBS. The cell suspension

was transferred into a 15 ml Falcon^{TM} tube and spun down (5 min, 350 x g, 4°C). The supernatant was discarded and the NALT cell pellet was resuspended in 10 ml FACS buffer. The spleen cell pellet was resuspended in 3 ml ACK buffer and incubated for 2 min for erythrocyte lysis. The lysis process was stopped by adding 10 ml FACS buffer. Spleen and NALT cell suspensions were pipetted trough a 30 µm cell strainer into a new 15 ml Falcon^{TM} tube and spun down (5 min, 350 x g, 4°C). The cell pellets were resuspended in FACS buffer (spleen: 3 ml, NALT: 100 µl). BALF was centrifuged (10 min, 1.700 x g, 4°C). The supernatant was discarded and the cell pellet was resuspended in 200 µl ACK buffer. After adding 1 ml PBS the cell suspension was spun down (10 min, 500 x g, 4°C) and the cell pellet was resuspended in 100 µl PBS. The obtained cells were used for subsequent flow cytometric analysis (3.2.8).

Procedure with subsequent CFU analysis. Lung, trachea, NALT, NALF and nasopharynx were obtained from mice, that had been infected with *S. pneumoniae* 19F. The organs were put in 1 ml ice-cold PBS and homogenized using a hand dispenser. Organ homogenates and NALF were serially diluted and 10 µl of each dilution was pipetted on a columbia blood agar plate and incubated over night at 37°C, 5 % CO_2. The number of CFU on the plate was counted and used to calculate the amount of CFU in the respective organ/fluid.

Procedure with subsequent histopathologic analysis. The abdomen of anesthetized mice was opened and 100 µl heparin solution (25000 IU) was intracardially injected trough the diaphragm to prevent coagulation. The *vena cava* was punctured, trachea was exposed and a thread was tied around it to prevent lung collapse. The esophagus was cut below the lung. Subsequently, thorax was opened completely, the trachea was cut above the thread and pulled upwards to remove the intact lung. The lung was placed carefully in an embedding cassette. The cassette was stored in saline-buffered PFA (4 %) solution for tissue fixation and preservation at room temperature (RT).

3.2.5 Histopathologic analysis

Histopathologic analyses were carried out by Dr. Olivia Kershaw (Institute of Veterinary Pathology, Free University of Berlin). The embedding cassette containing the fixated tissue was inserted into an

automatic sample preparation system where the organ was automatically dehydrated and transferred into liquid paraffin. The cassette was temporarily stored in a cryoconsole (60°C) and subsequently poured into a heated metallic pouring mold (60°C). The pouring mold was placed on a cooling plate (-9°C) for 10 min to harden the paraffin block. The paraffin embedded lung was cut into 1-2 µm thick slices using a microtome, transferred onto SuperFrost® microscope slides and dried for 20 min at 60°C. The organ slices were deparaffinized in xylene and rehydrated in a descending alcohol gradient (Table 14).

Table 14: Deparaffinization and rehydration of histologic slices

Step	Reagent	Time	Repetitions
1	Xylene	3 min	3x
2	Ethanol 100 %	2 min	2x
3	Ethanol 96 %	1 min	1x
4	Ethanol 80 %	1 min	1x
5	Ethanol 70 %	1 min	1x
6	H_2O	1 min	1x

Organ slices were stained in hemalum eosin (H&E) using a fully automated glass coverslipper. The stained slices were dehydrated in an ascending alcohol gradient (Table 15) and automatically covered in the glass coverslipper.

Table 15: Dehydration of histologic slices

Step	Reagent	Time	Repetitions
1	Ethanol 70 %	10 s	1x
2	Ethanol 80 %	1 min	1x
3	Ethanol 96 %	1 min	1x

Continued on next page

Step	Reagent	Time	Repetitions
4	Ethanol 100 %	1 min	2x
5	Xylene	2 min	4x

Images of the slides were captured and digitalized using a sample scanner and Aperio ImageScope software (version 12.3.2, Leica Biosystems).

3.2.6 *In vitro* stimulation

MLE-15 cells [135] were cultivated in Dulbecco's Modified Eagle Medium (DMEM) supplemented with 4.5 g/l glucose, 10 % FCS and 1 % penicillin/streptomycin. 3 x 10^5 cells were seeded in 12-well plates and incubated in 1 ml medium over night at 37°C, 5 % CO2. Cells were washed using 1 ml DMEM (4.5 g/l glucose, no additives). Recombinant murine IFN-γ was diluted in DMEM and added to the cells. After 24 h supernatants were removed, RNA was isolated from the cells using the RNeasy® Plus Mini Kit (QIAGEN) according to the manufacturer's instructions and used for cDNA synthesis (3.2.9).

3.2.7 Bead-based immunoassay

Cytokine levels in murine BALF and immunoglobulin levels in human NALF were determined using a LEGENDplex™ Multi-Analyte Flow Assay Kit (BioLegend) according to the manufacturer's instructions with slight modifications: 12.5 µl of assay buffer, standards, beads, detection antibodies and PE conjugated streptavidin were used instead of 25 µl.

3.2.8 Flow cytometric analysis

Flow cytometry was used for leukocyte subset quantification. 100 µl cell suspension from lung, spleen, NALT and BALF were transferred into a 96-well round bottom plate. Cells were washed by addition of 150 µl PBS to each well and plate was spun (5 min, 350 x g, 4°C). Supernatants were

discarded and the plate was briefly vortexed to loosen the cell pellet. For simultaneous viability staining and blocking of Fc receptors, 100 µl eBioscience™ fixable viability dye-Fc-block reagent was added to the cells and incubated in the dark for 30 min, RT. After incubation, reaction was stopped and cell samples were washed by addition of 100 µl FACS buffer per well. Afterwards, 100 µl antibody mix was added (Table 7) and incubated in the dark for 15 min at 4°C. After incubation, 150 µl FACS buffer was added and the cells were washed. The cells were resuspended in 250 µl FACS buffer and flow cytometric analyses were performed. For compensation purposes compensation beads (Table 5) were individually stained with each single fluorescence-labelled antibody and acquired as well. These controls were utilized to calculate a compensation matrix using FlowJo™ software (version 10, BD Biosciences).

3.2.9 cDNA synthesis

1 µg RNA in 11 µl DEPC-treated water was mixed with 0.5 µl Random Primers and 0.5 µl Oligo dT(20) Primers, incubated for 10 min at 70°C and cooled down for 10 min on ice. cDNA synthesis was performed using the SuperScript™ III Reverse Transcriptase Kit (Thermo Fisher Scientific) according to the manufacturer's instructions. Synthetized cDNA was utilized for qRT-PCR (3.2.10).

3.2.10 Quantitative real-time reverse transcription-PCR (qRT-PCR)

qRT-PCR was used to compare the relative gene expression between biological samples. The relative expression of the target gene was determined for every sample and normalized to the relative expression of a gene that is known to be constitutively expressed in all analysed tissues (house-keeping gene). The relative gene expression of the target gene normalized to the house-keeping gene was calculated using the delta Cp method [136]. Forward and reverse primers were each diluted to a final concentration of 10 µmol/l in DEPC-treated water. cDNA samples were diluted 1:4 in DEPC-treated water. For qRT-PCR the components were mixed in a 96-well PCR plate as shown in table 16 and briefly centrifuged. Each sample was analysed in duplicate.

Table 16: Pipetting scheme for qRT-PCR

Component	**Volume [µl]**
DEPC-treated water	4.4
Forward primer (10 µM)	0.8
Reverse primer (10 µM)	0.8
SensiFAST™ SYBR® No-ROX Kit	10
cDNA	4

The PCR temperature program is displayed in table 17. The data analysis was carried out using LightCycler® 480 software (version 1.5, Roche).

Table 17: Temperature profile of conducted qRT-PCR analyses

Step	**Temperature [°C]**	**Time**	**Cycles**
Incubation	95	2 min	
Amplification	95	5 s	40
	60	10 s	
	72	5 s	
Cooling down	40	10 s	

3.2.11 Enzyme-linked immunosorbent assay (ELISA) analysis

Relative levels of murine IgE and IgA (including monomeric IgA, dimeric IgA and SIgA molecules) and human SIgA were measured by ELISA. A 96-well ELISA plate was coated by pipetting 100 µl/well of the respective capture antibody (Table 8) into the plate and incubating over night at 4°C. The wells were washed four times with 200 µl/well wash buffer to remove unbound antibodies and blocked with 200 µl/well assay diluent for 1 h, RT on a plate shaker (180 rpm). After incubation, the

plate was washed again. 100 µl/well sample was added in duplicate (negative control: assay diluent), incubated for 2 h, RT on a plate shaker (180 rpm) and washed again. 100 µl/well of the respective secondary antibody was added (Table 8), incubated for 1 h, RT on a plate shaker (180 rpm) and washed again. 100 µl/well of the respective HRP conjugated detection antibody was added (Table 8), incubated for 30 min, RT on a plate shaker (180 rpm) and washed again. For the assessment of murine IgE this step was skipped as the utilized secondary anti-IgE antibody was conjugated to HRP. TMB substrate set was mixed according to the manufacturer's instructions. 100 µl/well substrate was added and incubated in the dark for 10 min, RT. Enzymatic reaction was stopped by adding 100 µl/well sulfuric acid (2N). The optical density (OD) per well was measured in a plate reader at 450 nm and 570 nm. These values were used to calculate the relative levels of the target substance (equation (2) - (4)).

$$\mathrm{OD}_{\mathrm{corr.}} = \mathrm{OD}_{450} - \mathrm{OD}_{570} \tag{2}$$

$$\overline{OD} = \frac{\mathrm{OD}_{1,\,\mathrm{corr.}} + \mathrm{OD}_{2,\,\mathrm{corr.}}}{2} \tag{3}$$

$$\text{Relative amount of target immunoglobulin} = \overline{OD}_{\mathrm{sample}} - \overline{OD}_{\mathrm{control}} \tag{4}$$

3.2.12 Human specimen collection and processing: nasopharynx and blood analyses

Analysis of respiratory parameters for the characterization of the asthma phenotype and asthma severity (Table 22) were carried out by Dr. med. Nadine Waldburg (Pulmonary Practice, Magdeburg). Blood was obtained from the arm vein using a venipuncture cannula and blood collection tubes with and without EDTA. Blood samples were further profiled by Prof. Dr. Thomas Wex (Medical Laboratory Prof. Schenk/Dr. Ansorge, Magdeburg) to assess selected immunological and allergy-related blood parameters (Table 22). Nasal microbiota was probed using nasal swabs. Swabs were stored in DNA/RNA Shield$^{\mathrm{TM}}$ solution and used for subsequent microbiota analysis (3.2.15).

NAL was performed by instilling 5 ml saline into one nostril and recovered NALF was spun down (10 min, 3.700 x g, 4°C). Supernatants were used for BCA test (3.2.13) and ELISA analysis (3.2.11). Nasal epithelial cell (NEC) biopsies were obtained using a nasal mucosal curette. The cells were counted using a counting chamber and stained in H&E solution for viability analysis. RNA and protein was isolated from the cells using the RNeasy® Plus Mini Kit (QIAGEN) according to the manufacturer's instructions. RNA was used for cDNA synthesis (3.2.9). Protein was resuspended in TPNE buffer, quantified by BCA test (3.2.13) and used for Western Blot analysis (3.2.14).

3.2.13 Protein quantification by BCA test

Protein concentrations in NEC and NALF samples were quantified prior Western Blot and ELISA/bead-based immunoassay analyses, respectively. Quantification was carried out using the Pierce™ BCA Protein Assay Kit (Thermo Fisher Scientific) according to the manufacturer's instructions. The calculation was performed using the software Gen5™ (version 2.04, BioTek).

3.2.14 SDS-PAGE and Western Blot

Protein samples from human NEC biopsies were analysed for pIgR and RPLP0 protein expression by SDS-PAGE (sodium dodecyl sulfate polyacrylamide gel electrophoresis) and subsequent Western Blot. RPLP0 protein expression was used to normalize pIgR protein expression (house-keeping protein).

Gel preparation. The composition of the agarose running gel was as follows (Table 18):

Table 18: Composition of the running gel

Solution	**Volume [ml]**
H_2O	3.3
30 % acrylamide	4.0
1.5 M TRIS	2.5
10 % SDS	0.1
10 % APS	0.1
TEMED	0.004

The liquid running gel was instilled between two sealed glass plates. 1 ml isopropanol was added on top of the gel. After gel polymerization isopropanol was removed and an agarose stacking gel was produced as follows (Table 19):

Table 19: Composition of the stacking gel

Solution	**Volume [ml]**
H_2O	2,7
30 % acrylamide	0,67
1 M TRIS	0,5
10 % SDS	0,04
10 % APS	0,04
TEMED	0,004

The liquid stacking gel was pipetted onto the running gel. A sample comb was inserted and removed after polymerization. The formed pockets in the stacking gel were used to apply the samples later

on. The glass plates containing the gel were inserted into an upright stand and placed in a gel electrophoresis chamber. Stand and chamber were filled with gel running buffer.

Sample preparation and gel electrophoresis. Samples containing 20 µg of protein were mixed at a ratio of 1:2 with 2x SDS buffer and incubated for 5 min at 90°C (denaturation and linearization step). The samples and a protein standard were instilled into the pockets of the stacking gel and a voltage of 80 V was applied. The gel electrophoresis was stopped after 1.5 h.

Western Blot. 10 Filter papers and a Western Blot PVDF transfer membrane were cut out (7 x 9 cm). The membrane was permeabilized in methanol for 5 min and subsequently washed for 5 min in transfer buffer. The filter papers were soaked in transfer buffer for 2 min. The acrylamide gel was removed from the glass plates and the blotting chamber was set up as shown in the following scheme:

Negative pole (top)

↓

5x filter paper

↓

Acrylamide gel

↓

Transfer membrane

↓

5x filter paper

↓

Positive pole (bottom)

An electric current of 220 mA was applied and the transfer was stopped after 2 h.

Antibody staining. The transfer membrane was recovered from the blotting chamber, washed in TBST and transferred into a 50 ml Falcon™ tube. 50 ml 3 % (w/v) BSA in TBST was added and

incubated for 1 h, RT on a roller mixer. Anti-human pIgR primary antibody (diluted 1:200 in 10 ml TBST containing 3 % BSA) was added to the membrane and incubated over night at 4°C on a roller mixer. Afterwards, the antibody solution was discarded, another 10 ml TBST was added and incubated for 15 min, RT on a roller mixer to remove unspecifically bound antibodies from the membrane. This wash step was repeated twice. The respective HRP conjugated detection antibody (diluted in 10 ml TBST containing 3 % (w/v) BSA) was added to the membrane (Table 9). After incubation (1 h, RT, protected from light) on a roller mixer, membrane was washed three times in 10 ml TBST for 15 min.

Development and detection. Working reagent containing peroxide and acridan was prepared using the Pierce™ ECL Plus Western Blotting Substrate Kit (Thermo Fisher Scientific) according to the manufacturer's instructions. 10 ml of this reagent was pipetted onto the membrane and incubated for 5 min (protected from light). Chemiluminescent reaction was detected using an imaging system at the following exposure times [min]: 1, 2, 3, 4, 5 and 6. The visible protein bands were quantified densitometrically using ImageJ software (version 1.8, Wayne Rasband). The same membrane was used to determine RPLP0 protein expression (house-keeping protein) for normalization purposes. To this end, the membrane was washed three times in 10 ml TBST for 15 min. Anti-human RPLP0 primary antibody (diluted 1:2.500 in 10 ml TBST containing 3 % (w/v) BSA) was added to the membrane and incubated over night at 4°C on a roller mixer. The subsequent steps were carried out as described before.

3.2.15 Microbiota analysis

Microbiota analysis was carried out by Dr. Lisa Hönicke and Prof. Till Strowig (HZI, Braunschweig).

Amplification of genomic DNA. Microbial genomic DNA (gDNA) was isolated from nasal swabs using ZymoBIOMICS™ DNA Miniprep Kit (Zymo Research) according to the manufacturer's instructions. 25 ng DNA was used for the amplification of the V4 region (515F/806R) of the 16S rRNA gene via PCR. The 16S rRNA gene is highly conserved. Its variable regions (V4) can be used as a marker for the identification and quantification of microbial families in a biological

sample by determining the abundance of species characteristic sequences and comparing them to respective genomic databases. Forward and reverse primers (515F/806R) were each diluted to a final concentration of 10 µmol/l in PCR-grade water. For the gDNA amplification the components were mixed as shown in table 20.

Table 20: Reaction mix for PCR on 16s rRNA gene

Component	**Volume [µl]**
PCR-grade water	13
Forward primer (10 µM)	0.5
Reverse primer (10 µM)	0.5
5Prime HotMasterMix®	10
gDNA	1

PCR amplification was performed in a thermocycler (see table 21). Each sample was run in triplicates and pooled afterwards. The amplicons were purified using the UltraClean®-htp 96 Well PCR Clean-Up Kit (MO BIO Laboratories) according to the manufacturer's instructions, diluted to a concentration of 10 nmol/l and used for sequencing. During amplification the primers bind specifically to the V4 region of the 16s rRNA gene on the gDNA.

Table 21: Temperature profile for 16S rRNA gene amplification PCR

Step	**Temperature [°C]**	**Time**	**Cycles**
Incubation	94	3 min	
Amplification	94	45 s	35
	50	60 s	
	72	90 s	

Continued on next page

Step	Temperature [°C]	Time	Cycles
	72	10 min	
Cooling down	4	hold	

Sequencing and 16S rRNA analysis. The PCR amplicons were sequenced on an illumina® MiSeq™ PE250 gene sequencing platform using the MiSeq™ Reagent Kit v2 (illumina®) according to the manufacturer's instructions. During the sequencing process the amplicons bound to the oligo-coated bottom of the flow cell via their adapter sequence. The sequencing primers then bound to the amplicons which initiated the complementary attachment of fluorescently tagged nucleotides to the amplicon strand. These fluorochromes were excited by a laser and in turn emitted a characteristic fluorescent signal cluster that depends on the sequence of the amplicon. This signal was detected and used for the classification of the sequences into clusters of operational taxonomic units (OTU). The obtained reads were pooled using -fastq_mergepairs with -fastq_maxdiffs 30. Quality filtering was carried out at a minimum read length of 200 bp with fastq_filter (-fastq_maxee 1). Similar sequences were grouped into OTU clusters by using the UPARSE algorithm [137]. The Silva database v128 [138] and the RDP Classifier [139] were utilized to perform taxonomy assignment of the OTU clusters. The bootstrap confidence cutoff was set to 80 %. Statistical analyses and visualization of data was carried out via the R statistical programming environment package phyloseq (Paul J. McMurdie) [140] based on the OTU absolute abundance table (software: RStudio, version 2021.09.2+382, RStudio PBC).

3.2.16 Statistical analysis

Statistical analyses were performed either by two-tailed, unpaired t-test (Gaussian distribution, two groups), Mann-Whitney test (no Gaussian distribution, two groups), one-way ANOVA (Gaussian distribution, more than two groups, post test: Bonferroni's Multiple Comparison Test) or Kruskal-Wallis test (no Gaussian distribution, more than two groups, post test: Dunn's Multiple Comparison Test) using the software GraphPad Prism (version 5.04, GraphPad Software Inc.).

4 Aims of the study

Active transport of secretory immunoglobulins (SIgs) across the airway epithelial cell (AEC) layer is exclusively mediated by the polymeric immunoglobulin receptor (pIgR). While the importance of SIgs and pIgR for respiratory mucosal immunity is well-acknowledged [37, 40], knowledge regarding their relative abundance and regulation throughout the whole respiratory tract during homeostasis as well as during chronic respiratory disease is still fragmentary. Therefore, the overall aim of this thesis was to elucidate the airway-associated secretory and antimicrobial immunity in response to exogenous and endogenous stimuli in the context of asthma. Specifically, the following aims were to be addressed in frame of this thesis:

Aim 1: Provide detailed insight into the regulation of basal airway-associated secretory immunity *in vivo*.

In order to dissect the impact of intrinsic (sex, age, cytokines) and extrinsic (microbial environment) factors to pIgR-mediated immunity, basal *Pigr* gene expression and IgA abundance in the upper respiratoty tract (URT) and lower respiratory tract (LRT) of mice was to be compared. It was shown that asthma is linked to impaired pulmonary PIGR expression resulting in deteriorated airway mucosal SIg-transport [44, 141] and increased susceptibility to severe pneumococcal infections of the respiratory tract [99, 100]. The upper airways are known to be an entry site and reservoir for respiratory pathogens like *Streptococcus pneumoniae* and a place of allergen sensitization during asthma development [142, 143]. It is unknown whether secretory and antipneumococcal immunity in the URT of asthmatic individuals is impaired as well. Therefore, the second aim of this work was defined as follows:

Aim 2: Investigate the impact of murine allergic asthma on pIgR-mediated airway immunity and pneumococcal colonization.

In order to analyse the impact of asthma on secretory and antipneumococcal immunity, two murine models of allergic asthma had to be established and characterized in depth. Subsequently, *Pigr*

gene expression and IgA abundance as well as pneumococcal colonization of the URT and LRT of asthmatic and non-asthmatic mice were to be assessed. In line with impaired pulmonary PIGR-expression and SIgA levels as well as altered pulmonary microbiota composition [133], the nasal microbiota was previously shown to be distinct between asthmatics and healthy subjects [144]. However, it is still unclear whether this is related to altered regulation of secretory immunity in the upper airways. In this context, the impact of allergy (reactivity to aeroallergens) on secretory immunity in the URT and composition of the nasal microbiota in asthma is generally unknown. Since the human nasopharynx is both a site of allergen sensitization during asthma development as well as an entry site and natural reservoir for respiratory pathogens [142, 143], it is crucial to investigate the impact of allergic and non-allergic asthma on the secretory immunity and the nasal microenvironment in the URT. Hence, the third aim of this work was formulated as follows:

Aim 3: Analyse the influence of human allergic and non-allergic asthma on secretory immunity and microbiota composition in the upper airways.

In order to investigate the impact of human asthma on secretory immunity and microbiota composition in the upper airways, *PIGR* gene expression, PIGR protein expression, SIgA abundance as well as immunoglobulin profile and bacterial abundance in the URT of asthmatic and non-asthmatic individuals were to be assessed.

5 Results

5.1 Part I: Insight into the regulation of basal airway-associated secretory immunity *in vivo*

5.1.1 Analysis of basal *Pigr* gene expression in the murine upper and lower respiratory tract

Nasal epithelial cells (NECs) represent the first line of defense against airborne pathogens. Here, NECs play an important role in antibody-mediated mucosal immunity. Multimeric IgA and IgM are actively transported through NECs by the polymeric immunoglobulin receptor (pIgR). Subsequently, these molecules are released into the mucosal lumen as secretory immunoglobulins (SIgs) [30]. Especially SIgA is known to avert pathogen adhesion, thus preventing microbial infiltration [37]. It is known that *Pigr*-deficiency manifests in susceptibility to mycobacterial respiratory infections [40], development of a COPD-like phenotype caused by an altered lung microbiome and bacterial invasion of the airway epithelium [41]. Furthermore, several human chronic airway diseases are associated with reduced PIGR expression in the bronchial epithelium, which causes increased disease severity (COPD) and deteriorated SIgA-mediated mucosal defense (asthma) [43, 44]. While several studies have already addressed the contribution of pIgR and secretory immunity to airway homeostasis, very little is known about their relative abundance and regulation in the airways.

Therefore, the first part of this thesis focussed on the detailed analysis of *Pigr* expression patterns in the airways. To this end, basal *Pigr* gene expression in different compartments of the upper (URT) and lower respiratory tract (LRT) of the two most commonly used laboratory mouse strains, BALB/c and C57BL/6J, was assessed using quantitative real-time RT-PCR (qPCR). Taking into account a potential impact of sex hormones and age on respiratory *Pigr* expression, analyses were performed using male and female mice of different ages.

BALB/c (Fig. 4a) as well as C57BL/6J (Fig. 4b) mice show highest *Pigr* expression in the trachea, followed by nasal-associated lymphoid tissue (NALT) and lung. Furthermore, comparative analyses of *Pigr* expression patterns in URT and LRT of BALB/c *vs.* C57BL/6J mice (Fig. 4c) and male *vs.* female C57BL/6J mice (Fig. 4d) revealed no significant sex- or strain-specific differences. Moreover, correlation analyses of airway *Pigr* gene expression analyses in mice of different ages

(Fig. 4e-4g) revealed no significant correlation between age and *Pigr* gene expression, neither in the URT nor in the LRT. Altogether, these analyses revealed tissue-specific differences in *Pigr* gene expression in the respiratory tract, which were however independent of genetic background, sex and age.

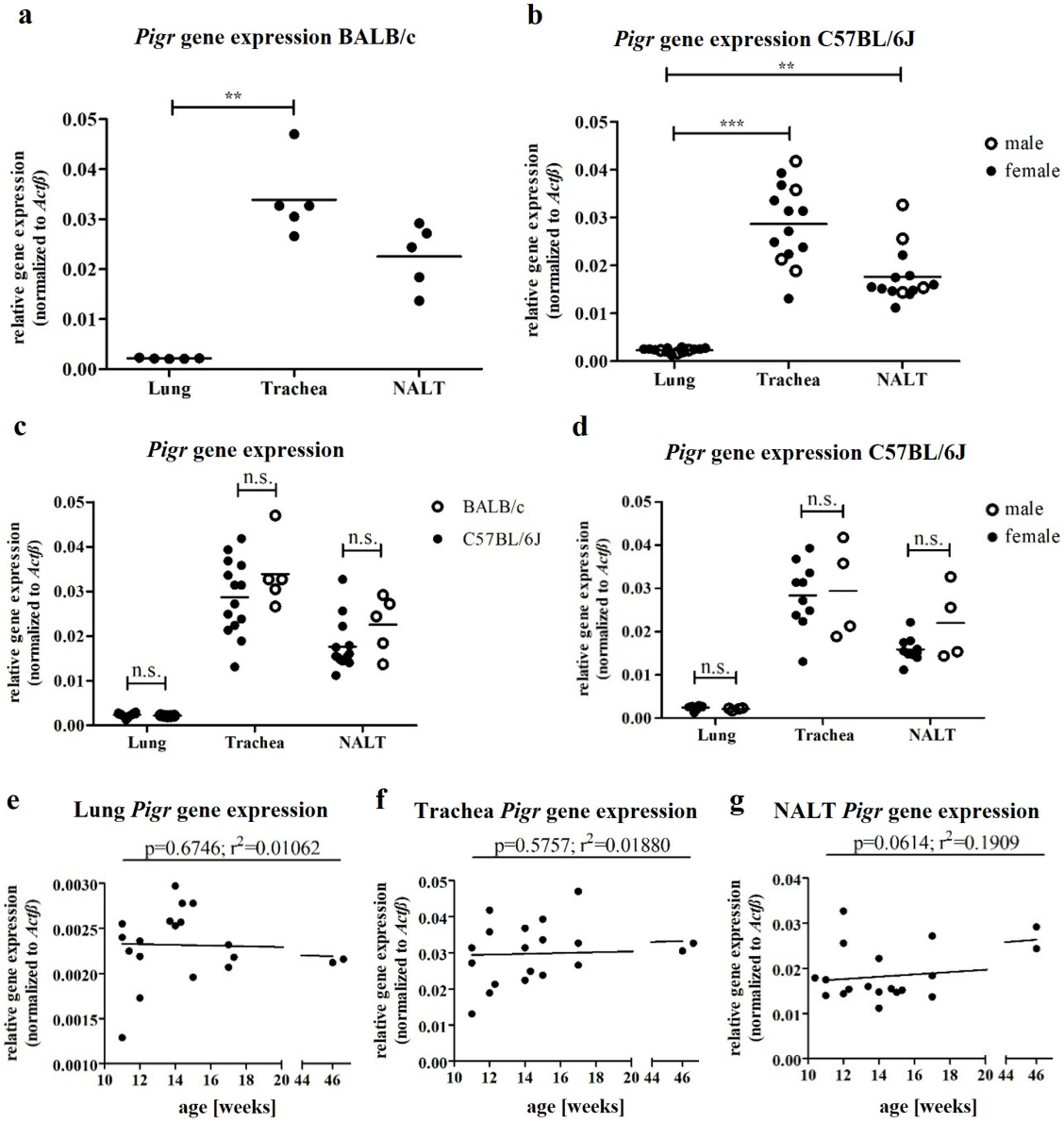

Figure 4: Analyses of basal *Pigr* expression in murine airways. RNA from lung tissue, trachea and nasal-associated lymphoid tissue (NALT) of female BALB/c mice (n=5) and male/female C57BL/6J mice (n=14) was isolated and reversely transcribed into cDNA. *Pigr* expression was assessed by qPCR. *Actb* served as reference gene (cumulative data from two experiments; data for individual mice are graphed; mean is indicated by horizontal line; correlation analysis was performed by linear regression; ** for $p \leq 0.01$; *** for $p \leq 0.001$; n.s.: not significant). Modified figure has already been published [145].

5.1.2 Secretory immunity in differentially colonized mice

It was previously shown that commensal intestinal bacteria induce the production of IgA in mice [146]. Furthermore, the abundance of lymphocytes in nasal mucosa depends on the exposure to microbial stimuli and housing conditions [147]. While those previous findings attest a strong impact of the microbiota on lymphocyte-mediated mucosal immunity in general, the relationship between the microbiota and airway-associated secretory immunity is largely unknown. Thus, in order to examine whether microbiota affect respiratory secretory immunity, *Pigr* expression and IgA levels in the airways of germ-free (GF) mice (no microbial exposure), specific pathogen-free (SPF) mice (IVCs, exposure to a limited microbial flora) and mice with an undefined microbiome (open cage maintenance, highest degree of exposure to airborne microorganisms) were determined using qPCR and ELISA, respectively (Fig. 5).

These comparative analyses revealed similar LRT *Pigr* expression in all three experimental groups, while *Pigr* expression was significantly lower in the NALT of mice with an undefined microbiome compared to SPF mice (Fig. 5a). In contrast to the unaltered (lung, trachea) or decreased (NALT) *Pigr* expression in mice with an undefined microbiome, IgA concentration was significantly elevated in the LRT (Fig. 5b) as well as URT (Fig. 5c) of this group. Interestingly, this finding was associated with an increase in systemic IgA (Fig. 5d).

Taken together, these data suggest that IgA-mediated secretory immunity in the airways is partly dependent on the degree of microbial exposure.

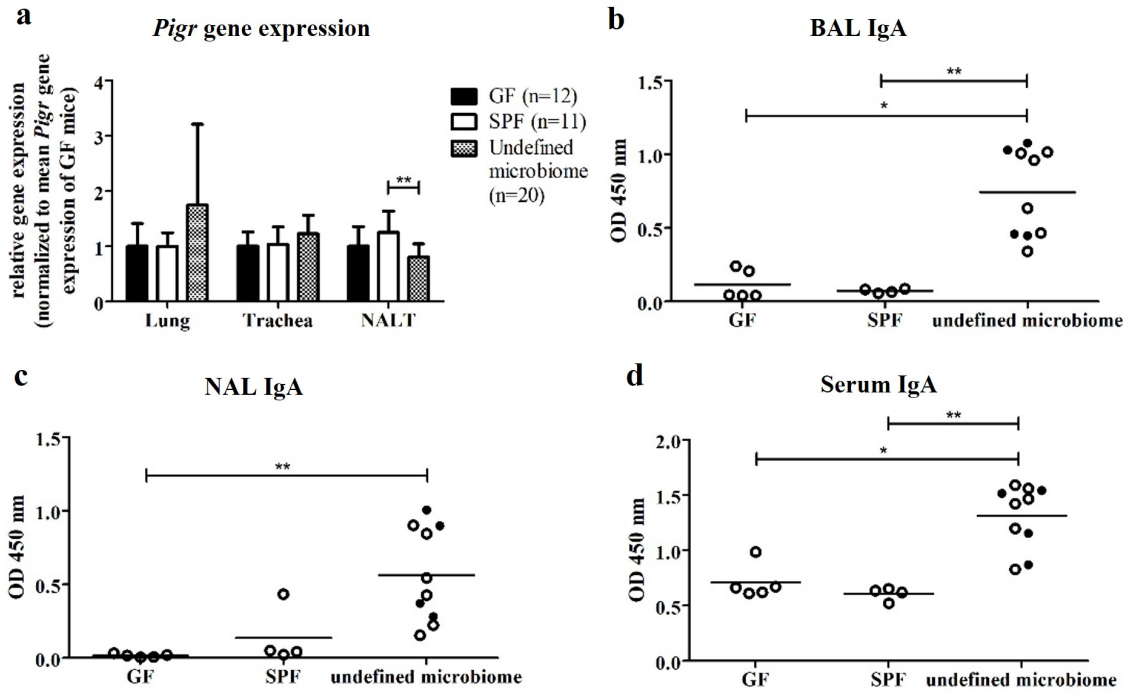

Figure 5: *Pigr* expression and IgA levels in differentially colonized mice. RNA from lung tissue, trachea and NALT of male specific pathogen-free (SPF), male germ-free (GF) and male mice with an undefined microbiome was isolated, reversely transcribed into cDNA and qPCR analysis was performed (● indicates female, ○ indicates male). (a) *Pigr* expression normalized to *Actb*. Normalized gene expression values of each organ were divided by the mean gene expression of the GF mice for the respective organ (mean expression values ± SD are graphed). Relative IgA levels were determined in (b) bronchoalveolar lavage (BAL), (c) nasal lavage (NAL) and (d) serum of GF (n=5), SPF (n=4) and mice with an undefined microbiome (n=10) by semi-quantitative ELISA (cumulative data from two experiments; data for individual mice are graphed; mean is indicated by horizontal line; * for $p \leq 0.05$; ** for $p \leq 0.01$). Modified figure has already been published [145].

5.1.3 Modulation of secretory immunity by LPS treatment

In line with previous experimental evidence, which attests a clear impact of microbial components on intestinal IgA production and *Pigr* expression [46, 146, 148], the results obtained in this study suggest that respiratory secretory immunity is similarly dependent on the presence of microbial components. It is however unclear, whether secretory immunity in the airways is boosted by the respiratory microbiota or solely dependent on the gut microbiome. In order to experimentally address this question, a LPS-based murine *in vivo* model, which mimics nasal bacterial stimulation, was employed. LPS is a TLR4 agonist and a highly abundant antigen on the surface of Gram-negative bacteria [149–151]. Moreover, previous studies revealed that human and murine intestinal epithelial cells exhibit increased *Pigr*/*PIGR* gene expression after LPS stimulation *in vitro* [45, 46, 152].

Mice were i.n. treated with LPS and 48 h later *Pigr* gene expression in URT (NALT) and LRT (trachea, lung tissue) was assessed by qPCR. Moreover, airway as well as systemic IgA levels were assessed by semi-quantitative ELISA (Fig. 6). These analyses revealed that *Pigr* expression in trachea and NALT was unaffected by LPS treatment (Fig. 6a). In the lung tissue however, LPS led to a significant, 2-fold increase of *Pigr* expression 48 h after treatment. Interestingly, and in discordance with the increased *Pigr* expression in lung, IgA levels in BAL and NAL fluid were significantly reduced in response to LPS treatment (Fig. 6b, 6c). In contrast to its effect on local (airway) mucosal IgA levels, systemic IgA levels (serum) were however unaffected (Fig. 6d) by LPS treatment.

It was shown that LPS induces intestinal epithelial barrier dysfunction *in vitro* [153]. Therefore, it is thinkable that LPS treatment caused alterations regarding the barrier function of NECs as well, resulting in epithelial leakage and dilution of the IgA signal. In order to test this hypothesis, expression of Claudins, *i.e.* epithelial molecules which are vital for tight-junction mediated cell-cell-contact, in lung and NALT was analysed by qPCR at 48 h post LPS treatment. As *Cldn18* expression is associated with altered epithelial barrier function in the lower respiratory tract and altered *Cldn7* expression affects epithelial barrier function in the upper respiratory tract [11, 12], these genes were chosen as candidates for gene expression analyses. However, no significant differences in *Cldn* gene expression, neither in lung nor NALT, could be observed upon LPS treatment (Fig. 6e, 6f).

These data suggest that TLR4 stimulation by bacterial ligands modulates airway *Pigr* expression

in a compartment-specific manner. However, the presence of LPS temporarily inhibits the IgA response in the respiratory mucosa. In contrast to the original hypothesis, LPS does not boost mucosal IgA immunity in the respiratory tract.

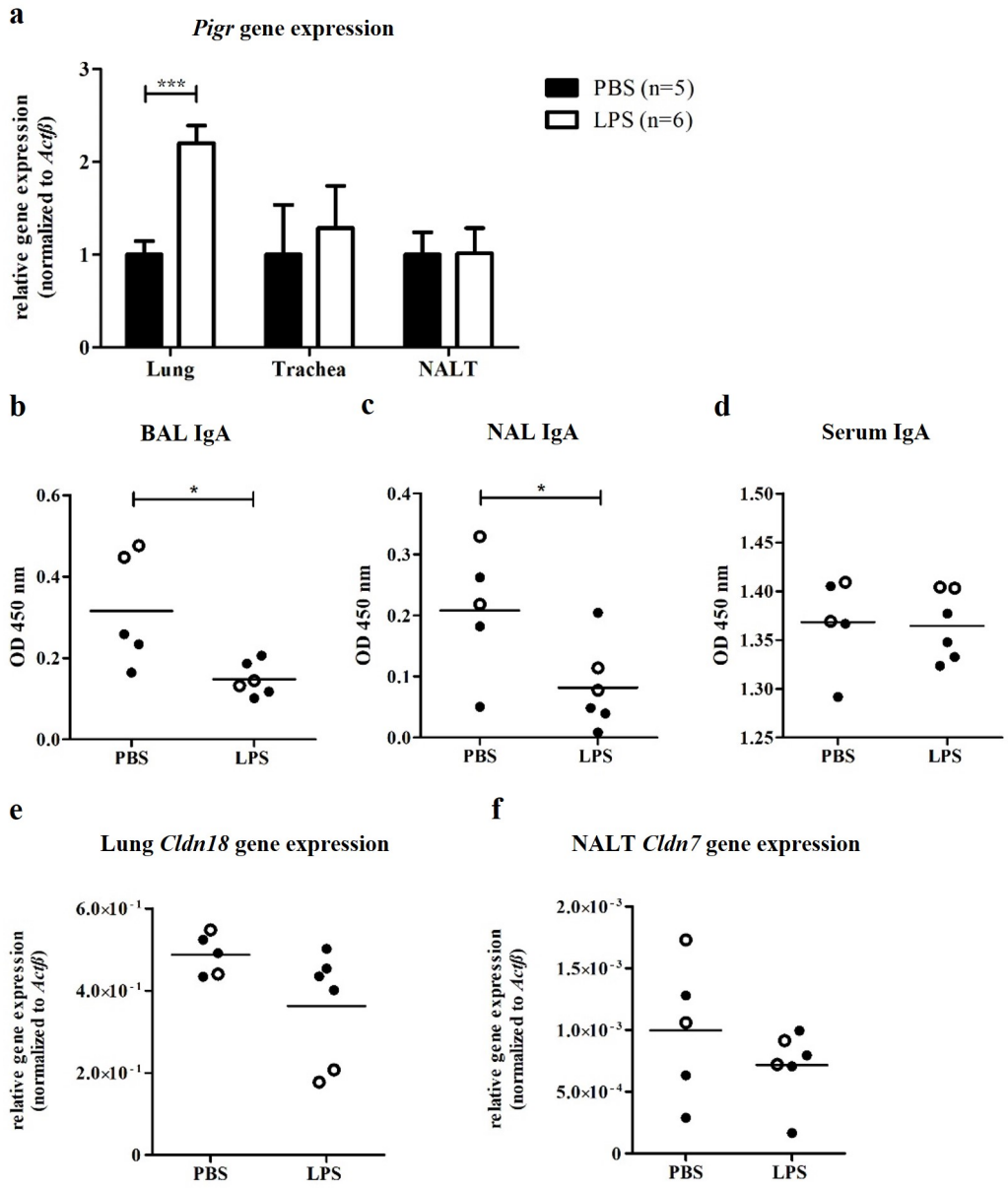

Figure 6: Effect of LPS treatment on airway secretory immunity and epithelial barrier function. Male and female BALB/c mice were treated i.n. with 10 µg of LPS (n=6) or solvent alone (n=5). 48 h post treatment RNA from lung tissue, trachea and NALT was isolated, reversely transcribed into cDNA and qPCR analysis was performed (• indicates female, ○ indicates male). (a) *Pigr* expression normalized to *Actb*. Normalized *Pigr* expression values of each organ were divided by the mean *Pigr* expression of the PBS-treated mice for the respective organ (mean expression values ± SD are graphed). IgA levels were determined in (b) BAL, (c) NAL and (d) serum by semi-quantitative ELISA. (e) *Cldn18* expression normalized to *Actb* and (f) *Cldn7* expression normalized to *Actb* (cumulative data from two experiments; data for individual mice are graphed; mean is indicated by horizontal line; * for $p \leq 0.05$; *** for $p \leq 0.001$). Modified figure has already been published [145].

5.1.4 Modulation of secretory immunity by IFN-γ treatment

Next to LPS, Interferon-γ (IFN-γ) was previously shown to induce human *PIGR* gene expression in a colon adenocarcinoma cell line (HT-29.74) [51]. In order to test whether this proinflammatory cytokine might also boost pIgR-mediated secretory immunity in the airways, a proof-of-concept *in vitro* study was initially conducted. Here, murine lung epithelial (MLE-15) cells were treated for 24 h with ascending concentrations of recombinant murine IFN-γ and *Pigr* gene expression was subsequently assessed (Fig. 7).

Well in line with its *PIGR*-inducing effect on intestinal epithelial cells [51], IFN-γ also induced a significant, dose-dependent increase in *Pigr* expression in murine respiratory epithelial cells. Based on the finding of the *Pigr*-inducing potential of IFN-γ *in vitro*, this cytokine was subsequently chosen for more detailed *in vivo* analyses aiming at elucidating the modulation of *Pigr* and airway-associated secretory immunity.

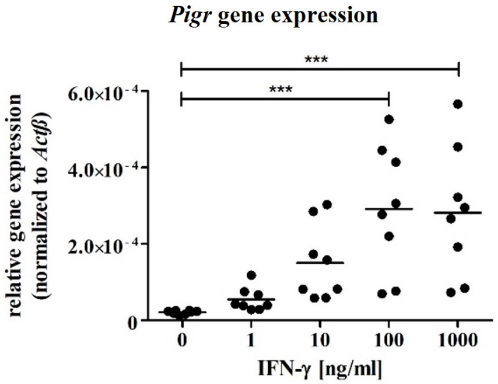

Figure 7: *Pigr* expression in MLE-15 cells upon IFN-γ treatment. Murine lung epithelial (MLE-15) cells (n=8 wells/experimental group) were treated with 1, 10, 100 or 1000 ng of IFN-γ in 1 ml medium or medium alone for 24 h. RNA was isolated and reversely transcribed into cDNA. *Pigr* expression was assessed by qPCR analysis. *Actb* was used as reference gene (cumulative data from two experiments; data for individual cell culture wells are graphed and mean is indicated by horizontal line; *** for $p \leq 0.001$). Modified figure has already been published [145].

In these *in vivo* analyses, mice were i.n. treated with 1 µg of recombinant IFN-γ and *Pigr* gene expression, IgA levels and *Cldn* gene expression in the airways were assessed on day 1 and day 2 post treatment (Fig. 8) by qPCR and ELISA, respectively.

While treatment with IFN-γ did neither affect *Pigr* expression in the URT nor in the LRT after 48 h (Fig. 8a), pulmonary mucosal IgA levels were significantly increased 48 h after IFN-γ treatment (Fig. 8b). This was however not associated with altered IgA levels in NAL or serum (Fig. 8c, 8d), indicating compartment-specific effects of IFN-γ treatment. In order to test whether altered *Cldn* gene expression might underlie altered pulmonary IgA levels, expression of *Cldn18* was analysed by qPCR. Moreover, *Cldn7* expression was examined in NALT. *Cldn* gene expression was however unaffected by IFN-γ treatment (Fig. 8e, 8f), indicating that the increase in pulmonary IgA was not the results of decreased tight-junction function and thus increased epithelial leakage. It was shown that IFN-γ plays an important role in the modulation of B cell proliferation *in vitro* [154]. To test whether IgA increase in lung might be caused by Ig-producing B cells which were induced by IFN-γ, gene expression of the joining chain (IgJ) of multimeric IgA and IgM was determined in lung and NALT. *IgJ* expression was unaffected by IFN-γ treatment (Fig. 8g, 8h), indicating that IgA increase in the airways was most likely not caused by IFN-γ-mediated activation of Ig-producing cells.

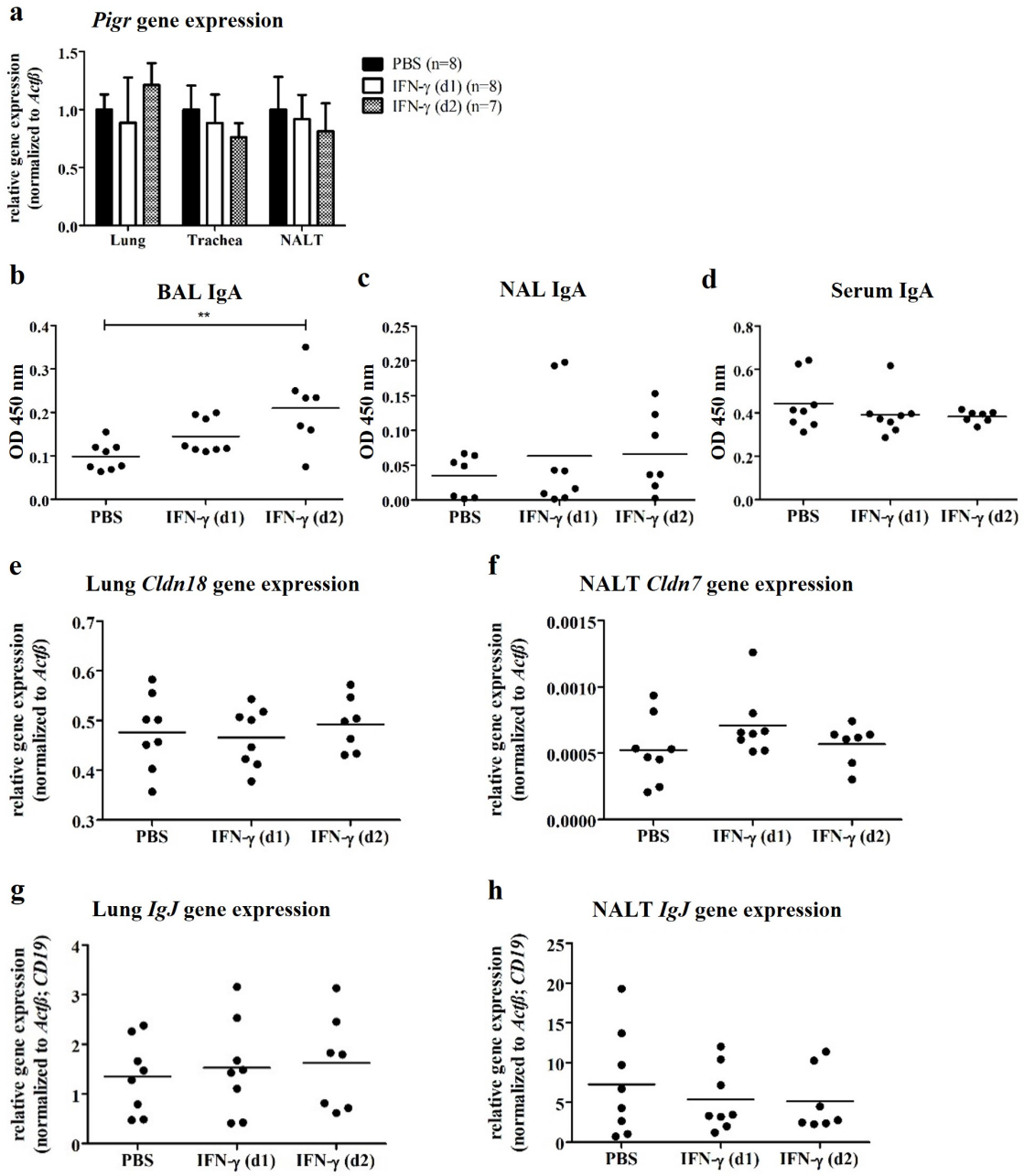

Figure 8: Effect of IFN-γ treatment on secretory immunity, epithelial barrier function and B cells. Female BALB/c and C57BL/6J mice were treated i.n. with 1 µg of IFN-γ (n=8 for d1, n=7 for d2) or solvent alone (n=8). Lung, trachea and NALT were removed on day 1 or day 2 post treatment, RNA was isolated, reversely transcribed into cDNA and qPCR analysis was performed. (a) *Pigr* expression normalized to *Actb*. Normalized *Pigr* expression values of each organ were divided by the mean *Pigr* expression of the PBS-treated group for the respective organ (mean expression values ± SD are graphed). IgA levels were determined in (b) BAL, (c) NAL and (d) serum by semi-quantitative ELISA. (e) *Cldn18* expression normalized to *Actb*, (f) *Cldn7* expression normalized to *Actb* and (g) + (h) *IgJ* gene expression normalized to *Actb* and *CD19* (cumulative data from two experiments; data for individual mice are graphed; mean is indicated by horizontal line; ** for $p \leq 0.01$). Modified figure has already been published [145].

5.1.5 Effect of IFN-γ treatment on immune cell influx in the respiratory tract

The increased pulmonary IgA levels observed upon IFN-γ treatment (Fig. 8b) were neither due to epithelial leakage (Fig. 8e, 8f) nor to increased activity of Ig-producing cells (Fig. 8g, 8h). Since intradermal IFN-γ injection stimulates intradermal lymphocyte migration in rats [155], it was next investigated whether i.n. IFN-γ treatment causes the influx of immune cells that do not express *Pigr* or *IgJ*, thereby leading to a dilution effect that would diminish the overall *Pigr* or *IgJ* signal in the respiratory tract. To analyse whether IFN-γ leads to an increased immune cell influx or alters the numbers of Ig producing B cells, mice were i.n. treated with 1 µg of recombinant IFN-γ and leukocyte subsets from lung and NALT were quantified by flow cytometric analysis (Fig. 9).
These analyses revealed a slight, yet non-significant increase of B cells, CD4+ T cells and CD8+ T cells upon IFN-γ treatment in NALT (Fig. 9b, 9d, 9f). The abundance of these subsets was unaffected in lung (Fig. 9a, 9c, 9e). Number of macrophages, neutrophils, DCs or eosinophils was unaltered in response to IFN-γ stimulation in lung and NALT (Fig. 9g-9n). These results indicate that the *Pigr* and *IgJ* signals were most likely not diluted by IFN-γ induced influx of immune cells. Moreover, the data suggest that the increased IgA levels in BAL of IFN-γ-treated mice are probably not due to increased numbers of Ig producing B cells.

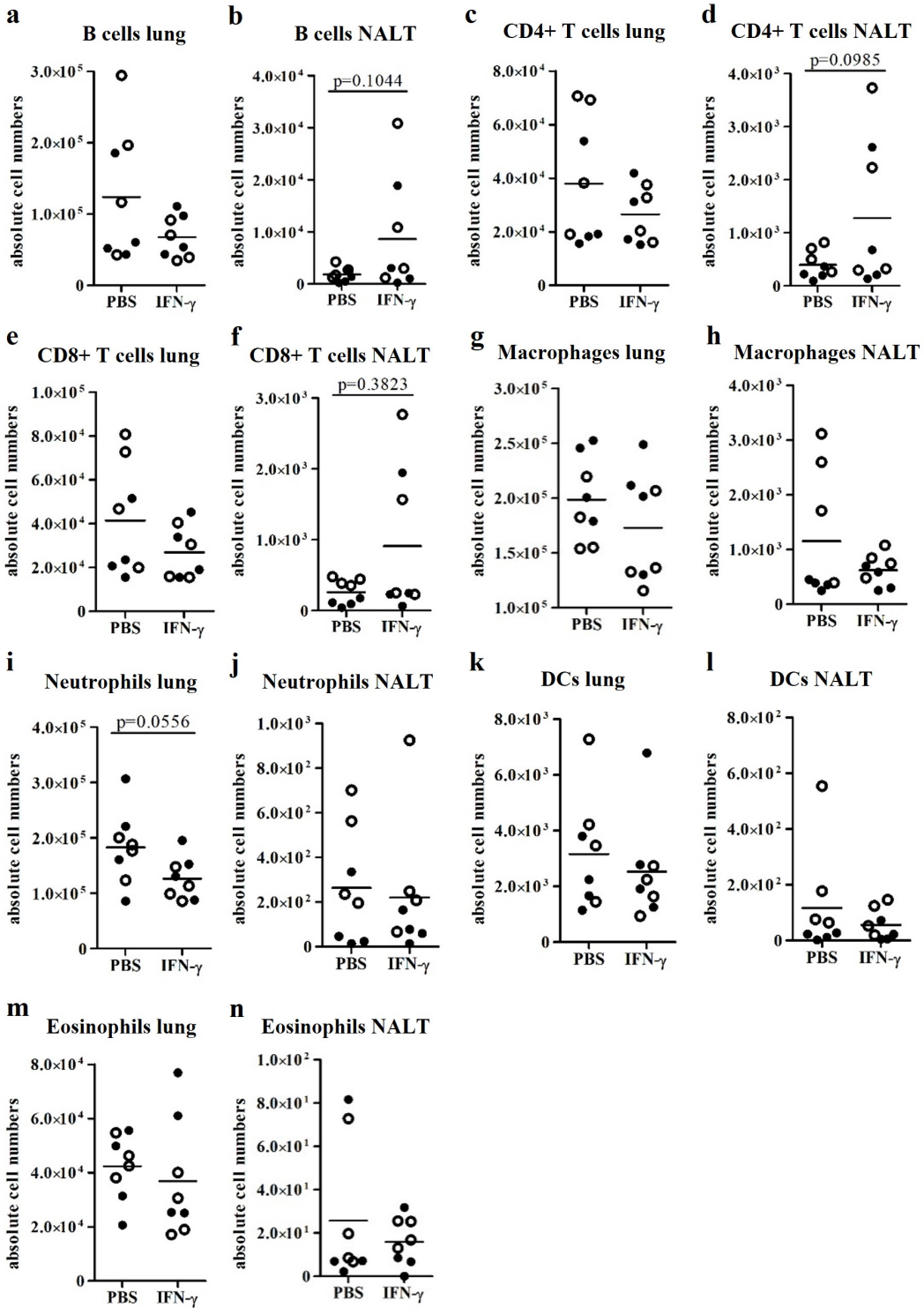

Figure 9: Effect of IFN-γ treatment on secretory immunity, epithelial barrier function and B cells. Female C57BL/6JRj mice were treated i.n. with 1 µg of IFN-γ (n=8) or solvent alone (n=8). Lung and NALT were removed 24 h post treatment, immune cells were isolated and flow cytometric analysis was performed. Absolute cell numbers of (a) + (b) B cells, (c) + (d) CD4+ T cells, (e) + (f) CD8+ T cells, (g) + (h) macrophages, (i) + (j) neutrophils, (k) + (l) dendritic cells (DCs) and (m) + (n) eosinophils were determined in lung and NALT (cumulative data from two experiments represented by • or ○; data for individual mice are graphed; mean is indicated by horizontal line).

Taken together, this first part of the thesis demonstrates that site-specific differences regarding basal *Pigr* gene expression are depending on microbial colonization as well as on yet unknown intrinsic effects. Moreover, secretory immunity in the URT and LRT can be partly modulated by exogenous (microbial-derived) as well as endogenous (host-derived) stimuli.

5.2 Part II: Impact of murine allergic asthma on pIgR-mediated airway immunity and pneumococcal colonization

5.2.1 Establishment & characterization of murine, house dust mite (HDM)-mediated allergic asthma models

While the first part of this thesis provided detailed insight into the regulation of *Pigr* expression and secretory immunity throughout the entire respiratory tract, the second part of this work focusses on elucidating the impact of allergic asthma on pIgR-mediated secretory antibacterial immunity. Chronic respiratory diseases including asthma are associated with differential *PIGR* expression resulting in altered airway mucosal SIg-transport in mice and humans [44,156,157]. It is also known that *Pigr* knockout mice showed an increased susceptibility to airway mycobacterial infections [40]. In this context, it was previously shown that asthma is associated with decreased pIgR abundance in the LRT and case-control studies identified asthma as a risk factor for severe pneumococcal disease [99,100].

In order to investigate the impact of allergic asthma on airway-associated secretory antibacterial immunity, two previously reported murine models [158,159] of house dust mite (HDM)-mediated allergic asthma (Fig. 10) were established in our laboratory and characterized in detail in frame of this study. HDM derived enzymes (*e.g. Der p1*) are naturally occurring asthma allergens in humans [59,60]. Due to its relevant roles in allergy and asthma pathogenesis, the use of HDM extract as a model allergen generally allows to mimic important features of human allergic asthma in murine *in vivo* models.

As visualized in figure 10, for model 1 mice were treated i.n. with 20 µg HDM extract in 30 µl PBS or PBS alone (control group) three times a week over the course of 5 weeks (low-dose, long-term treatment, fig. 10a). For model 2 100 µg HDM extract in 50 µl PBS or PBS alone (control group) was intranasally administered three times at intervals of 1 week (high-dose, mid-term treatment, fig. 10b). On day 3 and day 7 after the last treatment, all mice were sacrificed and analysed for immunological, histopathological and lung functional parameters in order to obtain detailed information about individual pathologic features of the asthmatic phenotype. Typical markers of allergic asthma are an increased abundance of eosinophils in the lower respiratory tract [160], goblet

cell hyperplasia in the lung [161, 162] and increased systemic IgE levels [163]. These key features were analysed initially (Fig. 11, 12).

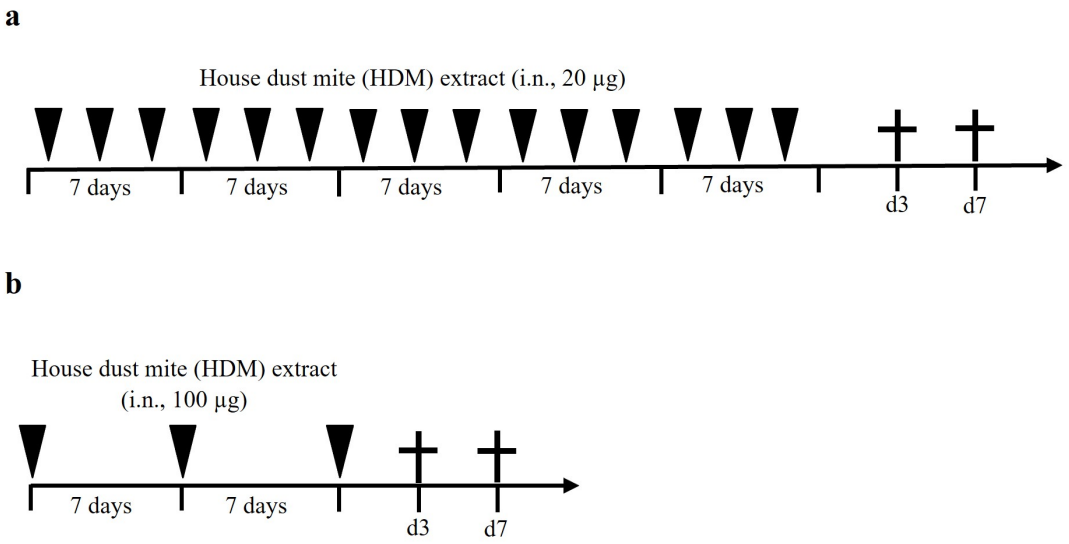

Figure 10: Schematic representation of HDM-induced murine asthma models. (a) Model 1: 20 µg HDM extract in 30 µl PBS or PBS alone (control group) was i.n. administered three times a week over the course of 5 weeks. (b) Model 2: 100 µg HDM extract in 50 µl PBS or PBS alone (control group) was i.n. administered three times at intervals of 1 week. Mice were sacrificed on day 3 and day 7 after the last treatment (black arrows indicate timepoint of i.n. HDM application; black crosses indicate timepoint of sacrifice).

Leukocyte subsets were quantified in lung, BAL and spleen by flow cytometric analysis. In both models HDM treatment led to significantly increased numbers of eosinophils on day 3 and day 7 post treatment in lung tissue (Fig. 11a, 12a) and airways (Fig. 11b, 12b). In model 1, eosinophil numbers in lung were 25 times higher in HDM treated mice compared to the control group on day 3 post treatment (PBS: $6.43x10^4 \pm 1.7x10^4$; HDM: $1.61x10^6 \pm 6.38x10^5$) and 13 times higher on day 7 (PBS: $2.7x10^4 \pm 4.8x10^3$; HDM: $3.5x10^5 \pm 1.36x10^5$). Eosinophil numbers in BAL were increased 44-fold upon HDM treatment on day 3 (PBS: $9.64x10^2 \pm 6.5x10^2$; HDM: $4.28x10^4 \pm 2.7x10^4$) and 360-fold on day 7 (PBS: $3.97x10^1 \pm 1.62x10^1$; HDM: $1.42x10^4 \pm 5.59x10^3$). In model 2, eosinophil numbers in lung were 50 times higher in HDM treated mice compared to the control group on day 3 (PBS: $6.27x10^4 \pm 1.8x10^4$; HDM: $3.23x10^6 \pm 4.47x10^5$) and 16 times higher on day 7 (PBS: $9.6x10^4 \pm 3.3x10^4$; HDM: $1.55x10^6 \pm 4.28x10^5$). Eosinophils in BAL were increased 68-fold upon HDM treatment on day 3 (PBS: $6.4x10^3 \pm 5.8x10^3$; HDM: $4.38x10^5 \pm 1.95x10^5$) and

15-fold on day 7 (PBS: $7.98x10^3 \pm 7.07x10^3$; HDM: $1.25x10^5 \pm 2.89x10^4$). Eosinophil numbers in spleen were unaffected (Fig. 11c, 12c). Well in line with these findings, histopathological analyses (performed on day 7 post last treatment) revealed increased eosinophil influx into the lung tissue as well as goblet cell hyperplasia exclusively in HDM treated mice (Fig. 11d, 11e, 12d, 12e) in both models. Moreover, HDM treatment caused increased systemic IgE levels on day 3 and day 7 post treatment in both models (Fig. 11f, 12f). The difference was however slightly more significant in model 2 when comparing the results at the early timepoint.

In summary, these initial experiments revealed that murine asthma, induced by applying two different treatment strategies, recapitulates hallmark histopathological and immunological features of human allergic asthma.

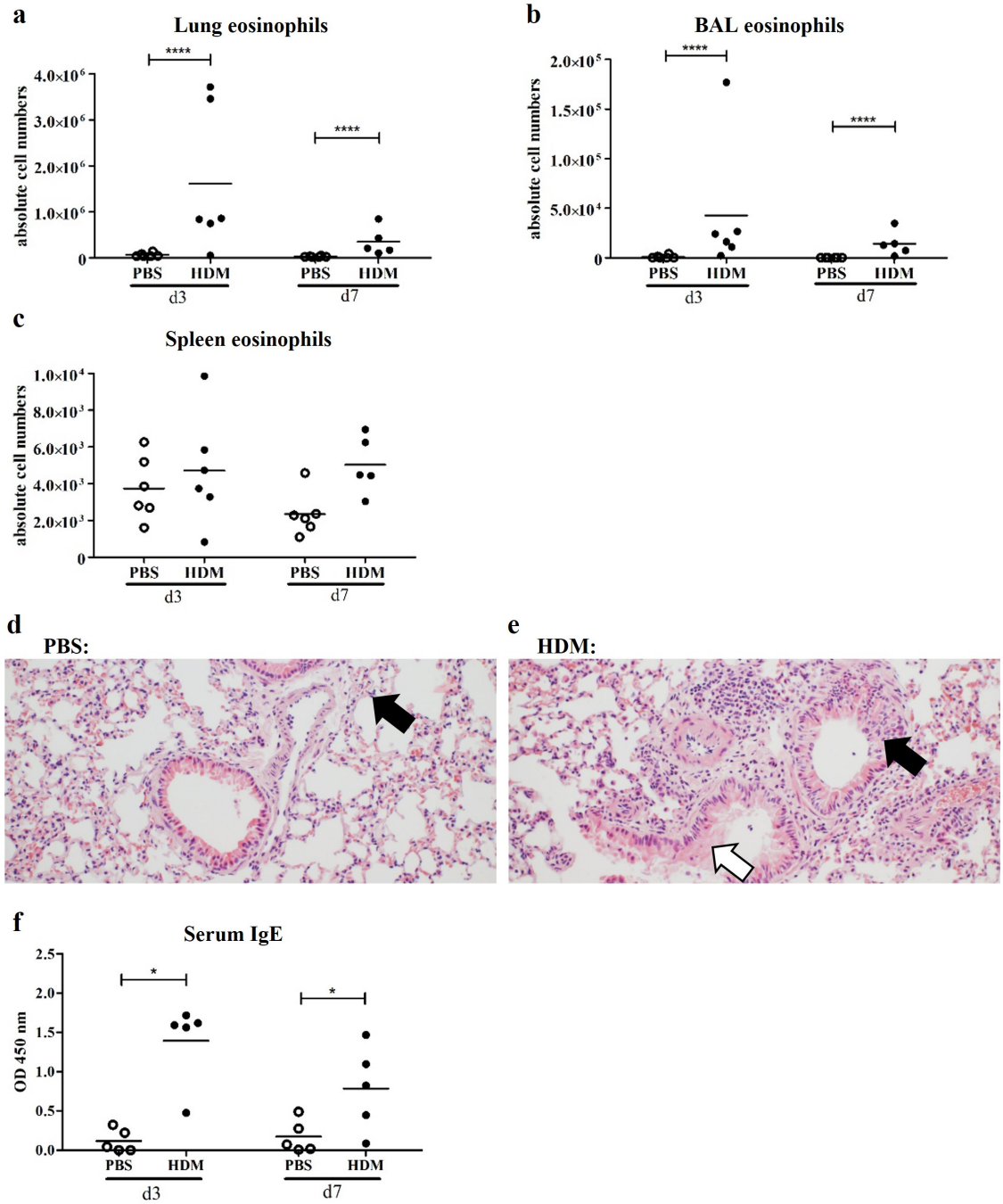

Figure 11: Eosinophil influx, histopathology and IgE levels during murine allergic asthma (model 1). Female C57BL/6JRj mice were treated i.n. with PBS (n=12) or HDM (n=11) according to scheme in Fig. 10a. On day 3 and day 7 after the last treatment, immune cells were isolated from (a) lung, (b) BAL and (c) spleen and absolute eosinophil numbers were determined by flow cytometric analysis. Histopathological analysis of lungs slices from (d) PBS and (e) HDM treated mice were performed by H&E staining. Black arrow indicates eosinophils, white arrow indicates goblet cell hyperplasia. Magnification: 200x. Scale bar: 50 µm. (f) IgE levels were determined in serum on day 3 and day 7 after the last treatment by semi-quantitative ELISA (cumulative data from two experiments; data for individual mice are graphed; mean is indicated by horizontal line; * for $p \leq 0.05$; **** for $p \leq 0.0001$). Histopathologic analyses were carried out by Dr. Olivia Kershaw (Institute of Veterinary Pathology, Free University of Berlin).

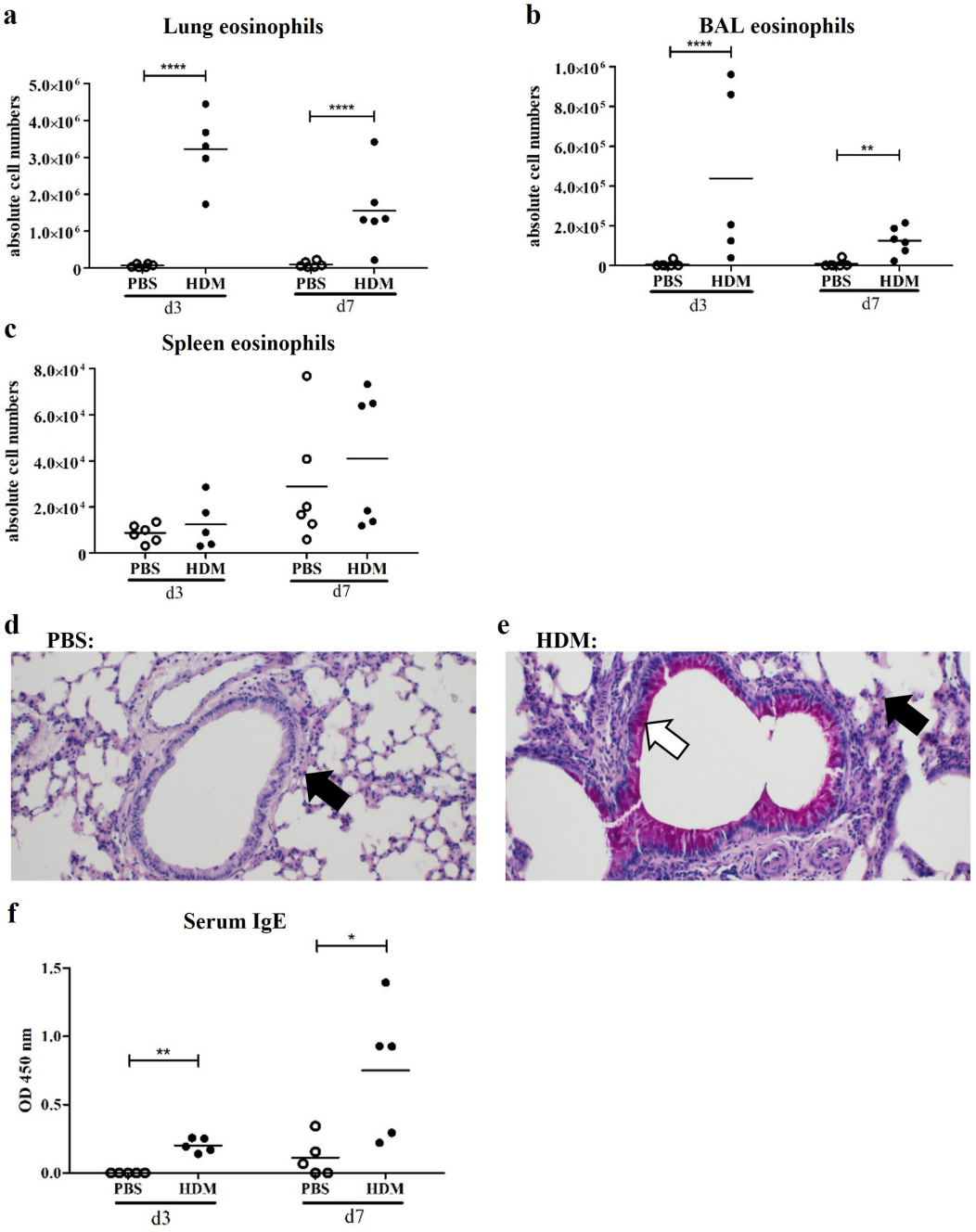

Figure 12: Eosinophil influx, histopathology and IgE levels during murine allergic asthma (model 2). Female C57BL/6JRj mice were treated i.n. with PBS (n=12) or HDM (n=11) according to scheme in Fig. 10b. On day 3 and day 7 after the last treatment, immune cells were isolated from (a) lung, (b) BAL and (c) spleen and absolute eosinophil numbers were determined by flow cytometric analysis. Histopathological analysis of lungs slices from (d) PBS and (e) HDM treated mice were performed by H&E staining. Black arrow indicates eosinophils, white arrow indicates goblet cell hyperplasia. Magnification: 200x. Scale bar: 50 µm. (f) IgE levels were determined in serum on day 3 and day 7 after the last treatment by semi-quantitative ELISA (cumulative data from two experiments; data for individual mice are graphed; mean is indicated by horizontal line; * for $p \leq 0.05$; ** for $p \leq 0.01$; **** for $p \leq 0.0001$). Histopathologic analyses were carried out by Dr. Olivia Kershaw (Institute of Veterinary Pathology, Free University of Berlin).

Next to goblet cell hyperplasia and pulmonary eosinophilia, human allergic asthma is characterized by increased abundance of several proinflammatory mediators (*e.g.* cytokines) in the airways. It is known that the cytokines IL-4 and IL-5 are crucial for the migration and activation of eosinophils during asthma sensitization [164, 165]. Moreover, IL-10, IL-13 and IL-17A play an important role regarding the induction of airway hyperreactivity and allergic inflammation [83, 84]. In addition, IL-6 in induced sputum and TNF-α in serum of allergic asthmatics were shown to be elevated [166, 167].

In order to further characterize the lung inflammatory micromilieu during experimental murine allergic asthma, cytokine levels (IL-2, 4, 5, 6, 9, 10, 13, 17A, 17F, 21, 22, IFN-γ, TNF-α) in BAL fluid were determined on day 3 and day 7 post last treatment by bead-based immunoassay. Interestingly – and in stark contrast to the profound cellular (lung pathology and eosinophil infiltrations) and molecular (increased serum IgE levels) allergic manifestations – none of the measured cytokines was significantly increased upon HDM treatment neither on day 3 nor day 7 post treatment in model 1. Furthermore, in many of the samples the measured cytokine levels were below the limit of detection (LOD). This was the case for every single cytokine (Fig. 13a-13m). In stark contrast to the unaltered cytokine microenvironment present in asthma model 1, HDM-extract treatment led to a significant increase in several proinflammatory cytokines in the airways in model 2. Here, IL-4 (PBS: 0.36 ± 0.13, HDM: 10.04 ± 1.92, 28-fold increase), IL-5 (PBS: 1.19 ± 0.09, HDM: 9.89 ± 2.73, 8-fold), IL-6 (PBS: 1.3 ± 0.82, HDM: 117.8 ± 10.96, 90-fold), IFN-γ (PBS: 0.58 ± 0.07, HDM: 1.86 ± 0.5, 3-fold), TNF-α (PBS: 3.33 ± 0.49, HDM: 7.52 ± 0.63, 2-fold) and IL-17A (PBS: 1.75 ± 0.23, HDM: 4.65 ± 0.84, 3-fold) levels in BAL fluid were increased on day 3 post HDM treatment. Interestingly, the increase in prototype cytokines of type 1 (IFN-γ, TNF-α), type 2 (IL-4, IL-5, IL-6) and type 3 (IL-17A) immunity suggests pleiotropic contributions of these mediators to the observed asthma phenotype. While the increase of these inflammatory mediators was ceased already 7 days post HDM-extract treatment, IL-17A was also slightly increased in HDM treated mice at this time. Moreover, TNF-α levels were slightly increased in the control group compared to the HDM group on day 7 post treatment. Again, the measured cytokine levels were below the limit of detection in many of the samples (especially those of the control group). The only cytokines that were detectable in every sample were IL-10 and IL-17A (Fig. 14a-14m).

Altogether, these results indicate that – despite its overt effects on pulmonary cellular characteristics

– model 1 has no measurable effect on inflammatory cytokine levels, while model 2 is associated with a proinflammatory, mixed type 1/2/3 immune response in the airways and thus recapitulates important aspects of human allergic asthma.

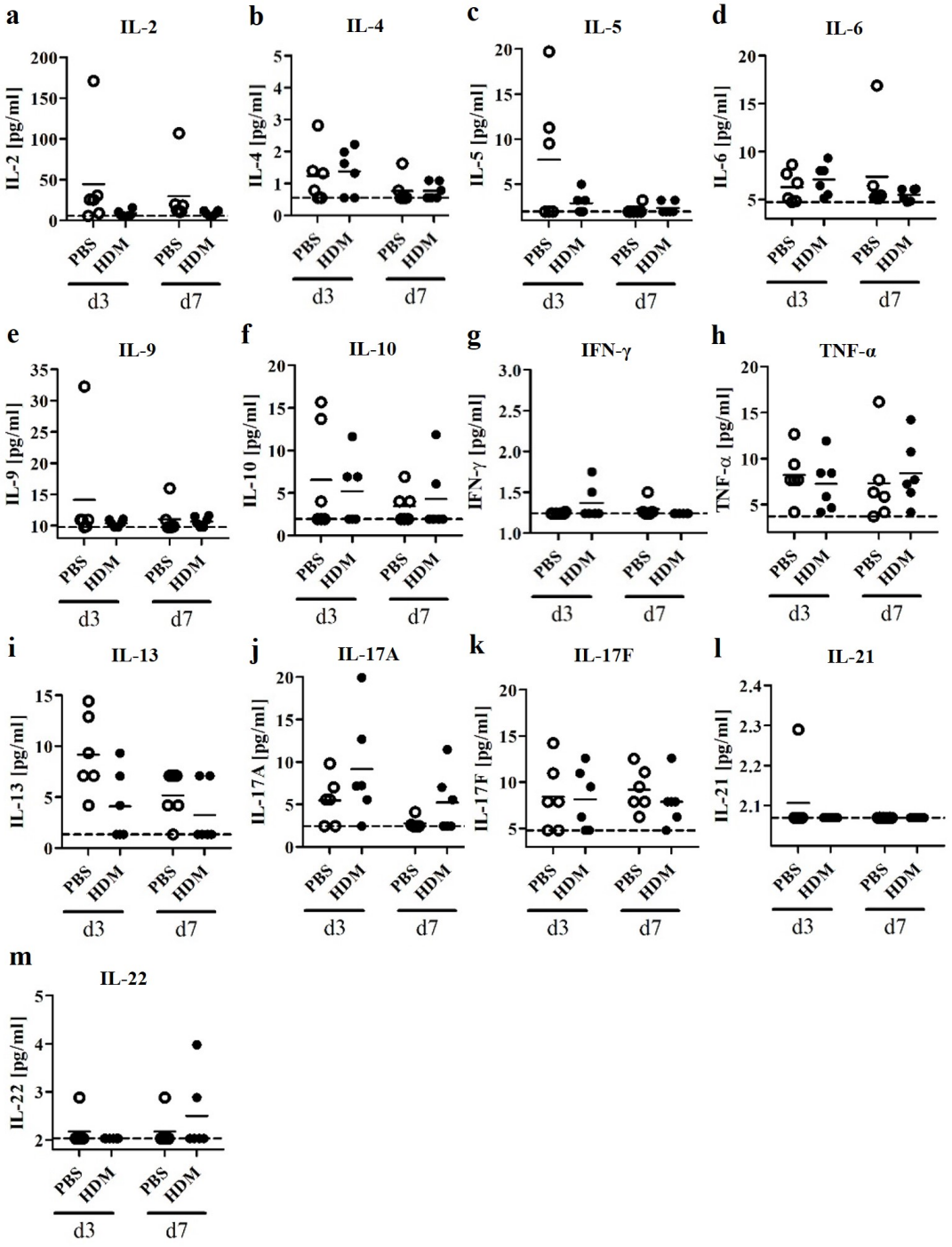

Figure 13: Airway cytokine profile during murine allergic asthma (model 1). Female C57BL/6JRj mice were treated i.n. with PBS (n=12) or HDM (n=12) according to scheme in Fig. 10a. Absolute levels of (a) IL-2, (b) IL-4, (c) IL-5, (d) IL-6, (e) IL-9, (f) IL-10, (g) IFN-γ, (h) TNF-α, (i) IL-13, (j) IL-17A, (k) IL-17F, (l) IL-21 and (m) IL-22 were determined in BAL on day 3 and day 7 after the last treatment by bead-based immunoassay (cumulative data from two experiments; data for individual mice are graphed; mean is indicated by horizontal line; detection limit is indicated by dashed line).

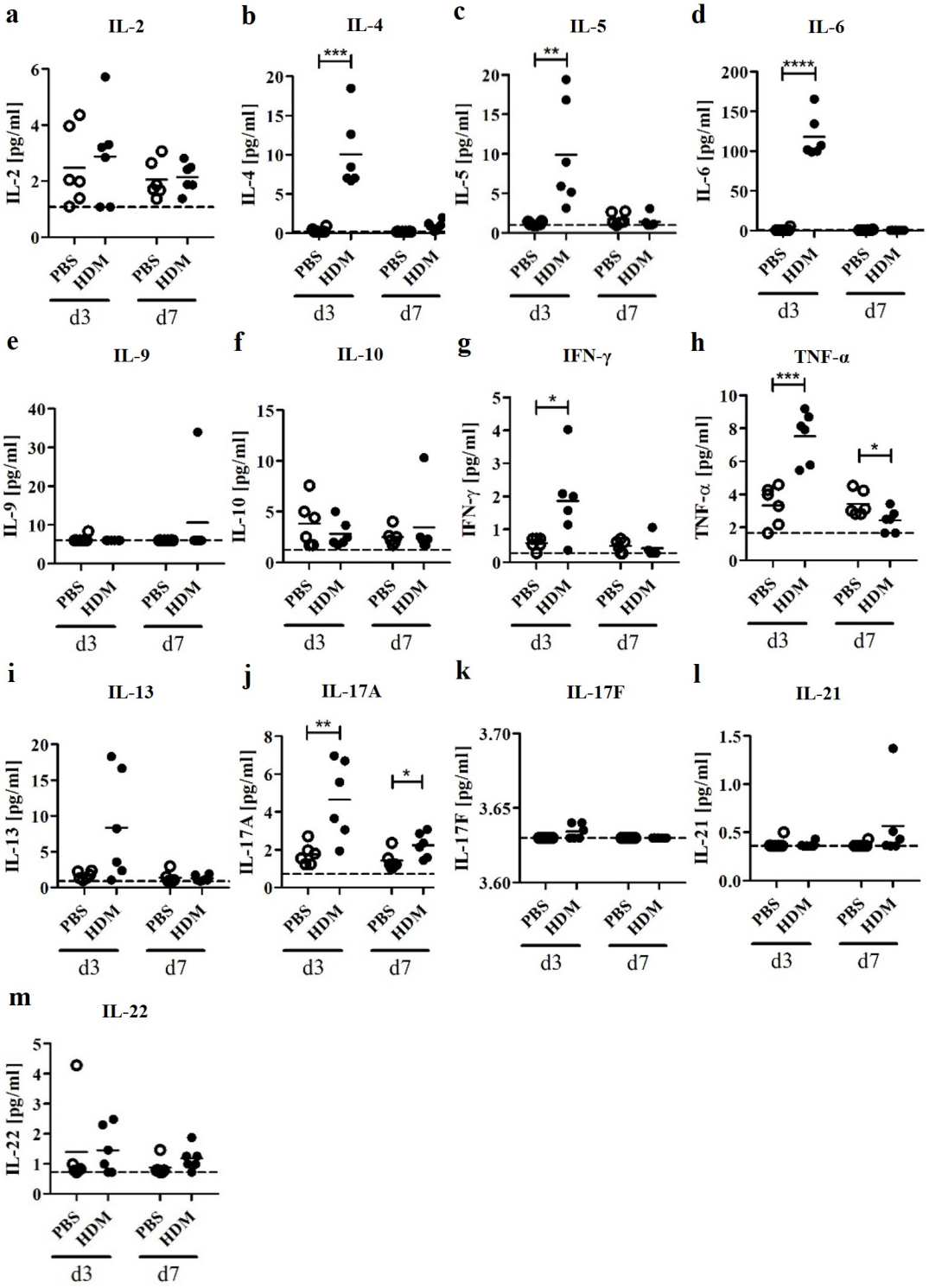

Figure 14: Airway cytokine profile during murine allergic asthma (model 2). Female C57BL/6JRj mice were treated i.n. with PBS (n=12) or HDM (n=12) according to scheme in Fig. 10b. Absolute levels of (a) IL-2, (b) IL-4, (c) IL-5, (d) IL-6, (e) IL-9, (f) IL-10, (g) IFN-γ, (h) TNF-α, (i) IL-13, (j) IL-17A, (k) IL-17F, (l) IL-21 and (m) IL-22 were determined in BAL on day 3 and day 7 after the last treatment by bead-based immunoassay (cumulative data from two experiments; data for individual mice are graphed; mean is indicated by horizontal line; detection limit is indicated by dashed line; * for $p \leq 0.05$; ** for $p \leq 0.01$; *** for $p \leq 0.001$; **** for $p \leq 0.0001$).

The overarching aim of the use of preclinical animal models is to provide the best possible representation of key disease patterns. While the previous experiments focussed on the comparison of important immunological and histopathological asthma characteristics in both *in vivo* models, the implications of HDM-induced allergic immune responses for lung function had not been addressed so far. It is known that human asthma manifests in bronchoconstriction, which can be diagnosed by lung functional analyses. Here, asthmatic individuals display increased airway resistance following inhalation of nebulized methacholine chloride (MCh) [96]. In order to clarify whether the chosen experimental models of murine allergic asthma would be associated with similar effects on pulmonary function, airway resistance was measured in reaction to ascending doses of inhaled MCh in HDM treated mice and the PBS control groups using a resistance and compliance system (Fig. 15, 16).

As expected, the airway resistance gradually increased with increasing MCh concentrations in all experimental groups on day 3 and day 7 post treatment. Surprisingly, the individual extent of MCh-induced airway resistance did not differ between PBS and HDM treated mice in model 1 neither on day 3 (Fig. 15a) nor day 7 (Fig. 15b) post treatment for any of the applied MCh doses. In model 2 however, airway resistance of HDM treated mice was slightly increased compared to the control group on day 3 post treatment (Fig. 16a). On day 7 post treatment the HDM group exhibited a significant, 2-fold increase in airway resistance compared to the control group at a MCh concentration of 100 mg/ml (Fig. 16b).

In summary, the extensive comparative analyses performed in 5.2.1 indicated that despite its capacity to promote individual pathologic traits of allergy (eosinophil accumulation, goblet cell hyperplasia, IgE response), model 1 failed to fully recapitulate hallmarks of human allergic asthma. In contrast, model 2 caused a stable phenotype of allergic asthma that is characterized by increased pulmonary eosinophil influx, goblet cell hyperplasia, elevated systemic IgE levels as well as proinflammatory cytokine response and increased bronchoconstriction.

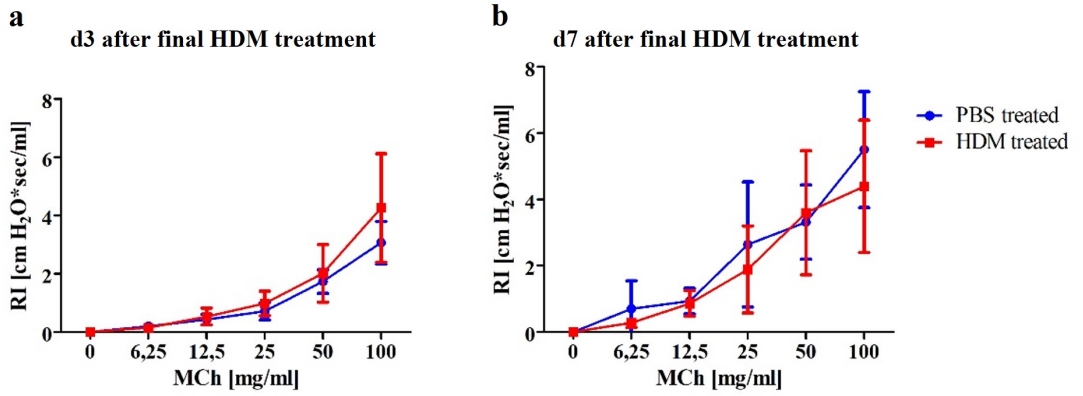

Figure 15: Airway resistance during murine allergic asthma (model 1). Female C57BL/6JRj mice were treated i.n. with PBS (n=10) or HDM (n=10) according to scheme in Fig. 10a. On day 7 post treatment, airway resistance (R) was determined upon inhalation of increasing MCh concentrations using a resistance and compliance system (cumulative data from two experiments; mean airway resistance values ± SD are graphed).

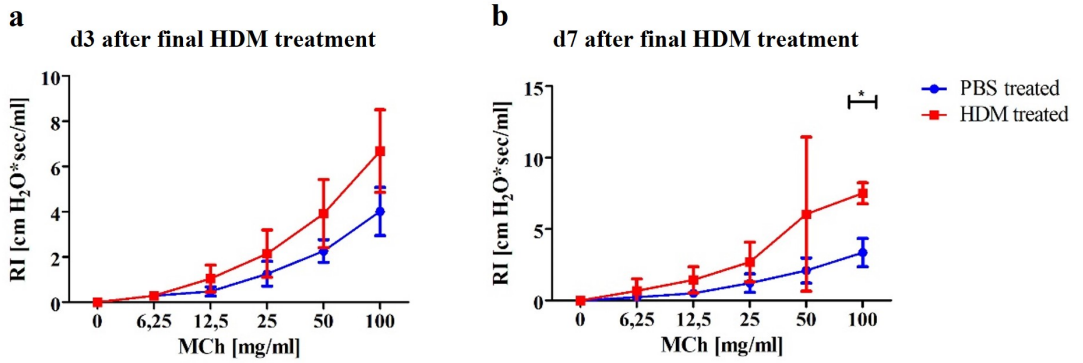

Figure 16: Airway resistance during murine allergic asthma (model 2). Female C57BL/6JRj mice were treated i.n. with PBS (n=10) or HDM (n=10) according to scheme in Fig. 10b. On day 7 post treatment, airway resistance (R) was determined upon inhalation of increasing MCh concentrations using a resistance and compliance system (cumulative data from two experiments; mean airway resistance values ± SD are graphed; * for $p \leq 0.05$).

Based on these findings, model 2 was chosen as a suitable *in vivo* mouse model to investigate the impact of allergic asthma on airway-associated secretory immunity and antibacterial defense in subsequent experiments.

5.2.2 Antimicrobial immunity during murine allergic asthma

It is known that asthma affects several aspects of epithelial-mediated defense. For example, it was shown that asthmatic patients exhibit an impaired epithelial PIGR expression [Ladjemi et al., 2018] and diminished IgA responses in lung [141]. Furthermore, bronchial mucus secretion was found to be increased during asthma [168]. Airway mucus is produced mainly by goblet cells in the respiratory tract and plays a crucial role for the antimicrobial defense [169]. Lysozyme is another important antimicrobial protein that is produced in the airway epithelium and secreted into the mucosal lumen [170]. It was shown that the lysozyme concentration is increased in bronchial secretions of asthmatic children [171].

In order to analyse the secretory immunity and antimicrobial defense of mice with HDM-induced, allergic asthma (model 2), *Pigr*, *Muc5ac* and *Lyz2* gene expression in lung, trachea and NALT and IgA levels in BAL and NAL fluid were determined on day 3 and 7 after the last HDM treatment by qPCR and ELISA, respectively (Fig. 17). Since the nasopharynx is seen as a place of antigen sensitization in asthmatic children [143] and the trachea is an anatomical part of the LRT [2], NALT, NAL fluid and trachea were included in these analyses.

Interestingly, and in contrast to the findings in human asthmatic individuals [44], pulmonary *Pigr* gene expression in murine asthma was significantly increased (3-fold) compared to the non-asthmatic control group on day 7 after the last HDM treatment (Fig. 17a), while *Pigr* gene expression in trachea and NALT was unaffected (Fig. 17b, 17c). In line with increased *Pigr* expression in lung tissue, IgA levels were significantly elevated in BAL fluid of asthmatic mice on day 3 and ten times higher on day 7. Surprisingly, nasal IgA levels were significantly increased upon day 7 post treatment, while they were unaltered on day 3 (Fig. 17d, 17e). *Muc5ac* gene expression was 6-fold increased in lung of HDM treated mice on day 3 and 4-fold on day 7 (Fig. 17f) while trachea and NALT showed no alterations (Fig. 17g, 17h). *Lyz2* gene expression was unaltered upon HDM treatment in lung, trachea and NALT on day 3 and day 7 (Fig. 17i-17k).

In summary, these results indicate that while epithelial mucus production is generally boosted by allergic asthma, murine *vs.* human allergic asthma most likely exert differential effects on *Pigr*-mediated secretory immunity.

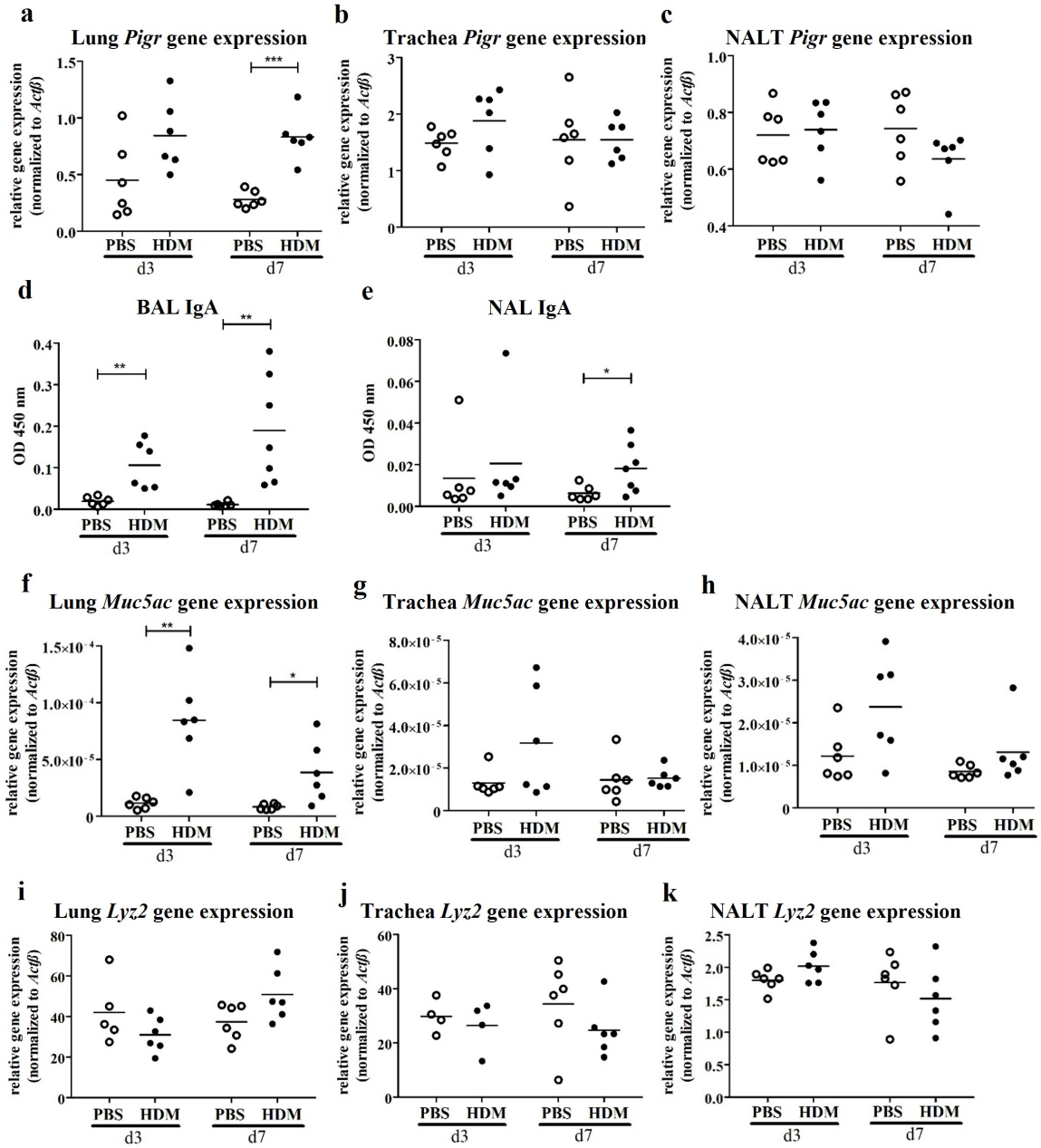

Figure 17: Antimicrobial immunity during murine allergic asthma. Female C57BL/6JRj mice were treated i.n. with PBS (n=12) or HDM (n=13) according to scheme in Fig. 10b. Lung, trachea and NALT were removed on day 3 or day 7 after the last treatment, RNA was isolated, reversely transcribed into cDNA and qPCR analysis was performed. *Pigr* expression normalized to *Actb* in (a) lung, (b) trachea and (c) NALT. IgA levels were determined in (d) BAL and (e) NAL by semi-quantitative ELISA. *Muc5ac* expression normalized to *Actb* in (f) lung, (g) trachea and (h) NALT. *Lyz2* expression normalized to *Actb* in (i) lung, (j) trachea and (k) NALT (cumulative data from two experiments; data for individual mice are graphed; mean is indicated by horizontal line; * for $p \leq 0.05$; ** for $p \leq 0.01$; *** for $p \leq 0.001$).

5.2.3 Establishment of a murine model of pneumococcal colonization

In a next step the newly established and characterized murine model of allergic asthma was employed to investigate the impact of allergic asthma on antipneumococcal immunity. *Streptococcus pneumoniae* is a frequent colonizer of the human nasopharynx. This Gram-positive bacterium persists mostly asymptomatic in healthy individuals, while it causes respiratory diseases like bronchitis and pneumonia in immunosuppressed individuals [102, 103]. Moreover, asthma is associated with an increased susceptibility to severe pneumococcal infections in humans [99, 100]. The nasopharynx is a place of allergen sensitization during asthma development as well as an entry site and reservoir for respiratory pathogens [142, 143]. However, there are no experimental data that describe the impact of asthma on the antipneumococcal immunity in the upper airways.

In order to investigate the impact of allergic asthma on pathogen burden as well as potential bacterial dissemination *in vivo*, a pneumococcal colonization model mimicking human nasal colonization had to be established in the first place. To this end, mice were inoculated intranasally (i.n.) with 10^8 CFU of *Streptococcus pneumoniae* strain BHN 100 (serotype 19F), which is known to be a non-invasive colonizer of the upper respiratory tract [134]. Subsequently, colony-forming units (CFU) were determined in nasopharynx, NAL fluid, NALT, trachea and lung on day 1, 3, 7, 9 and 14 post infection (Fig. 5.2.3).

On day 1 post inoculation bacteria in nasopharynx, NAL fluid, NALT and trachea were detected (Fig. 5.2.3a-5.2.3d). The number of CFU decreased gradually over time in all four compartments. The highest number of bacteria was observed on day 1 post inoculation in NAL fluid with an average of $4x10^3$ CFU followed by nasopharynx with $2x10^3$ CFU. In these two compartments pneumococci were detectable up to 7 days post inoculation, with an amount of $3x10^2$ CFU in NAL and $6x10^2$ CFU in nasopharynx. In NALT and trachea rapid bacterial clearance was observed from day 3 onward. In general, no bacteria were detected in the lung tissue (data not shown), indicating that the chosen inoculation strategy was able to mimic pneumococcal nasopharyngeal colonization *in vivo*. In summary, these results show that the murine upper respiratory tract could be effectively colonized by *Streptococcus pneumoniae* 19F up to 7 days post inoculation. Therefore, this colonization model was employed for all subsequent *in vivo* colonization experiments.

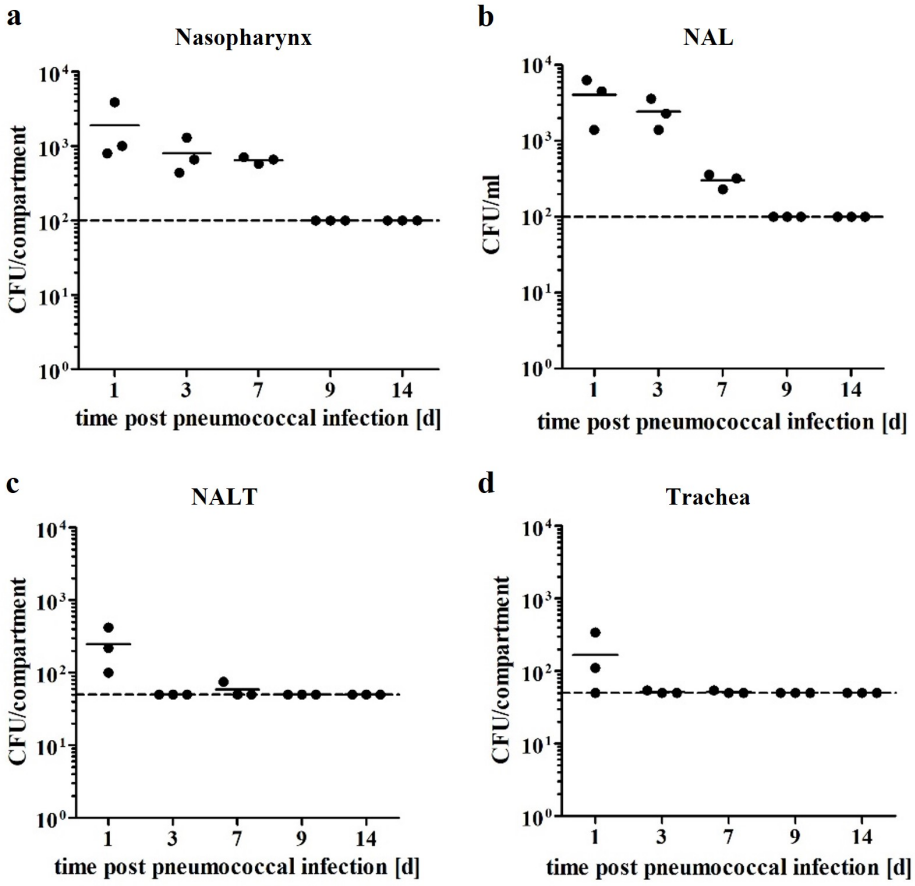

Figure 18: Colonization of mice with *Streptococcus pneumoniae* 19F. Female C57BL/6JRj mice (n=15) were i.n. inoculated with 10^8 CFU of *Streptococcus pneumoniae* 19F and bacterial burden was assessed on day 1, 3, 7, 9 and 14 post infection in (a) nasopharynx, (b) NAL, (c) NALT and (d) trachea (representative data from one experiment; data for individual mice are graphed; mean is indicated by horizontal line; detection limit is indicated by dashed line).

5.2.4 Effect of LPS/IFN-γ treatment on pneumococcal colonization

As described earlier, i.n. LPS *vs.* i.n. IFN-γ treatments had opposing effects on secretory immunity in mice (LPS: decreased IgA levels in BAL and NAL fluid (Fig. 6b, 6c), IFN-γ: increased IgA levels in BAL fluid (Fig. 8b)). Since it is known that IgA plays a key role in the immunity to *Streptococcus pneumoniae* [39], it was tested whether prophylactic i.n. treatment with the aforementioned molecules could affect pneumococcal colonization *in vivo*.

Therefore, mice were treated i.n. with either 10 µg LPS, 1 µg IFN-γ or solvent alone (control group). Two days later the mice were inoculated i.n. with 10^8 CFU of *Streptococcus pneumoniae* serotype 19F. CFU were determined in nasopharynx, NAL fluid, NALT, trachea and lung 1 day post infection (Fig. 19a).

As expected, LPS/IFN-γ treated mice and the respective control groups exhibited highest bacterial burden in the URT (NAL fluid and nasopharynx, Fig. 19b, 19c). CFU numbers in trachea and NALT were below the limit of detection for almost all of the samples. No bacteria were detected in lung. CFU numbers in NAL fluid and nasopharynx were comparable between LPS treated mice and the control group, indicating no effect of prophylactic LPS-stimulation on pneumococcal colonization. Likewise, bacterial burden in nasopharynx was unaltered between IFN-γ treated mice and the control group, whereas IFN-γ treatment reduced the amount of CFU in NAL fluid almost by half (PBS: 1408.0 ± 221.5, IFN-γ: 825.0 ± 129.0).

These data suggest that IFN-γ partly improves antibacterial immunity in the URT, most likely via IgA independent mechanisms, which makes this cytokine a candidate for further immunomodulatory experiments.

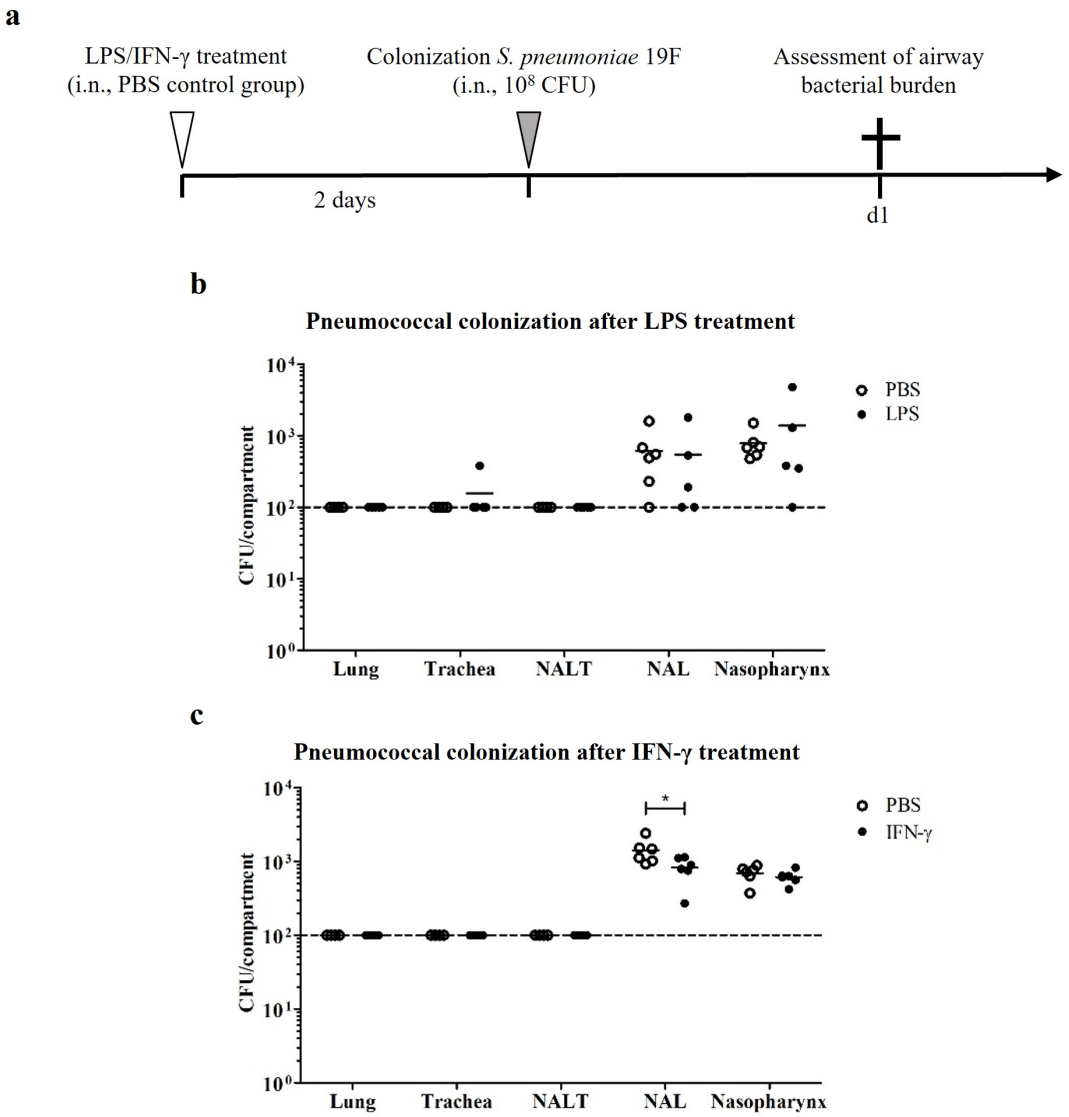

Figure 19: Effect of LPS or IFN-γ treatment on pneumococcal colonization. (a) Schematic representation of the experimental setup. (b) Female C57BL/6JRj mice were treated i.n. with 10 µg of LPS (n=5), control mice received PBS only (n=6). (c) C57BL/6JRj mice were treated i.n. with 1 µg of IFN-γ (n=6), control mice received PBS only (n=6). 2 days post treatment all mice were i.n. inoculated with 10^8 CFU of *Streptococcus pneumoniae* 19F and airway bacterial burden was assessed 18 h post infection (white arrow indicates timepoint of i.n. LPS/IFN-γ application; grey arrow indicates timepoint of i.n. *S. pneumoniae* 19F colonization; black cross indicates timepoint of sacrifice; representative data from one experiment; data for individual mice are graphed; mean is indicated by horizontal line; detection limit is indicated by dashed line; * for $p \leq 0.05$). Modified figure has already been published [145].

5.2.5 Impact of murine allergic asthma on pneumococcal colonization

Previous studies have shown that asthma facilitates the spread of pneumococci from the upper to the lower respiratory tract, which might cause pneumonia in humans [99, 100]. It is yet unknown, whether increased incidence of invasive pneumococcal disease or pneumonia is the result of increased translocation of pathogenic bacteria from URT to LRT or rather ineffective antibacterial immunity in the lower airways. In order to experimentally address this question, it was evaluated whether asthmatic mice are more susceptible to the colonization with *Streptococcus pneumoniae* and the spread of the bacterium from the upper to the lower respiratory tract than non-asthmatic mice. Therefore, pneumococcal colonization of these two groups was compared. Since SIgA is crucial for the protection against pneumococcal nasal colonization of mice [39], it was also tested whether the IgA response differs between *Streptococcus pneumoniae* infected asthmatic and non-asthmatic mice.

Allergic asthma was induced by HDM-extract treatment according to Fig. 10b and asthmatic *vs.* control mice were inoculated i.n. with 10^8 CFU of *Streptococcus pneumoniae* serotype 19F three days after the last HDM treatment. CFU were determined in nasopharynx, NAL fluid, NALT, trachea and lung on day 1, 3, 7, 9 and 14 post infection. IgA levels were determined in NAL fluid by semi-quantitative ELISA at the same timepoints (Fig. 20a).

Similar to the results obtained in 5.2.3, bacteria were detectable in nasopharynx, NAL fluid, NALT and – partly – trachea (Fig. 20b-20e) on day 1 post inoculation. The highest number of bacteria were observed on day 1 post inoculation in NAL fluid followed by nasopharynx. In both compartments CFU numbers decreased gradually over time. In nasopharynx the number of bacteria was above the detection limit until day 7 post infection for all samples, while in NAL fluid it was only until day 3 post infection. In nasopharynx no differences regarding CFU numbers were observed between asthmatic and non-asthmatic mice for any of the analysed timepoints. In NAL fluid of asthmatic mice however, there was a 2-fold increase in CFU on day 1 post infection (PBS: 2062.0 ± 527.9, HDM: 4550.0 ± 578.4) and a 3-fold increase on day 3 post infection (PBS: 830.0 ± 143.6, HDM: 2604.0 ± 443.2) compared to non-asthmatic mice, indicating that bacterial persistence in the URT is partly facilitated by allergic asthma. In NALT and trachea the number of bacteria was below the limit of detection for the majority of the samples from day 3 onward. In lung no bacteria were

detected (data not shown). Interestingly, nasal IgA levels proved to be similar between healthy *vs.* asthmatic mice early after inoculation. However, IgA gradually increased in NAL fluid of non-asthmatic as well as asthmatic mice even after accomplished bacterial clearance. Here, nasal IgA proved to be significantly increased in asthmatic mice compared to non-asthmatic mice on day 9 and day 14 post infection (Fig. 20f).

Altogether, these data indicate that allergic asthma significantly promotes pneumococcal colonization of the upper respiratory tract. Moreover, allergic asthma boosts stronger overall IgA response upon pneumococcal colonization.

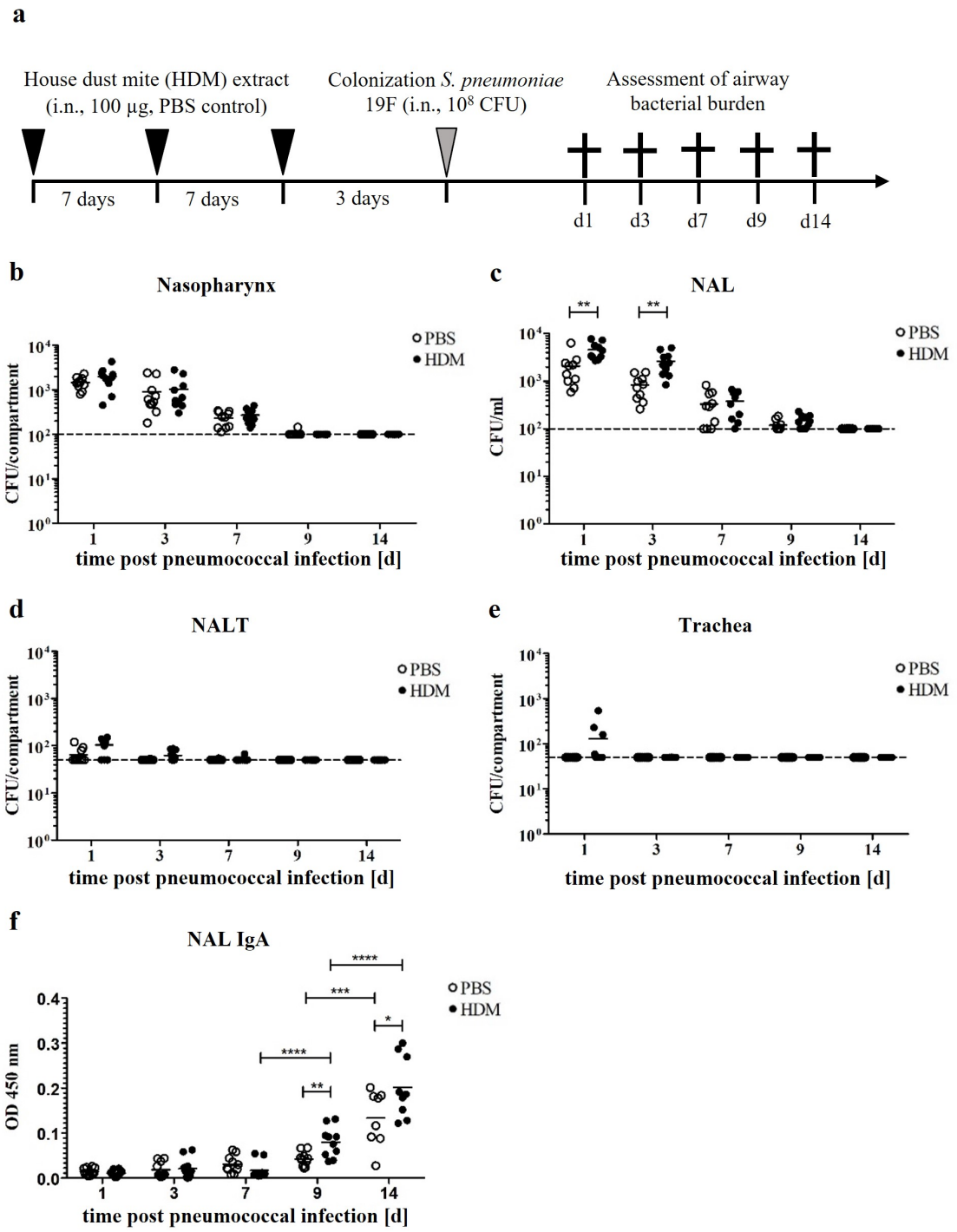

Figure 20: Colonization of healthy and asthmatic mice with *Streptococcus pneumoniae* 19F. (a) Schematic representation of the experimental setup. Female C57BL/6JRj mice were treated i.n. with PBS (n=50) or HDM (n=50) according to scheme in Fig. 10b. 3 days after the last treatment, mice were i.n. inoculated with 10^8 CFU of *Streptococcus pneumoniae* 19F and bacterial burden was assessed on day 1, 3, 7, 9 and 14 post infection in (b) nasopharynx, (c) NAL, (d) NALT and (e) trachea. (f) IgA levels were determined in NAL by semi-quantitative ELISA on day 1, 3, 7, 9 and 14 post infection (black arrows indicate timepoint of i.n. HDM application (PBS control); grey arrow indicates timepoint of i.n. *S. pneumoniae* 19F colonization; black crosses indicate timepoint of sacrifice; cumulative data from two experiments; data for individual mice are graphed; mean is indicated by horizontal line; detection limit is indicated by dashed line; * for $p \leq 0.05$; ** for $p \leq 0.01$; *** for $p \leq 0.001$; **** for $p \leq 0.0001$).

5.2.6 Impact of IFN-γ on secretory immunity of asthmatic mice

As mentioned before, i.n. IFN-γ treatment of non-asthmatic mice led to increased IgA levels in BAL fluid (Fig. 8b) and improved antipneumococcal immunity in the URT (Fig. 19c). Therefore, it was investigated whether immunomodulation by prophylactic IFN-γ treatment would likewise enhance secretory antibacterial immunity during allergic asthma.

In a first step, asthmatic mice were treated i.n. with 1 µg IFN-γ or solvent alone (control group) one day after the last HDM application. On day 1 and day 2 post treatment *Pigr* gene expression and IgA levels were assessed by qPCR and semi-quantitative ELISA, respectively (Fig. 21a).

In contrast to unaltered *Pigr* gene expression in URT and LRT upon IFN-γ treatment at both timepoints (Fig. 21b-21d), pulmonary IgA levels were significantly decreased on day 1 post IFN-γ treatment (Fig. 21e) while IgA levels in NAL fluid were unaffected by IFN-γ (Fig. 21f).

These data indicate that – despite its IgA-promoting effect in the airways of healthy individuals – IFN-γ decreases pulmonary IgA levels in allergic asthma and thus has a context-dependent role in promoting secretory immunity.

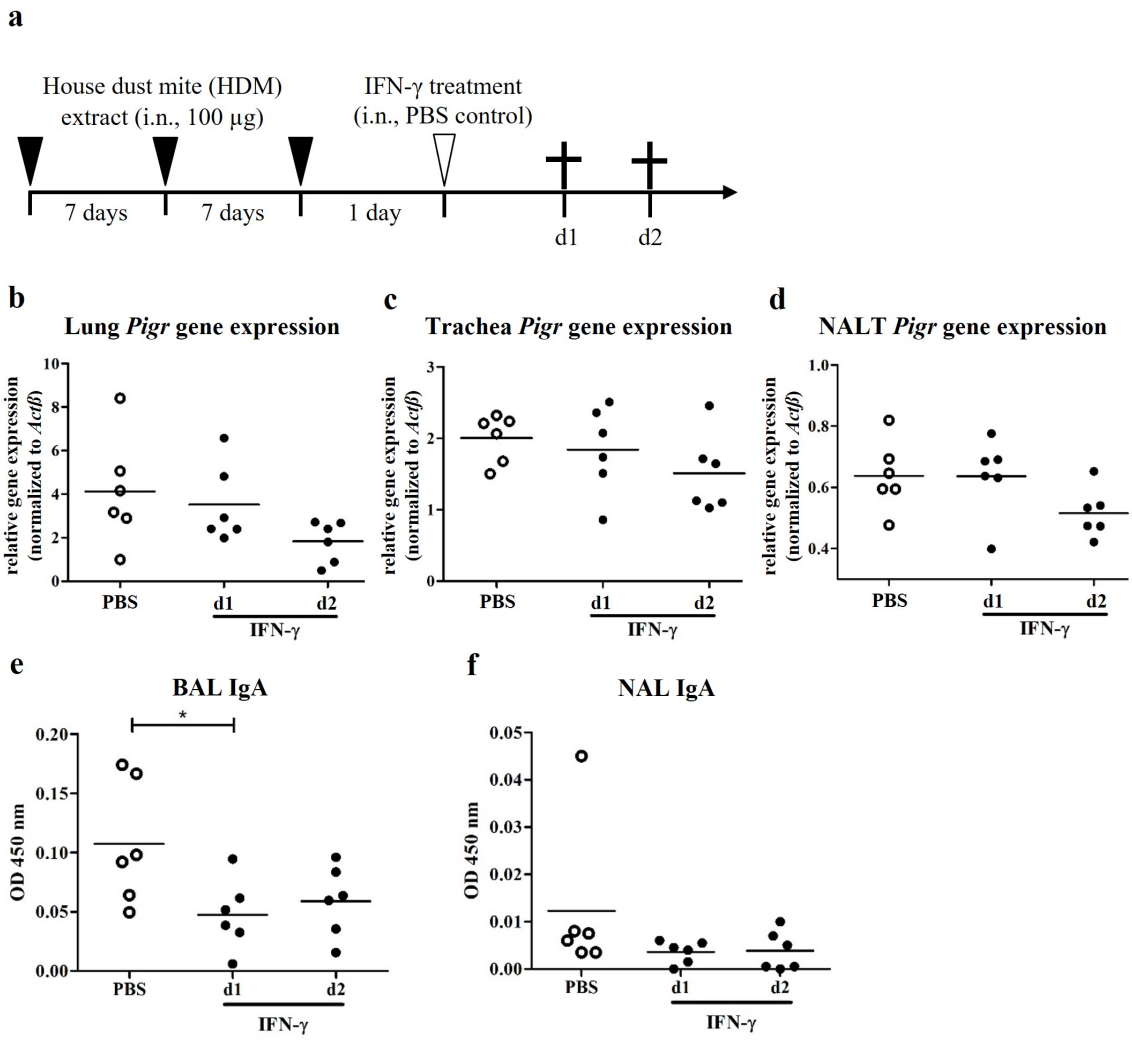

Figure 21: Effect of IFN-γ treatment on secretory immunity during murine allergic asthma. (a) Schematic representation of the experimental setup. Female C57BL/6JRj mice were treated i.n. with HDM (n=18) according to scheme in Fig. 10b. 1 day after the last treatment, mice were treated i.n. with 1 µg of IFN-γ (n=12), control mice received PBS only (n=6). Lung, trachea and NALT were removed on day 1 or day 2 post IFN-γ treatment, RNA was isolated, reversely transcribed into cDNA and qPCR analysis was performed. *Pigr* expression normalized to *Actb* in (b) lung, (c) trachea and (d) NALT. IgA levels were determined in (e) BAL and (f) NAL by semi-quantitative ELISA on day 1 or day 2 post IFN-γ treatment (black arrows indicate timepoint of i.n. HDM application; white arrow indicates timepoint of i.n. IFN-γ application; black crosses indicate timepoint of sacrifice; cumulative data from two experiments; data for individual mice are graphed; mean is indicated by horizontal line; * for $p \leq 0.05$).

5.2.7 Impact of IFN-γ treatment on pneumococcal colonization of asthmatic mice

In view of the fact that prophylactic IFN-γ treatment was shown to promote bacterial clearance in the URT (Fig. 19c), the role of this proinflammatory cytokine for antipneumococcal defense in the URT of asthmatic individuals was subsequently addressed.

It was analysed whether pneumococcal colonization of the respiratory tract of asthmatic mice is also affected by IFN-γ treatment. To this end, allergic asthma was induced according to Fig. 10b and asthmatic mice were treated i.n. with 1 µg IFN-γ or solvent alone (control group) one day after the last HDM application. Two days later the mice were colonized i.n. with 10^8 CFU of *Streptococcus pneumoniae* serotype 19F. CFU were determined in nasopharynx, NAL fluid, NALT, trachea and lung on day 1, 3, 7, 9 and 14 post inoculation (Fig.22a).

CFU counts were highest in nasopharynx (Fig.22b) followed by NAL fluid (Fig. 22c). As observed before (Fig. 20b, 20c), the bacterial burden decreased gradually over time in these two compartments and was above the detection limit up to 7 days post infection in nasopharynx and up to 3 days post infection in NAL fluid. In NALT and trachea the number of bacteria was below the limit of detection for almost all of the samples (Fig. 22d, 22e). No bacteria were detected in lung (data not shown). Moreover, no differences regarding bacterial burden were observed upon IFN-γ treatment in any of the analysed compartments.

Altogether, these data suggest that IFN-γ stimulation exerts no effect on host antibacterial defense in the asthmatic URT and supports the finding of the context-dependent role of this cytokine on antipneumococcal immunity in healthy *vs.* pre-diseased individuals.

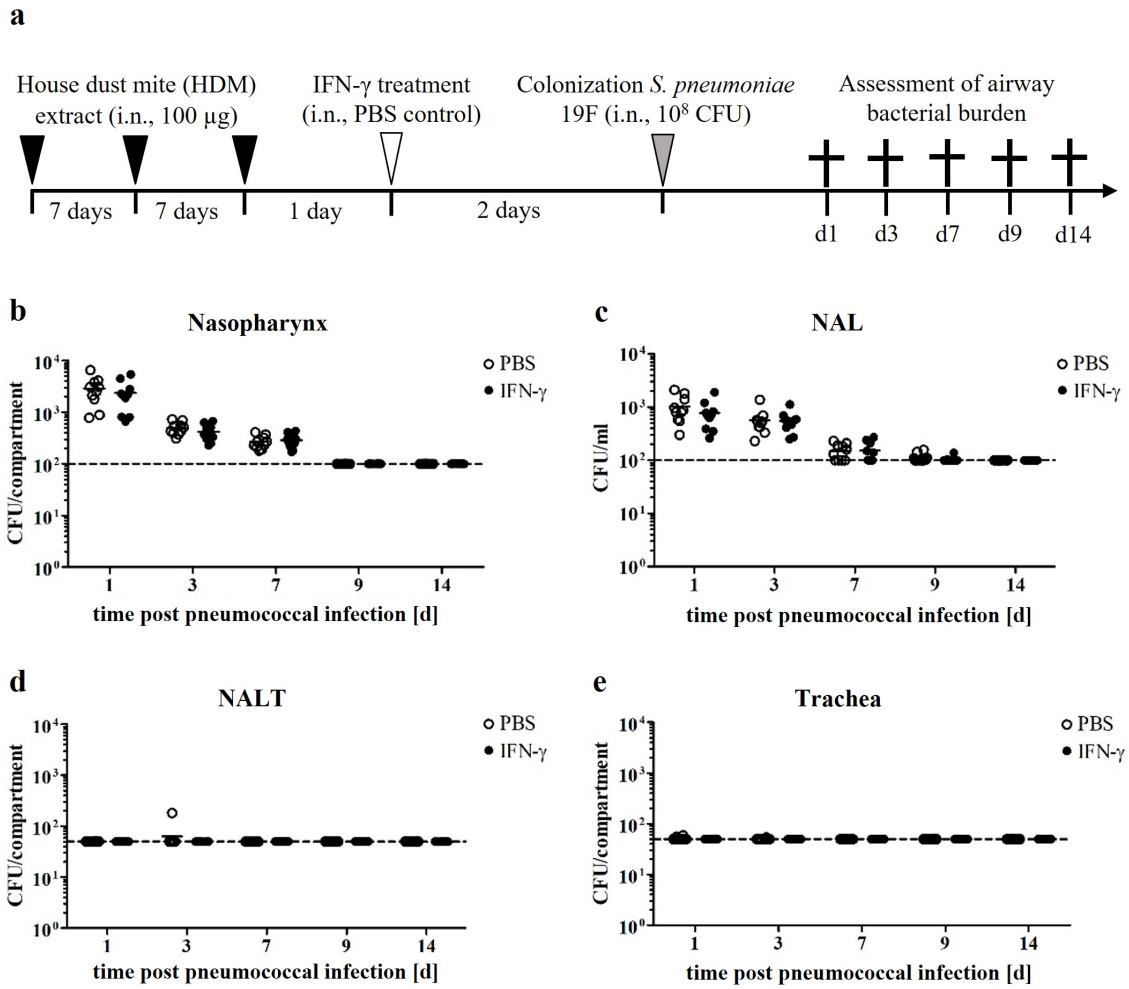

Figure 22: Effect of IFN-γ treatment on pneumococcal colonization in murine allergic asthma. (a) Schematic representation of the experimental setup. Female C57BL/6JRj mice were treated i.n. with HDM (n=100) according to scheme in Fig. 10b. 1 day after the last treatment, mice were treated i.n. with 1 µg of IFN-γ (n=50), control mice received PBS only (n=50). 2 days post IFN-γ treatment, mice were i.n. inoculated with 10^8 CFU of *Streptococcus pneumoniae* 19F and bacterial burden was assessed on day 1, 3, 7, 9 and 14 post infection in (b) nasopharynx, (c) NAL, (d) NALT and (e) trachea (black arrows indicate timepoint of i.n. HDM application; white arrow indicates timepoint of i.n. IFN-γ application; grey arrow indicates timepoint of i.n. *S. pneumoniae* 19F colonization; black crosses indicate timepoint of sacrifice; cumulative data from two experiments; data for individual mice are graphed; mean is indicated by horizontal line; theoretical detection limit is indicated by dashed line).

5.3 Part III: Influence of human allergic and non-allergic asthma on secretory immunity and microbiota composition in the upper airways

5.3.1 Impact of the asthma phenotype on secretory and antibacterial immunity in the upper respiratory tract of humans

While the second part of this thesis employed a pre-clinical murine model of aeroallergen-induced asthma to study the impact of asthma on a) secretory immunity and b) antibacterial defense, the third and last part of this work addressed these aspects in a clinical cohort study in healthy and asthmatic subjects. As already mentioned, asthmatic patients exhibit decreased PIGR expression in the bronchial epithelium, which results in impaired SIgA-mediated mucosal defense [44] and might be linked to the increased risk for severe pneumococcal infections reported in asthmatics [99, 100]. While previous studies attest distinct nasal microbiota in asthmatics [144], it is not clear whether this is due to an altered secretory immunity in the upper airways. In this context, the role allergy plays regarding the composition of the nasal microbiota in asthma is still unknown. Therefore, the impact of allergic and non-allergic asthma on nasal secretory immunity as well as the nasal microbiota was investigated. Since the human nasopharynx is considered a place of allergen sensitization during asthma development as well as an entry site and natural reservoir for respiratory pathogens [142], it is vital to analyse the impact of allergic and non-allergic asthma on secretory immunity in the URT and the nasal microenvironment, in general. However, there is no true consensus about the impact of asthma on the secretory immunity in the human URT.

Since this study aimed at quantifying the impact of allergic asthma on PIGR expression in the URT, acquisition of nasal epithelial cell (NEC) biopsies had to be initially established to make sure a sufficient amount of viable cells could be obtained for subsequent gene and protein expression analysis. Thus, in a first step, cells were obtained from nasal biopsies of healthy human donors using a curette, counted and stained in H&E solution. Viable nasal epithelial cells were acquired (Fig. 23a) with an average cell number of about $3x10^6$ viable cells per donor (Fig. 23b), indicating that the applied sampling method yields a high number of viable target cells.

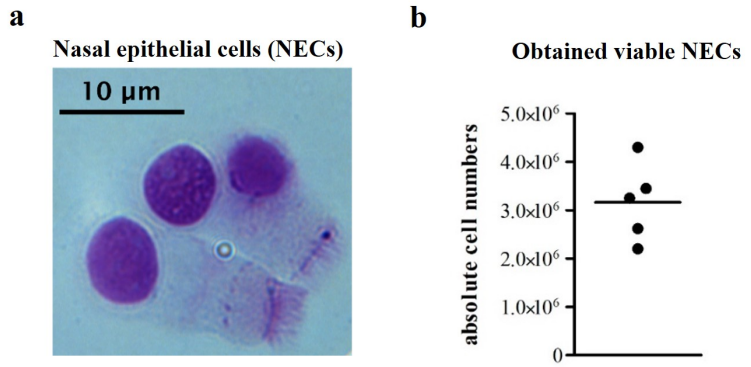

Figure 23: Visualization and quantification of human NECs. Human NEC biopsies were obtained using a mucosal curette. (a) Cells were H&E stained and visualized using a light microscope (magnification: 40x). (b) Numbers of viable cells obtained from individual donors were determined using a counting chamber and a light microscope (mean is indicated by horizontal line).

In a next step, 112 male and female patients (control subjects, n=30; asthmatics, n=82) at the age of 18-82 years were enrolled in a cross-sectional study. The asthmatic donors were subdivided into exogenous asthmatics (reactivity to aeroallergens, increased specific IgE response, n=33), endogenous asthmatics (no reactivity to aeroallergens, infection-associated exacerbations, n=24) and patients with a mixed asthma phenotype (characteristics of both exogenous and endogenous asthmatics, n=25). Nasal microbiota was probed using swabs. NAL was obtained by flushing the nostrils with 5 ml saline. Nasal epithelial cell (NEC) biopsies were acquired as described above using a nasal mucosal curette (Fig. 24). The donors were analysed with regard to different asthma-specific immunological and respiratory parameters to characterize and distinguish the different subgroups (Table 22).

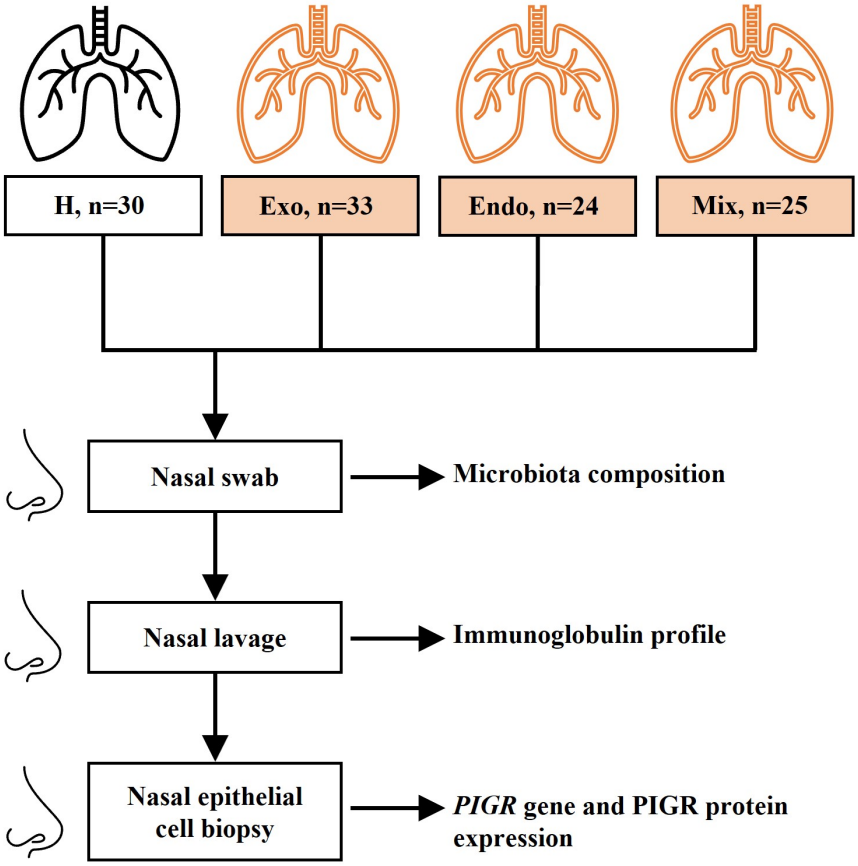

Figure 24: Schematic representation of the clinical study design. H: healthy; Exo: exogenous asthmatics; Endo: endogenous asthmatics; Mix: subjects with mixed asthma phenotypes. Used pictograms were provided by PowerPoint software (version 2203, Microsoft).

Table 22: Patient characterization

		Asthmatics		
	Healthy	**Exogenous**	**Endogenous**	**Mixed**
Subjects, N	30	33	24	25
Age, years (mean ± SD)	47.3 ± 14.9[*]	46.5 ± 14.7[#]	58.8 ± 14.1[*,#]	50.3 ± 15.4
Sex, male/female, n	7/23	12/21	4/20	9/16
FEV1, % predicted, (N=81; mean ± SD)	-	94.0 ± 11.8	95.5 ± 18.9	100.1 ± 19.3
FEV1/FVC ratio, (N=81; mean ± SD)	-	79.8 ± 2.7	77.7 ± 2.5	79.0 ± 2.9
Control of asthma, yes/no, n (N=82)	-	25/8	13/11	15/10
Allergy to aeroallergens, n (N=112)	0	33	0	25
Allergen immunotherapy, n (N=82)	-	25	0	14
Medication				
ICS, n (N=112)	0	7	9	2
ICS + LABA, n (N=112)	0	24	11	21
ICS + LABA + LAMA, n (N=112)	0	0	3	2
Antileukotrienes, n (N=112)	0	1	0	2
Blood parameters				
CRP, mg/l, (N=111; mean ± SD)	2.5 ± 3.2	2.2 ± 3.1	2.3 ± 2.7	3.1 ± 4.9
Leukocytes, K/µl (N=111; mean ± SD)	6.8 ±1.5	7.1 ±1.9	7.1 ± 2.2	7.2 ± 2.0
Eosinophils, Gpt/l (N=110; mean ± SD)	0.15 ± 0.11	0.21 ± 0.12	0.24 ± 0.24	0.23 ± 0.17
α-1 antitrypsin, g/l (N=111; mean ± SD)	-	1.4 ± 0.2	1.4 ± 0.1	1.3 ± 0.3
IgE-total, IU/ml (N=109; mean ± SD)	31.1 ± 32.8	246.5 ± 296.1	165.0 ± 415.9	476.5 ± 606.0
Spec. IgE ad inhalation mixture ip8, kU/l (N=81; mean ± SD)	0	19.1 ± 29.3	0.03 ± 0.07	29.7 ± 35.1

*: Kruskal-Wallis Test and Dunn's Multiple Comparison Test between healthy and endogenous group ($p \leq 0.05$). #: Kruskal-Wallis Test and Dunn's Multiple Comparison Test between exogenous and endogenous group ($p \leq 0.05$) [A Pausder, P Mras et al., submitted for publication].

Secretory immunity (Fig. 25) and immunoglobulin profile (Fig. 26) in the URT of the patients was analysed to investigate whether there are differences regarding URT-associated mucosal immunity between healthy and asthmatic individuals as well as amongst allergic and non-allergic asthma subgroups. In order to analyse the impact of allergic asthma and reactivity to aeroallergens on PIGR-mediated secretory immunity and the humoral microenvironment in general, *PIGR* gene and PIGR protein expression were determined in NEC biopsies by qPCR and Western Blot, respectively. Moreover, total protein concentration, SIgA, IgG and IgE levels were measured in NAL by BCA assay, ELISA and bead-based immunoassay, respectively.

Interestingly - and in stark contrast to the deteriorated bronchial PIGR expression observed in asthmatic humans [44] - nasal *PIGR* gene and PIGR protein expression levels between healthy and asthmatic individuals were unaltered (Fig. 25a, 25b). Since slightly varying alterations in NAL total protein concentration were detected (Fig. 25c), Ig protein levels were normalized to the respective protein concentration. Nasal SIgA levels were similar between healthy and asthmatic individuals as well as between the asthma subgroups (Fig. 25d), which is in line with the unchanged *PIGR*/PIGR expression. Interestingly, IgG2 levels were significantly increased in the combined asthma group, which was attributable to elevated IgG2 in exogenous and endogenous asthmatics (Fig. 26b). However, IgG1, IgG3 and IgG4 levels were unaltered (Fig. 26a, 26c, 26d). Although there was an increase in total and aeroallergen (mixed and exogenous subtype)-specific IgE in the sera of asthmatic subjects (Table 22), nasal mucosal IgE levels were unaltered in these cohorts (Fig. 26e).

These data suggest that the secretory immunity as well as the mucosal IgE response in the human nasopharynx are not affected by asthmatic disease. Moreover, patients that show either characteristics of allergic or non-allergic asthma appear to exhibit a stronger, URT-associated IgG2 response than non-asthmatic individuals.

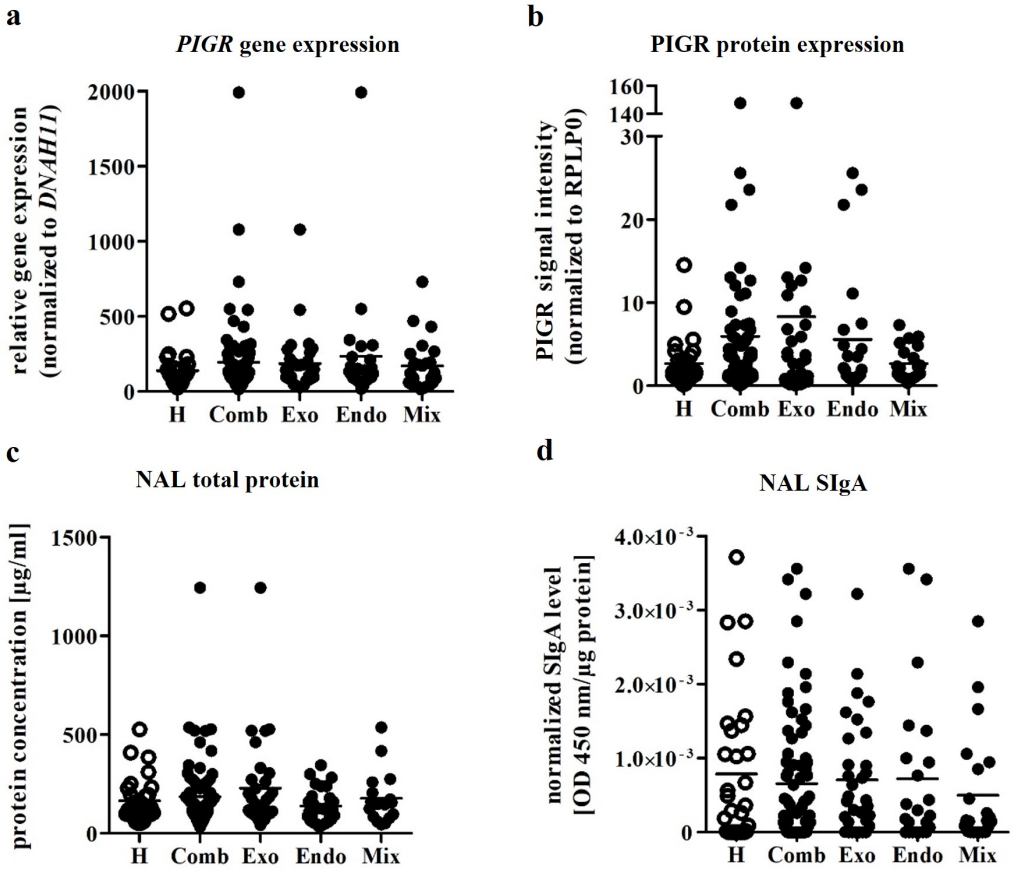

Figure 25: Secretory immunity in the upper airways of healthy and asthmatic patients. 112 male and female subjects (30 healthy, 33 exogenous asthma, 24 endogenous asthma, 25 mixed asthma) at the age of 18-82 years were analysed. RNA and protein were isolated from nasal epithelial cell biopsies. RNA was reversely transcribed into cDNA and qPCR analysis was performed. Protein expression was determined by Western Blot. (a) *PIGR* expression normalized to *DNAH11*. (b) PIGR protein expression normalized to RPLP0. (c) Protein concentration was determined in NAL by BCA protein assay. (d) SIgA levels were determined in NAL by semi-quantitative ELISA and normalized to the respective protein concentration (data for individual subjects are graphed; mean is indicated by horizontal line; H: healthy; Comb: all asthmatics combined; Exo: exogenous asthmatics; Endo: endogenous asthmatics; Mix: subjects with mixed asthma phenotypes) [A Pausder, P Mras et al., submitted for publication].

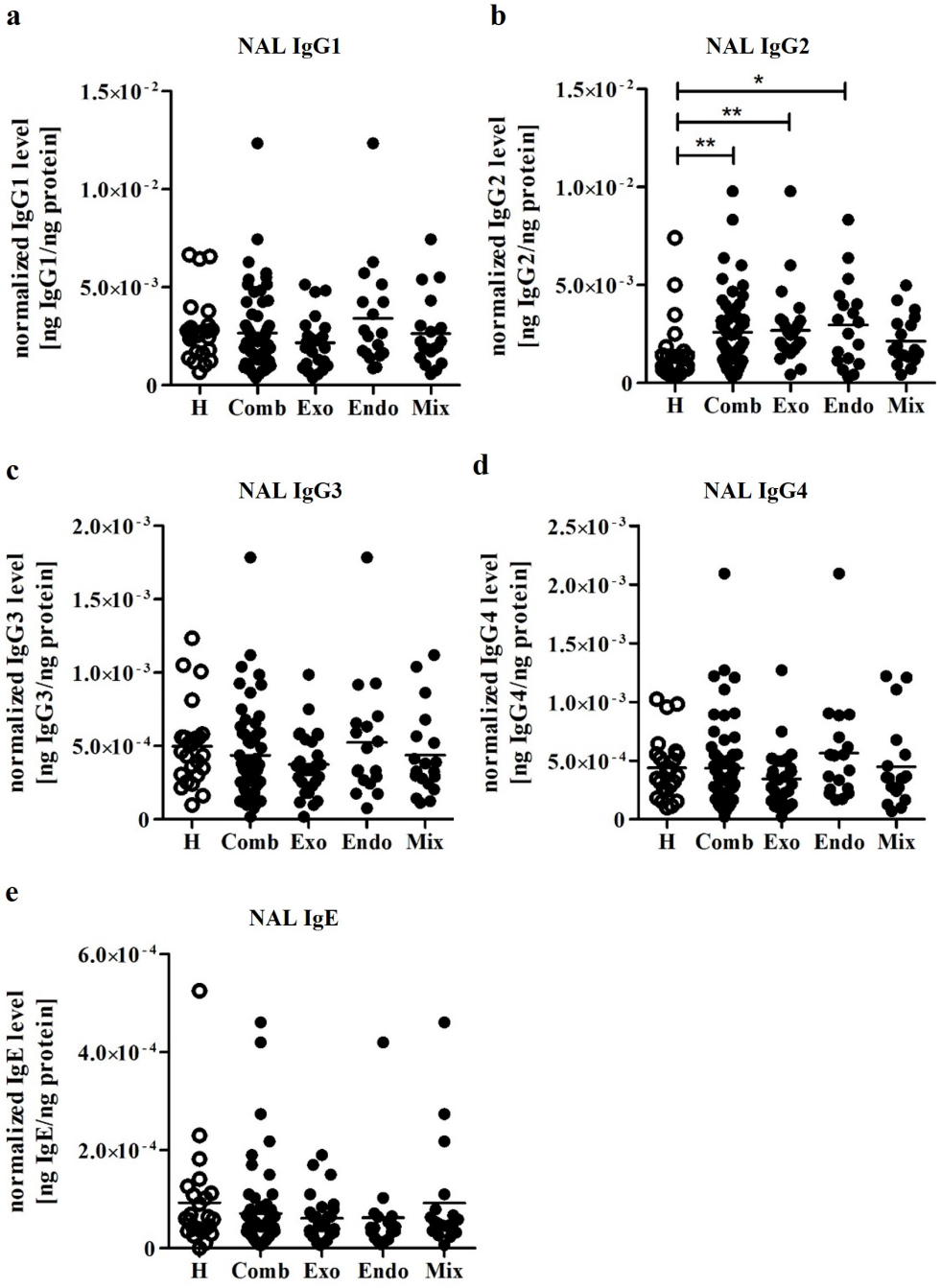

Figure 26: Immunoglobulin profile in the upper airways of healthy and asthmatic patients. 112 male and female subjects (30 healthy, 33 exogenous asthma, 24 endogenous asthma, 25 mixed asthma) at the age of 18-82 years were analysed. (a) IgG1, (b) IgG2, (c) IgG3, (d) IgG4 and (e) IgE levels were determined in NAL by bead-based immunoassay and normalized to the respective protein concentration (data for individual subjects are graphed; mean is indicated by horizontal line; H: healthy; Comb: all asthmatics combined; Exo: exogenous asthmatics; Endo: endogenous asthmatics; Mix: subjects with mixed asthma phenotypes; * for $p \leq 0.05$; ** for $p \leq 0.01$) [A Pausder, P Mras et al., submitted for publication].

5.3.2 Impact of the asthma phenotype on microbiota composition in the upper respiratory tract of humans

Microbiota composition in the URT of the subjects was analysed to examine whether asthma as well as the reactivity to aeroallergens has an impact on microbial diversity and relative bacterial abundance in general (Fig. 27). Therefore, abundance of various bacteria families was determined in nasal swabs by gene sequencing analysis of the V4 region of the 16S rRNA gene.

The analysis revealed distinct differences in nasal microbiota composition between asthmatic and healthy individuals. Specifically, an increased number of different bacterial species, which is a measure for the so-called alpha diversity, was observed in asthmatic patients (combined asthma group as well as exogenous and mixed subgroups) (Fig. 27a). Since IgG2 is known to be targeted against bacterial polysaccharides [172] and nasal IgG2 levels were increased in exogenous and endogenous asthmatics (Fig. 26b), alpha diversity was plotted against IgG2 levels. However, there was no correlation between microbial diversity and the amount of IgG2 (Fig. 27b). Principle coordinates analysis (PCoA) of the beta diversity of the microbial communities uncovered significant differences between asthmatic and healthy individuals (ADONIS: p=0.0035), although a large overlap was observed (Fig. 27c). Linear discriminant analysis (LDA) and effect size (LEfSe) analysis (LDA score > 2.0) revealed that various bacteria families were more abundant in asthmatic patients than in healthy individuals (*e.g.* Chitinophagaceae, Burkholderiaceae, Prevotellaceae, Bacteroidaceae). However, Carnobacteriaceae and Corynebacteriaceae exhibited a lower abundance in asthmatics (Fig. 27d). Comparison of relative bacterial abundance on family level revealed no significant differences between asthmatic and healthy subjects (Fig. 27e).

These data indicate that the microbial diversity and general abundance in the URT is affected by asthma. Moreover, increased microbial diversity in asthmatics that exhibit reactivity to aeroallergens is most likely not caused by alterations regarding IgG2 abundance.

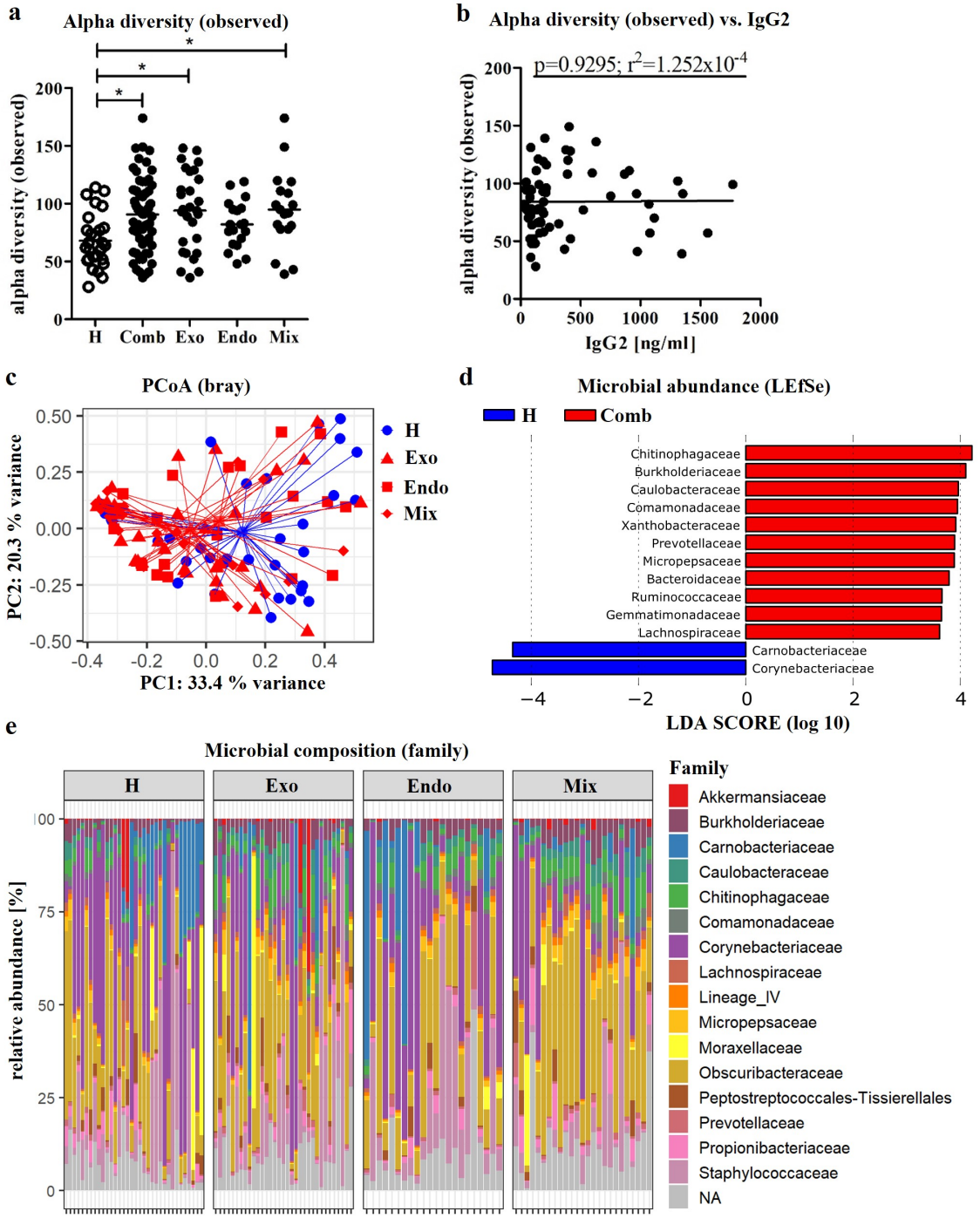

Figure 27: Microbiota composition in the upper airways of healthy and asthmatic patients. 112 male and female subjects (30 healthy, 33 exogenous asthma, 24 endogenous asthma, 25 mixed asthma) at the age of 18-82 years were analysed. DNA was extracted from nasal swabs and nasal microbiota composition was analysed via 16S rRNA gene sequencing of the V4 region. (a) Alpha diversity was determined using observed species per sample. (b) Alpha diversity was plotted against IgG2 levels. (c) PCoA plot showing an overlap in the nasal microbiota composition between healthy and asthmatic individuals. (d) LEfSe analysis was performed and bacterial families with LDA score > 2 are displayed. (e) Relative abundance of bacterial families (data for individual patients are graphed; mean is indicated by horizontal line; H: healthy subjects; Comb: all asthmatic subjects combined; Exo: subjects with exogenous asthma; Endo: subjects with endogenous asthma; Mix: subjects with mixed asthma phenotypes; correlation analysis was performed by linear regression; statistical test: Kruskal-Wallis Test and Dunn's Multiple Comparison Test; * for $p \leq 0.05$) [A Pausder, P Mras et al., submitted for publication].

6 Discussion

Epithelial transport of secretory immunoglobulins via the polymeric immunoglobulin receptor (pIgR) constitutes a vital component of mucosal antimicrobial host defense. While there are many studies investigating the secretory immunity and its modulation in the murine and human intestinal tract [45, 46, 51, 146, 148, 152], little is known about the roles of secretory immunoglobulins in the upper and lower airways under homeostatic and infectious conditions and during chronic respiratory diseases like asthma.

The data obtained in frame of this thesis will be discussed in the following sections according to the previously announced aims of this study:

Aim 1: Provide detailed insight into the regulation of basal airway-associated secretory immunity *in vivo*.

Aim 2: Investigate the impact of murine allergic asthma on pIgR-mediated airway immunity and pneumococcal colonization.

Aim 3: Analyse the influence of human allergic and non-allergic asthma on secretory immunity and microbiota composition in the upper airways.

6.1 Aim 1: Provide detailed insight into the regulation of basal airway-associated secretory immunity *in vivo*.

Basal secretory immunity and its modulation

Previous studies on *Pigr* gene and PIGR protein expression in the airways mainly applied *in vitro* approaches [173, 174] or analysed tissue from patients with chronic respiratory diseases [37, 43, 157, 175]. Murine studies either analysed *Pigr* expression in reaction to interleukin treatment [176] or exposure to pathogen-associated molecules like cholera toxin or amoeba lysates [177]. These studies showed that PIGR/*Pigr* expression is strongly impacted by exogenous and endogenous stimuli that are present in the airway microenvironment. In this study, compartment-specific and age/sex-independent differences in basal airway *Pigr* gene expression were detected. BALB/c as well as C57BL/6J mice exhibited highest *Pigr* expression in trachea, followed by NALT and lung. This effect might be caused by inherent differences in microbial density between the compartments. Due to their anatomical localization, trachea and nasopharynx are in more frequent contact to microbial stimuli than the lung [21]. It is conceivable that a higher microbial density in the murine URT provides more signals that trigger *Pigr* gene expression and SIg transport compared to the LRT. This in turn might contribute to preventing the spread of bacteria from URT to LRT, and ultimately the low bacterial density in the lung. Unexpectedly, no alterations regarding *Pigr* expression were observed between germ-free and microbially colonized mice. This indicates that overall *Pigr* expression in the murine respiratory tract might be unaffected by microbial colonization. However, since *Pigr* gene expression levels were determined at the whole-tissue level, it is possible that signal dilution effects (*e.g.* from leukocytes) have an impact on compartment-specific *Pigr* expression.

It is known that commensal intestinal bacteria induce IgA production in mice [146]. Furthermore, it was shown that housing conditions and exposure to microbial stimuli affects lymphocyte numbers in nasal mucosa [147]. While those findings clearly demonstrate the impact of the microbiota on lymphocyte-associated mucosal immunity, the connection between the level of microbial exposure and airway-associated secretory immunity is still poorly understood. It was revealed in this study that *Pigr* expression in NALT of mice with an undefined microbiome was lower than in mice maintained under SPF conditions, while airway and systemic IgA levels were increased in these

mice. Since fecal IgA levels are affected by the composition of the intestinal microflora [178], it is possible that a comparable effect might be present in murine airways. However, since *Pigr* expression in NALT is decreased while IgA levels are increased it is likely that there is no correlation between IgA abundance and *Pigr* expression at the whole-tissue level. Of note, *Pigr* expression levels were not exclusively assessed in stromal cells but in whole tissue. As it was shown that the microbial environment affects the cell composition in the mucosa, it is conceivable that the accumulation of leukocytes in mice with a high microbial exposure leads to a dilution effect and ultimately to the reduction of the net *Pigr* signal.

It was shown that human and murine intestinal epithelial cells exhibit elevated *Pigr*/*PIGR* gene expression levels upon LPS stimulation *in vitro* [45, 46, 152]. In this study, LPS treatment caused increased pulmonary *Pigr* expression *in vivo*. However, LPS treatment did not affect *Pigr* expression in trachea or NALT. This might be due to the fact that bacterial colonization - and therefore exposure to *e.g.* LPS - is more pronounced in the URT [21], which results in a decreased sensitivity of URT airway stromal cells to LPS. However, it is known that the upper airways are mainly inhabited by Gram-positive bacteria [179, 180] and LPS is solely found in the membrane of Gram-negative bacteria [181]. This contradicts the hypothesis that URT airway stromal cells are in more frequent contact to LPS and therefore exhibit a lower sensitivity to the molecule. Since the bacterial density in URT is about 10 times higher than in the LRT [21], this effect might however be compensated. It is known that the intracytoplasmic toxin pneumolysin, which is found in *S. pneumoniae*, induces a TLR4-dependent proinflammatory immune response [182]. Since *PIGR* gene expression in human intestinal epithelial cells increases upon TLR4 stimulation [45, 46], pneumolysin constitutes an interesting candidate for the modulation of the airway-associated secretory immunity. In contrast to the increased pulmonary *Pigr* expression, LPS treatment caused decreased airway IgA levels, while systemic IgA was not affected. Decreased IgA levels might result from decreased epithelial leakage, which was tested by determining *Cldn18* and *Cldn7* expression. Claudins are proteins that are crucial for maintaining epithelial barrier function. Altered claudin expression is an indicator for an altered AEC barrier function in the LRT (*Cldn18*) and URT (*Cldn7*) [10–12]. However, LPS treatment had no effect on *Cldn18* or *Cldn7* expression. It is known that IgA binds LPS [183]. Therefore, it is conceivable that administered LPS was already bound to mucosal IgA. This might lead to the reduction of detectable IgA, as the ELISA detects free IgA molecules with the highest

affinity. However, since *Pigr* expression in lung was increased while IgA in BAL was decreased and *Pigr* expression in NALT was unaltered while IgA in NAL was increased, it seems that there is no consistent correlation between the two molecules in whole-tissue analysis of LPS-treated mice. IFN-γ is also known to be an inducer of *PIGR* expression in a human lung epithelial cell line as well as in HT-29 human colon carcinoma cells [51, 174], while its impact on airway *Pigr* expression and secretory immunity *in vivo* has not been analysed before. IFN-γ treatment caused increased pulmonary IgA levels, while airway *Pigr* expression was unaffected. Since *Cldn* expression was unaffected, increased IgA levels were most likely not caused by epithelial leakage. It was hypothesized that IFN-γ treatment leads to the activation of mucosal B cells which in turn produce increased amounts of IgA. However, as *IgJ* expression was unaffected, this hypothesis was rejected. As mentioned before, *Pigr* gene expression was not determined exclusively in stromal cells but in whole tissue samples. It was shown that intradermal IFN-γ injection stimulates intradermal lymphocyte migration in rats [155]. Therefore, it is possible that i.n. IFN-γ treatment causes the accumulation and activation of lymphocytes in the airways, which might lead to the reduction of the net *Pigr* signal. IFN-γ treatment caused no significant alterations regarding the influx of immune cells in lung or NALT. However, there is a slight increase in absolute cell numbers of B cells, CD4+ T cells and CD8+ T cells in NALT upon IFN-γ treatment, which might be causing the aforementioned dilution effect.

In summary, these results show that secretory immunity in URT and LRT is differentially regulated by endogenous (cytokines) and exogenous (microbial ligands) stimuli and is partly amenable for immunomodulatory treatment.

6.2 Aim 2: Investigate the impact of murine allergic asthma on pIgR-mediated airway immunity and pneumococcal colonization.

HDM-induced murine model of allergic asthma

The second aim of this thesis was to analyse the impact of allergic asthma on pIgR abundance and secretory immunity in the entire respiratory tract. Therefore, a murine model of HDM-induced, allergic asthma was established that is characterized by a stable, eosinophilic and proinflammatory phenotype. HDM derived enzymes (*e.g. Der p1*, *Der p2*) are common aero- and skin allergens in asthmatic humans and patients with atopic dermatitis [59, 184]. Because of the relevance of HDM as aeroallergen and its role in asthma, HDM-extract induced asthma constitutes a valid model to perform preclinical studies in rodents. Allergic asthma is associated with increased numbers of eosinophils in the lower respiratory tract [160], goblet cell hyperplasia in the lung [161, 162] and increased systemic IgE levels [163]. The low-dose, long-term (model 1) as well as the high-dose, mid-term HDM (model 2) model of murine allergic asthma used in this study caused increased eosinophil influx in lung, goblet cell hyperplasia and elevated serum IgE levels to a similar degree. This shows that both models of i.n. HDM administration lead to a phenotype of eosinophilic, allergic asthma that is comparable to that observed in humans. Moreover, the aforementioned parameters seem to be mostly independent of the individually administered dose of HDM and the duration of the treatment. Since the total amount of administered HDM is the same for both models, it is possible that these parameters might be dependent on the overall application dose.

It is known that various cytokines are involved in shaping of the asthma phenotype. IL-4 and IL-5 are important for the migration and activation of eosinophils during asthma sensitization [164, 165]. It was shown that IL-4 and IL-5 mRNA and protein levels were increased in bronchial biopsies of asthmatic patients [185]. IL-10, IL-13 and IL-17A are crucial for the induction of airway hyperreactivity and allergic inflammation. Elevated IL-10 and IL-13 mRNA levels were observed in nasal mucosal biopsies of patients allergic to grass pollen, while bronchial IL-17A expression was increased in asthmatic patients [83–85]. Furthermore, elevated levels of IL-6 in induced sputum and TNF-α in serum were observed in allergic asthmatics [166, 167]. The low-dose, long-term asthma model did not lead to alterations in any of the measured cytokines, while the high-dose, mid-term model caused increased levels of IL-4, IL-5, IL-6, IFN-γ, TNF-α and IL-17A in BAL

fluid on day 3 after the last HDM treatment. These results show that only the latter asthma model caused a proinflammatory, allergic cytokine response that is comparable to that observed in allergic asthmatics. The increased IL-4/IL-5 levels observed in the high-dose, mid-term model might be the cause for the elevated influx of eosinophils. The fact that eosinophil influx was also increased in the low-dose, long-term model, while IL-4/IL-5 levels were unaffected seems to contradict this hypothesis. However, it is conceivable that these cytokines were increased right after HDM treatment and declined to their initial state shortly after.

Increased airway reactivity is a hallmark of asthma. Airway hyperreactivity can be diagnosed by an increased airway resistance in reaction to MCh inhalation. The low-dose, long-term model failed to induce increased airway resistance. This finding is well in line with the unaltered IL-10, IL-13 and IL-17A levels observed in this model, since these cytokines are important for the induction of airway hyperreactivity. On the other hand, the high-dose, mid-term model caused increased airway resistance, which fits the increased IL-17A levels found in this model. The fact that IL-10 and IL-13 levels were unaltered, suggests that these cytokines might not play an important role during the allergic reaction to HDM-extract even though they are involved in the induction of airway hyperreactivity in patients allergic to grass pollen [83]. Since only the high-dose, mid-term model generated a proinflammatory, allergic cytokine response and increased airway reactivity, these parameters seem to be dependent on the amount of individually administered HDM, rather than on the total amount or the frequency of the treatments. Exclusively the high dose, mid-term treatment led to an asthma phenotype that mimics important immunological, histopathological and functional characteristics of human allergic asthma.

It was shown that PIGR protein expression in the bronchial epithelium and IgA secretion in lung are impaired in asthmatic patients [44]. In contrast to these observations, the utilized murine asthma model (model 2) led to increased *Pigr* gene expression in lung and elevated IgA levels in NAL and BAL fluid. Analysis of murine pIgR protein expression might present a possibility to investigate whether HDM-extract treatment affects this molecule in a similar way as in asthmatic humans. Moreover, it is known that IFN-γ plays an important role in the upregulation of *PIGR* gene expression in HT-29 human colon carcinoma cells [186]. Since HDM-extract treated mice exhibited increased IFN-γ levels in BAL fluid, one might speculate that this causes the upregulation of *Pigr* gene expression and thus the IgA increase in the lower airways. Since *Pigr* gene expression

is unaltered in the upper airways of HDM-extract treated mice, it is unlikely that the same effect causes increased IgA levels in NAL fluid. However, asthmatics that show an allergic reaction to HDM also exhibit increased levels of HDM-specific SIgA in lung [187]. Therefore, it is possible that increased IgA levels in BAL and NAL fluid of the asthmatic mice are caused by an increase in HDM-specific SIgA, since the ELISA detects monomeric IgA, dimeric IgA and SIgA and does not allow discrimination between them. Measurement of HDM-specific SIgA presents a possibility to determine whether the increased IgA signal is due to such an effect. It was shown that bronchial mucus secretion is increased in asthmatic patients [169]. In line with this, HDM treated mice exhibited increased *Muc5ac* gene expression. This finding is well in line with the finding of goblet cell hyperplasia observed in the aforementioned histopathological analysis, since airway mucus is produced mainly by these cells [169].

Taken together, these data show that the chosen *in vivo* model of aeroallergen-(HDM) mediated allergic asthma leads to the formation of a proinflammatory, allergic phenotype of eosinophilic, allergic asthma mimicking important hallmarks of human allergic asthma. However, the impact asthma of on the secretory immunity in humans could not be reproduced in this murine asthma model. This might be tackled by a different methodical approach (*e.g.* analysis of pIgR protein expression, HDM-specific IgA ELISA).

Impact of murine allergic asthma on antimicrobial immunity

Streptococcus pneumoniae 19F strains are commonly used as model pathogen to study nasal colonization in murine models. It was shown that i.n. colonization of the murine URT with the bacterium was stable for up to 7 days post inoculation [188]. In the present study, the utilized *S. pneumoniae* 19F strain (BHN 100) was detectable in nasopharynx and NAL fluid of mice until day 7 post infection, which is in line with previously published data [188]. Since it was shown here that intranasal application of IFN-γ leads to increased IgA levels (Fig. 8) and IgA was previously described to enhance antipneumococcal immunity [189–191], the effect of this molecule on pneumococcal colonization was investigated. Prophylactic IFN-γ treatment led to a decline in nasal pneumococcal counts which indicates an improved antibacterial immunity. However, this effect was not due to increased IgA levels, since IFN-γ treatment caused increased IgA levels only in BAL and not in NAL. In this context, it was previously shown that IFN-γ induces antibacterial

activity in pulmonary macrophages [192] and macrophages are known to be present in the murine NALT [193]. Therefore, it is possible that IFN-γ triggers antibacterial activity in these cells as well. Moreover, IFN-γ induces the production of antibacterial molecules like β-defensins [194], which might also explain the observed effect. In order to elucidate the antimicrobial effect of IFN-γ in the URT, more detailed analyses aiming at characterization of the soluble *vs.* cellular microenvironment would be useful (*e.g.* analysis of macrophage activity by measurement of H_2O_2 production, analysis of cellular β-defensin expression in URT and LRT).

It is known that asthmatic patients are more susceptible to severe pneumococcal infections of the respiratory tract [99, 100]. However, it is unknown whether this is the result of increased translocation of pathogenic bacteria from the URT to the LRT or rather deteriorated antibacterial immunity in the lower airways. In order to address this question, it was investigated whether asthmatic mice are more susceptible to the colonization of the respiratory tract with *Streptococcus pneumoniae* and the spread of the bacterium from the upper to the lower airways than non-asthmatic mice. HDM-extract treated mice showed unaltered pneumococcal counts in nasopharynx compared to untreated animals. This is in line with a previous study that analysed bacterial load in nasopharynx of HDM treated, neonatal mice 1 day post i.n. *S. pneumoniae* 19F infection [195]. However, CFU counts in NAL fluid of HDM treated mice were increased on day 1 and 3 post infection, while they were on the same level on day 7. These results suggest that the murine model of allergic asthma is associated with a significant susceptibility to *S. pneumoniae* colonization in the upper airways that was however transient. Since elevated IgA levels were observed in NAL fluid of HDM treated mice on day 7 after the last treatment, while they were unaffected on day 3, it is possible that this late IgA response led to a decrease in pneumococcal counts causing equal bacterial loads in the two groups. It is also conceivable that the observed IgA response was triggered by the last HDM-extract treatment. To investigate the effect of increased IgA levels on bacterial clearance, it would be helpful to analyse the reactivity of IgA. This could be accomplished by flow cytometric quantification of IgA bound pneumococci in NAL fluid and might contribute to better understand the impact of asthma on secretory, IgA-mediated antipneumococcal immunity in the upper airways. However, the generated data suggest that this model of murine allergic asthma mimics the detrimental effects of human asthma on antipneumococcal immunity.

IgA levels in NAL fluid of *S. pneumoniae* infected, asthmatic mice were increased on day 9 and 14

post infection compared to non-asthmatic mice. Since the strength of an immune reaction often correlates with the pathogen load [196, 197], it is possible that the more pronounced pneumococcal colonization observed in asthmatic mice also led to a stronger IgA increase. The fact that IgA levels were unaltered on day 1, 3 and 7 post infection seems to contradict this hypothesis. However, since pneumococcal load was increased in HDM treated mice, it is conceivable that more IgA molecules were bound to the bacteria, which led to the decrease of the detected IgA signal at the early timepoints. It is also possible that this effect is again caused by an increase of HDM-specific IgA in the asthmatic mice that is detected as a part of the overall IgA signal.

As already mentioned, i.n. IFN-γ treatment of non-asthmatic mice caused increased IgA levels in BAL fluid on day 2 post treatment. In asthmatic mice however, IFN-γ treatment led to a decrease of IgA levels in BAL fluid on day 1 post treatment, while they were unaltered on day 2. These results clearly indicate that IFN-γ likely has opposing effects on airway secretory immunity in homeostasis *vs.* chronic respiratory disease. It is known that IFN-γ induces proinflammatory processes until inflammation reaches an inflammatory threshold. After reaching the threshold level, high IFN-γ levels activate opposing regulatory machanisms that induce negative feedback and trigger antiinflammatory processes [198]. Since IFN-γ levels were increased in BAL fluid of asthmatic mice, it is conceivable that i.n. IFN-γ treatment caused such an autoregulatory negative feedback loop that ultimately led to decreased IgA levels. It is possible that – next to IgA production and secretion – other antimicrobial mechanisms are affected by altered IFN-γ levels in asthmatic airways. This might also explain why the antipneumococcal immunity of asthmatic mice was unaffected by IFN-γ treatment, while non-asthmatic mice exhibited a decreased bacterial burden upon IFN-γ treatment. To further investigate the impact of IFN-γ on the antimicrobial immunity in asthma, IFN-γ neutralizing antibodies could be administered. Since IFN-γ levels were increased in asthmatic mice and the cytokine is known to play a critical role during eosinophilic inflammation in asthmatic patients [199], it may contribute to the shaping of the asthma phenotype. Therefore, its therapeutical use to improve antipneumococcal immunity in asthmatic patients is debatable.

These data suggest that HDM-induced murine allergic asthma promotes pneumococcal colonization of the URT. Moreover, the antibacterial effect of IFN-γ observed in non-asthmatic mice could not be reproduced in asthmatic mice.

6.3 Aim 3: Analyse the influence of human allergic and non-allergic asthma on secretory immunity and microbiota composition in the upper airways.

Impact of human asthma on the airway-associated secretory immunity

The third aim of this thesis was to analyse the impact of allergic *vs.* non-allergic asthma on the secretory immunity and microbiota composition in the human URT, which is still a widely unexplored topic. The human nasopharynx is considered a place of allergen sensitization during asthma development as well as an entry site and natural reservoir for respiratory pathogens [142]. Since first contact to aeroallergens takes place here, analysis of its microenvironment in frame of asthma has a high clinical relevance.

In this study, patients that exhibit other diseases that affect respiratory parameters or the immune system in general (*e.g.* COPD, cancer, diabetes mellitus, autoimmune diseases, chronic cardiac insufficiency) or are in a certain life situation (nicotine consumption, pregnancy) were excluded to prevent bias of the data. Moreover, by subdividing the patients into exogenous and endogenous asthmatics, it was possible to analyse whether the nasal microenvironment is affected by the reactivity to aeroallergens. It is known that asthmatic patients exhibit decreased bronchial PIGR expression that is associated with impaired epithelial IgA secretion in lung [44]. Interestingly, there were no significant differences in gene and protein expression levels of *PIGR*/PIGR in nasal epithelial cell biopsies between healthy and asthmatic individuals as well as between the asthma subgroups. This suggests that *PIGR*/PIGR expression in the human nasopharynx is unaffected by asthmatic disease. Moreover, nasal *PIGR*/PIGR expression seems to be independent of the reactivity against aeroallergens within the asthma cohort. These hypotheses are supported by the fact that nasal SIgA levels were unaltered between healthy and asthmatic subjects as well as between the asthma subgroups. The fact that secretory immunity in the LRT of asthmatics is impaired, while it is unaltered in the URT suggests that the effect asthma has on secretory immunity is site-specific and might be facilitated by asthma characteristics that are mainly found in the LRT (*e.g.* goblet cell hyperplasia, epithelial thickening) [200]. Increased total and aeroallergen-specific IgE was observed in the sera of asthmatic patients compared to healthy subjects, which is in line with previously published data [163]. However, nasal mucosal IgE levels were unaltered between these groups, which suggests that the effects causing systemic IgE increase have no impact on nasal

IgE levels. Furthermore, increased amounts of IgG2 were detected in exogenous and endogenous asthmatics and the combined asthma group compared to the healthy subjects, whereas IgG1, IgG3 and IgG4 levels were unchanged between the groups. Since IgG2 is targeted against bacterial polysaccharides [172], it is conceivable that the increased IgG2 levels are a reaction to an altered microbial flora in these asthmatic cohorts.

Impact of human asthma on the respiratory microbiota composition

It was shown that asthmatic patients exhibit increased microbial diversity in the lower airways [133]. However, knowledge on microbial diversity in the upper airways of asthmatics is still fragmentary. Here, asthmatic patients that show reactivity to aeroallergens (exogenous and mixed subgroup) exhibited increased microbial diversity in the URT. However, there was no correlation between this and the amount of nasal IgG2, indicating that nasal microbial diversity is not impacted by increased amounts of antimicrobial immunoglobulins and *vice versa*. It is more likely that the increased diversity is caused by asthma characteristics found exclusively in patients with and exogenous or mixed asthma phenotype (*e.g.* reactivity to aeroallergens). The decreased abundance of Corynebacteriaceae as well as the increased abundance of Prevotellaceae and Burkholderiaceae observed in the upper airways of asthmatic patients is in line with previously published literature [130]. However, abundance increase of the other bacteria families in the upper airways of asthmatics has not been described before.

Taken together, these results suggest that asthma disrupts the microbial equilibrium of the URT, which is comparable to the effect described in the LRT. Interestingly and in stark contrast to the lower airways however, microbial alterations in the upper airways were not associated with changes regarding PIGR-mediated secretory immunity. This suggests that the role of secretory immunity for microbial homeostasis in the URT might be less important than in the LRT. Since increased microbiota diversity was observed exclusively in exogenous and mixed asthmatics, it would be of high interest to analyse possible correlations between the degree of aeroallergen-reactivity and microbiota diversity as well as microbiota composition.

7 Appendix

7.1 References

[1] E Fröhlich, A Mercuri, S Wu and S Salar-Behzadi. Measurements of deposition, lung surface area and lung fluid for simulation of inhaled compounds. *Frontiers in pharmacology*, 7:181, 2016.

[2] A Patwa and A Shah. Anatomy and physiology of respiratory system relevant to anaesthesia. *Indian journal of anaesthesia*, 59(9):533–541, 2015.

[3] RG Crystal, SH Randell, JF Engelhardt, J Voynow and ME Sunday. Airway epithelial cells: current concepts and challenges. *Proceedings of the American Thoracic Society*, 5(7):772–777, 2008.

[4] WM Haschek., editor. *Handbook of toxicologic pathology*. Academic Press, San Diego, 2. ed. edition, 20XX-.

[5] DF Rogers. The airway goblet cell. *The International Journal of Biochemistry & Cell Biology*, 35(1):1–6, 2003.

[6] MJ Sanderson and ER Dirksen. Mechanosensitivity of cultured ciliated cells from the mammalian respiratory tract: implications for the regulation of mucociliary transport. *Proceedings of the National Academy of Sciences of the United States of America*, 83(19):7302–7306, 1986.

[7] W Hicks, L Hall, L Sigurdson, C Stewart, R Hard, J Winston and J Lwebuga-Mukasa. Isolation and characterization of basal cells from human upper respiratory epithelium. *Experimental cell research*, 237(2):357–363, 1997.

[8] C Hideki, O Makoto, M Masaki, K Takashi and S Norimasa. Transmembrane proteins of tight junctions. *Biochimica et biophysica acta*, 1778(3):588–600, 2008.

[9] B Gumbiner. Structure, biochemistry, and assembly of epithelial tight junctions. *The American journal of physiology*, 253(6 Pt 1):C749–58, 1987.

[10] S Tsukita and M Furuse. Occludin and claudins in tight-junction strands: leading or supporting players? *Trends in Cell Biology*, 9(7):268–273, 1999.

[11] MJ LaFemina, KM Sutherland, T Bentley, LW Gonzales, L Allen, CJ Chapin, D Rokkam, KA Sweerus, LG Dobbs, PL Ballard and JA Frank. Claudin-18 deficiency results in alveolar barrier dysfunction and impaired alveologenesis in mice. *American journal of respiratory cell and molecular biology*, 51(4):550–558, 2014.

[12] TB Clarke, N Francella, A Huegel and JN Weiser. Invasive bacterial pathogens exploit tlr-mediated downregulation of tight junction components to facilitate translocation across the epithelium. *Cell host & microbe*, 9(5):404–414, 2011.

[13] S Varsano, I Frolkis, L Rashkovsky, D Ophir and Z Fishelson. Protection of human nasal respiratory epithelium from complement-mediated lysis by cell-membrane regulators of complement activation. *American journal of respiratory cell and molecular biology*, 15(6):731–737, 1996.

[14] HS Kulkarni, MK Liszewski, SL Brody and JP Atkinson. The complement system in the airway epithelium: An overlooked host defense mechanism and therapeutic target? *The Journal of allergy and clinical immunology*, 141(5):1582–1586.e1, 2018.

[15] R Bals. Epithelial antimicrobial peptides in host defense against infection. *Respiratory research*, 1(3):141–150, 2000.

[16] PR Mills, RJ Davies and JL Devalia. Airway epithelial cells, cytokines, and pollutants. *American journal of respiratory and critical care medicine*, 160(5 Pt 2):S38–43, 1999.

[17] CA Janeway, Jr, P Travers, M Walport and MJ Shlomchik. *Immunobiology: The immune system in health and disease*. Garland Publ, New York, NY, 5. ed. edition, 2001.

[18] JRC García, A Krause, S Schulz, FJ Rodríguez-Jiménez, E Klüver, K Adermann, U Forssmann, A Frimpong-Boateng, R Bals and WG Forssmann. Human β–defensin 4: a novel inducible peptide with a specific salt–sensitive spectrum of antimicrobial activity. *The FASEB Journal*, 15(10):1819–1821, 2001.

[19] SM Travis, PK Singh and MJ Welsh. Antimicrobial peptides and proteins in the innate defense of the airway surface. *Current Opinion in Immunology*, 13(1):89–95, 2001.

[20] JR Luque-Ortega, W van't Hof, ECI Veerman, JM Saugar and L Rivas. Human antimicrobial peptide histatin 5 is a cell-penetrating peptide targeting mitochondrial atp synthesis in leishmania. *The FASEB Journal*, 22(6):1817–1828, 2008.

[21] WH Man, P Steenhuijsen, AA de Wouter and D Bogaert. The microbiota of the respiratory tract: gatekeeper to respiratory health. *Nature reviews. Microbiology*, 15(5):259–270, 2017.

[22] HW Schroeder and L Cavacini. Structure and function of immunoglobulins. *The Journal of allergy and clinical immunology*, 125(2 Suppl 2):S41–52, 2010.

[23] R Geisberger, M Lamers and G Achatz. The riddle of the dual expression of igm and igd. *Immunology*, 118(4):429–437, 2006.

[24] M Boes. Role of natural and immune igm antibodies in immune responses. *Molecular Immunology*, 37(18):1141–1149, 2000.

[25] ME Koshland. The coming of age of the immunoglobulin j chain. *Annual review of immunology*, 3:425–453, 1985.

[26] NJ Dimmock. Mechanisms of neutralization of animal viruses. *The Journal of general virology*, 65 (Pt 6):1015–1022, 1984.

[27] BJ Underdown and JM Schiff. Immunoglobulin a: strategic defense initiative at the mucosal surface. *Annual review of immunology*, 4:389–417, 1986.

[28] MR Neutra, P Michetti and JP Kraehenbuhl. Secretory immunoglobulin a: induction, biogenesis and function. *Physiology of the gastrointestinal tract*, 685, 1994.

[29] KE Mostov, JP Kraehenbuhl and G Blobel. Receptor-mediated transcellular transport of immunoglobulin: synthesis of secretory component as multiple and larger transmembrane forms. *Proceedings of the National Academy of Sciences of the United States of America*, 77(12):7257–7261, 1980.

[30] A Phalipon and B Corthésy. Novel functions of the polymeric ig receptor: well beyond transport of immunoglobulins. *Trends in Immunology*, 24(2):55–58, 2003.

[31] CS Kaetzel and K Mostov. Immunoglobulin transport and the polymeric immunoglobulin receptor. In *Mucosal Immunology*, pages 211–250. Elsevier, 2005.

[32] CS Kaetzel. The polymeric immunoglobulin receptor: bridging innate and adaptive immune responses at mucosal surfaces. *Immunological reviews*, 206:83–99, 2005.

[33] KE Mostov. Transepithelial transport of immunoglobulins. *Annual review of immunology*, 12:63–84, 1994.

[34] A Almogren, BW Senior, LM Loomes and MA Kerr. Structural and functional consequences of cleavage of human secretory and human serum immunoglobulin a1 by proteinases from proteus mirabilis and neisseria meningitidis. *Infection and immunity*, 71(6):3349–3356, 2003.

[35] P Crottet and B Corthésy. Secretory component delays the conversion of secretory iga into antigen-binding competent f(ab')2: a possible implication for mucosal defense. *Journal of immunology (Baltimore, Md. : 1950)*, 161(10):5445–5453, 1998.

[36] A Phalipon, A Cardona, JP Kraehenbuhl, L Edelman, PJ Sansonetti and B Corthésy. Secretory component. *Immunity*, 17(1):107–115, 2002.

[37] C Pilette, Y Ouadrhiri, V Godding, JP Vaerman and Y Sibille. Lung mucosal immunity: immunoglobulin-a revisited. *The European respiratory journal*, 18(3):571–588, 2001.

[38] GH Jorgensen, A Gardulf, MI Sigurdsson, S Th Sigurdardottir, I Thorsteinsdottir, S Gudmundsson, L Hammarström and BR Ludviksson. Clinical symptoms in adults with selective iga deficiency: a case-control study. *Journal of clinical immunology*, 33(4):742–747, 2013.

[39] Y Fukuyama, JD King, K Kataoka, R Kobayashi, RS Gilbert, K Oishi, SK Hollingshead, DE Briles and K Fujihashi. Secretory-iga antibodies play an important role in the immunity to streptococcus pneumoniae. *Journal of immunology (Baltimore, Md. : 1950)*, 185(3):1755–1762, 2010.

[40] A Tjärnlund, A Rodríguez, PJ Cardona, E Guirado, J Ivanyi, M Singh, M Troye-Blomberg and C Fernández. Polymeric igr knockout mice are more susceptible to mycobacterial infections in the respiratory tract than wild-type mice. *International immunology*, 18(5):807–816, 2006.

[41] BW Richmond, RM Brucker, W Han, RH Du, Y Zhang, DS Cheng, L Gleaves, R Abdolrasulnia, D Polosukhina, PE Clark, SR Bordenstein, TS Blackwell and VV Polosukhin. Airway bacteria drive a progressive copd-like phenotype in mice with polymeric immunoglobulin receptor deficiency. *Nature communications*, 7:11240, 2016.

[42] VV Polosukhin, BW Richmond, RH Du, JM Cates, P Wu, H Nian, PP Massion, LB Ware, JW Lee, AV Kononov, WE Lawson and TS Blackwell. Secretory iga deficiency in individual small airways is associated with persistent inflammation and remodeling. *American journal of respiratory and critical care medicine*, 195(8):1010–1021, 2017.

[43] ST Gohy, BR Detry, M Lecocq, C Bouzin, BA Weynand, GD Amatngalim, YM Sibille and C Pilette. Polymeric immunoglobulin receptor down-regulation in chronic obstructive pulmonary disease. persistence in the cultured epithelium and role of transforming growth factor-β. *American journal of respiratory and critical care medicine*, 190(5):509–521, 2014.

[44] MZ Ladjemi, D Gras, S Dupasquier, B Detry, M Lecocq, C Garulli, C Fregimilicka,C Bouzin, S Gohy, P Chanez and C Pilette. Bronchial epithelial iga secretion is impaired in asthma. role of il-4/il-13. *American journal of respiratory and critical care medicine*, 197(11):1396–1409, 2018.

[45] Tracey A. Schneeman, Maria E. C. Bruno, Hilde Schjerven, Finn-Eirik Johansen, Laura Chady, and Charlotte S. Kaetzel. Regulation of the polymeric ig receptor by signaling through tlrs 3 and 4: linking innate and adaptive immune responses. *Journal of immunology (Baltimore, Md. : 1950)*, 175(1):376–384, 2005.

[46] M. E. C. Bruno, A. L. Frantz, E. W. Rogier, F-E Johansen, and C. S. Kaetzel. Regulation of the polymeric immunoglobulin receptor by the classical and alternative nf-ϰb pathways in intestinal epithelial cells. *Mucosal immunology*, 4(4):468–478, 2011.

[47] KR Youngman, C Fiocchi and CS Kaetzel. Inhibition of ifn-gamma activity in supernatants from stimulated human intestinal mononuclear cells prevents up-regulation of the polymeric

ig receptor in an intestinal epithelial cell line. *Journal of immunology (Baltimore, Md. : 1950)*, 153(2):675–681, 1994.

[48] JO Phillips, MP Everson, Z Moldoveanu, C Lue and J Mestecky. Synergistic effect of il-4 and ifn-gamma on the expression of polymeric ig receptor (secretory component) and iga binding by human epithelial cells. *Journal of immunology (Baltimore, Md. : 1950)*, 145(6):1740–1744, 1990.

[49] D Kvale, D Løvhaug, LM Sollid and P Brandtzaeg. Tumor necrosis factor-alpha up-regulates expression of secretory component, the epithelial receptor for polymeric ig. *Journal of immunology (Baltimore, Md. : 1950)*, 140(9):3086–3089, 1988.

[50] LM Sollid, D Kvale, P Brandtzaeg, G Markussen and E Thorsby. Interferon-gamma enhances expression of secretory component, the epithelial receptor for polymeric immunoglobulins. *Journal of immunology (Baltimore, Md. : 1950)*, 138(12):4303–4306, 1987.

[51] JF Piskurich, JA France, CM Tamer, CA Willmer, CS Kaetzel and DM Kaetzel. Interferon-γ induces polymeric immunoglobulin receptor mrna in human intestinal epithelial cells by a protein synthesis dependent mechanism. *Molecular Immunology*, 30(4):413–421, 1993.

[52] SS Braman. The global burden of asthma. *Chest*, 130(1 Suppl):4S–12S, 2006.

[53] CM Averell, D Hinds, J Fairburn-Beech, B Wu and R Lima. Characteristics of treated asthmatics experiencing exacerbations in a us database: A retrospective cohort study. *Journal of asthma and allergy*, 14:755–771, 2021.

[54] G Globe, M Martin, M Schatz, I Wiklund, J Lin, R von Maltzahn and MS Mattera. Symptoms and markers of symptom severity in asthma–content validity of the asthma symptom diary. *Health and quality of life outcomes*, 13:21, 2015.

[55] AR Rubinfeld and MCF Pain. Perception of asthma. *The Lancet*, 307(7965):882–884, 1976.

[56] JA Krishnan, RF Lemanske, GJ Canino, KS Elward, M Kattan, EC Matsui, H Mitchell, ER Sutherland and M Minnicozzi. Asthma outcomes: symptoms. *The Journal of allergy and clinical immunology*, 129(3 Suppl):S124–35, 2012.

[57] KF Rabe, M Adachi, CKW Lai, JB Soriano, PA Vermeire, KB Weiss and ST Weiss. Worldwide severity and control of asthma in children and adults: the global asthma insights and reality surveys. *The Journal of allergy and clinical immunology*, 114(1):40–47, 2004.

[58] T Plattsmills, P Heymann, J Longbottom and S Wilkins. Airborne allergens associated with asthma: Particle sizes carrying dust mite and rat allergens measured with a cascade impactor. *Journal of Allergy and Clinical Immunology*, 77(6):850–857, 1986.

[59] R Voorhorst, FThM Spieksma, H Varekamp, MJ Leupen and AW Lyklema. The house-dust mite (dermatophagoides pteronyssinus) and the allergens it produces. identity with the house-dust allergen. *Journal of Allergy*, 39(6):325–339, 1967.

[60] LG Arlian and TA Platts-Mills. The biology of dust mites and the remediation of mite allergens in allergic disease. *Journal of Allergy and Clinical Immunology*, 107(3 Suppl):S406–13, 2001.

[61] CA Herbert, ST Holgate, C Robinson, PJ Thompson and GA Stewart. Effect of mite allergen on permeability of bronchial mucosa. *The Lancet*, 336(8723):1132, 1990.

[62] CA Herbert, CM King, PC Ring, ST Holgate, GA Stewart, PJ Thompson and C Robinson. Augmentation of permeability in the bronchial epithelium by the house dust mite allergen der p1. *American journal of respiratory cell and molecular biology*, 12(4):369–378, 1995.

[63] CR Hewitt, AP Brown, BJ Hart and DI Pritchard. A major house dust mite allergen disrupts the immunoglobulin e network by selectively cleaving cd23: innate protection by antiproteases. *The Journal of experimental medicine*, 182(5):1537–1544, 1995.

[64] NA Kalsheker, S Deam, L Chambers, S Sreedharan, K Brocklehurst and DA Lomas. The house dust mite allergen der p1 catalytically inactivates alpha 1-antitrypsin by specific reactive centre loop cleavage: a mechanism that promotes airway inflammation and asthma. *Biochemical and biophysical research communications*, 221(1):59–61, 1996.

[65] A Jacquet. Innate immune responses in house dust mite allergy. *ISRN allergy*, 2013:735031, 2013.

[66] V Kaza, V Bandi and KK Guntupalli. Acute severe asthma: recent advances. *Current opinion in pulmonary medicine*, 13(1):1–7, 2007.

[67] HP Lambert and H Stern. Infective factors in exacerbations of bronchitis and asthma. *British medical journal*, 3(5822):323–327, 1972.

[68] TE Minor. Viruses as precipitants of asthmatic attacks in children. *JAMA: The Journal of the American Medical Association*, 227(3):292, 1974.

[69] PJM Openshaw and M Turner-Warwick. Observations on sputum production in patients with variable airflow obstruction; implications for the diagnosis of asthma and chronic bronchitis. *Respiratory Medicine*, 83(1):25–31, 1989.

[70] DJ Jackson, A Sykes, P Mallia and SL Johnston. Asthma exacerbations: origin, effect, and prevention. *The Journal of allergy and clinical immunology*, 128(6):1165–1174, 2011.

[71] Y Zhao, J Yang, YD Gao and W Guo. Th17 immunity in patients with allergic asthma. *International archives of allergy and immunology*, 151(4):297–307, 2010.

[72] S Romagnani, P Parronchi, MM D'Elios, P Romagnani, F Annunziato, MP Piccinni, R Manetti, S Sampognaro, C Mavilia, M de Carli, E Maggi and GF Del Prete. An update on human th1 and th2 cells. *International archives of allergy and immunology*, 113(1-3):153–156, 1997.

[73] THM Ottenhoff, D Kumararatne and JL Casanova. Novel human immunodeficiencies reveal the essential role of type-1 cytokines in immunity to intracellular bacteria. *Immunology Today*, 19(11):491–494, 1998.

[74] RL Modlin and TB Nutman. Type 2 cytokines and negative immune regulation in human infections. *Current Opinion in Immunology*, 5(4):511–517, 1993.

[75] TA Wynn. Type 2 cytokines: mechanisms and therapeutic strategies. *Nature reviews. Immunology*, 15(5):271–282, 2015.

[76] D Robinson, S Ying, A Bentley, Q Meng, J North, S Durham, A Kay and Q Hamid. Relationships among numbers of bronchoalveolar lavage cells expressing messenger ribonucleic acid

for cytokines, asthma symptoms, and airway methacholine responsiveness in atopic asthma. *Journal of Allergy and Clinical Immunology*, 92(3):397–403, 1993.

[77] N Krug, VJ Erpenbeck, K Balke, J Petschallies, T Tschernig, JM Hohlfeld and H Fabel. Cytokine profile of bronchoalveolar lavage-derived cd4(+), cd8(+), and gammadelta t cells in people with asthma after segmental allergen challenge. *American journal of respiratory cell and molecular biology*, 25(1):125–131, 2001.

[78] C Zuany-Amorim, C Ruffié, S Hailé, BB Vargaftig, P Pereira and M Pretolani. Requirement for gammadelta t cells in allergic airway inflammation. *Science (New York, N.Y.)*, 280(5367):1265–1267, 1998.

[79] G Brusselle, J Kips, G Joos, H Bluethmann and R Pauwels. Allergen-induced airway inflammation and bronchial responsiveness in wild-type and interleukin-4-deficient mice. *American journal of respiratory cell and molecular biology*, 12(3):254–259, 1995.

[80] JW Park, C Taube, ES Yang, A Joetham, A Balhorn, K Takeda, N Miyahara, A Dakhama, DD Donaldson and EW Gelfand. Respiratory syncytial virus-induced airway hyperresponsiveness is independent of il-13 compared with that induced by allergen. *Journal of Allergy and Clinical Immunology*, 112(6):1078–1087, 2003.

[81] PS Foster, SP Hogan, AJ Ramsay, KI Matthaei and IG Young. Interleukin 5 deficiency abolishes eosinophilia, airways hyperreactivity, and lung damage in a mouse asthma model. *The Journal of experimental medicine*, 183(1):195–201, 1996.

[82] JJ Lee, D Dimina, MP Macias, SI Ochkur, MP McGarry, KR O'Neill, C Protheroe, R Pero, T Nguyen, SA Cormier, E Lenkiewicz, D Colbert, L Rinaldi, SJ Ackerman, CG Irvin and NA Lee. Defining a link with asthma in mice congenitally deficient in eosinophils. *Science (New York, N.Y.)*, 305(5691):1773–1776, 2004.

[83] A KleinJan, MD Dijkstra, SS Boksa, LWFM Severijnen, PGH Mulder and WJ Fokkens. Increase in il-8, il-10, il-13, and rantes mrna levels (in situ hybridization) in the nasal mucosa after nasal allergen provocation. *Journal of Allergy and Clinical Immunology*, 103(3):441–450, 1999.

[84] S Lajoie, IP Lewkowich, Y Suzuki, JR Clark, AA Sproles, K Dienger, AL Budelsky and M Wills-Karp. Complement-mediated regulation of the il-17a axis is a central genetic determinant of the severity of experimental allergic asthma. *Nature immunology*, 11(10):928–935, 2010.

[85] C Doe, M Bafadhel, S Siddiqui, D Desai, V Mistry, P Rugman, M McCormick, J Woods, R May, MA Sleeman, IK Anderson and CE Brightling. Expression of the t helper 17-associated cytokines il-17a and il-17f in asthma and copd. *Chest*, 138(5):1140–1147, 2010.

[86] L Maddox and DA Schwartz. The pathophysiology of asthma. *Annual review of medicine*, 53:477–498, 2002.

[87] S Romanet-Manent, D Charpin, A Magnan, A Lanteaume and D Vervloet. Allergic vs nonallergic asthma: what makes the difference? *Allergy*, 57(7):607–613, 2002.

[88] J Bousquet, P van Cauwenberge and N Khaltaev. Allergic rhinitis and its impact on asthma. *Journal of Allergy and Clinical Immunology*, 108(5 Suppl):S147–334, 2001.

[89] N Novak and T Bieber. Allergic and nonallergic forms of atopic diseases. *Journal of Allergy and Clinical Immunology*, 112(2):252–262, 2003.

[90] M Schatz and L Rosenwasser. The allergic asthma phenotype. *The journal of allergy and clinical immunology. In practice*, 2(6):645–8; quiz 649, 2014.

[91] D Raedler, N Ballenberger, E Klucker, A Böck, R Otto, O Da Prazeres Costa, O Holst, T Illig, T Buch, E von Mutius and B Schaub. Identification of novel immune phenotypes for allergic and nonallergic childhood asthma. *The Journal of allergy and clinical immunology*, 135(1):81–91, 2015.

[92] SP Peters. Asthma phenotypes: nonallergic (intrinsic) asthma. *The journal of allergy and clinical immunology. In practice*, 2(6):650–652, 2014.

[93] VV Jain, B Abejie, MH Bashir, T Tyner and J Vempilly. Lung volume abnormalities and its correlation to spirometric and demographic variables in adult asthma. *The Journal of asthma : official journal of the Association for the Care of Asthma*, 50(6):600–605, 2013.

[94] DN Payne, IM Adcock, NM Wilson, T Oates, M Scallan and A Bush. Relationship between exhaled nitric oxide and mucosal eosinophilic inflammation in children with difficult asthma, after treatment with oral prednisolone. *American journal of respiratory and critical care medicine*, 164(8 Pt 1):1376–1381, 2001.

[95] A Jatakanon, S Lim, SA Kharitonov, KF Chung and PJ Barnes. Correlation between exhaled nitric oxide, sputum eosinophils, and methacholine responsiveness in patients with mild asthma. *Thorax*, 53(2):91–95, 1998.

[96] F Hargreave, G Ryan, N Thomson, P Obyrne, K Latimer, E Juniper and J Dolovich. Bronchial responsiveness to histamine or methacholine in asthma: measurement and clinical significance. *Journal of Allergy and Clinical Immunology*, 68(5):347–355, 1981.

[97] PJ Barnes. Glucocorticosteroids: current and future directions. *British journal of pharmacology*, 163(1):29–43, 2011.

[98] RC Strunk and GR Bloomberg. Omalizumab for asthma. *The New England journal of medicine*, 354(25):2689–2695, 2006.

[99] TR Talbot, TV Hartert, E Mitchel, NB Halasa, PG Arbogast, KA Poehling, W Schaffner, AS Craig and MR Griffin. Asthma as a risk factor for invasive pneumococcal disease. *The New England journal of medicine*, 352(20):2082–2090, 2005.

[100] YJ Juhn, H Kita, BP Yawn, TG Boyce, KH Yoo, ME McGree, AL Weaver, P Wollan and RM Jacobson. Increased risk of serious pneumococcal disease in patients with asthma. *The Journal of allergy and clinical immunology*, 122(4):719–723, 2008.

[101] KJ Ryan., editor. *Sherris medical microbiology: An introduction to infectious diseases*. McGraw-Hill, New York, 4th ed. edition, 2004.

[102] R Austrian. Pneumococcal pneumonia. diagnostic, epidemiologic, therapeutic and prophylactic considerations. *Chest*, 90(5):738–743, 1986.

[103] V Bohr, OB Paulson and N Rasmussen. Pneumococcal meningitis. late neurologic sequelae and features of prognostic impact. *Archives of neurology*, 41(10):1045–1049, 1984.

[104] JT Macfarlane, MJ Ward, RG Finch and AD Macrae. Hospital study of adult community-acquired pneumonia. *The Lancet*, 320(8292):255–258, 1982.

[105] A Håkansson, I Carlstedt, J Davies, AK Mossberg, H Sabharwal and C Svanborg. Aspects on the interaction of streptococcus pneumoniae and haemophilus influenzae with human respiratory tract mucosa. *American journal of respiratory and critical care medicine*, 154(4 Pt 2):S187–91, 1996.

[106] C Feldman, R Read, A Rutman, PK Jeffery, A Brain, V Lund, TJ Mitchell, PW Andrew, GJ Boulnois and HC Todd. The interaction of streptococcus pneumoniae with intact human respiratory mucosa in vitro. *The European respiratory journal*, 5(5):576–583, 1992.

[107] B Andersson, EH Beachey, A Tomasz, E Tuomanen and C Svanborg-Edén. A sandwich adhesin on streptococcus pneumoniae attaching to human oropharyngeal epithelial cells in vitro. *Microbial Pathogenesis*, 4(4):267–278, 1988.

[108] JC Knecht, G Schiffman and R Austrian. Some biological properties of pneumococcus type 37 and the chemistry of its capsular polysaccharide. *The Journal of experimental medicine*, 132(3):475–487, 1970.

[109] A Tomasz. Choline in the cell wall of a bacterium: novel type of polymer-linked choline in pneumococcus. *Science (New York, N.Y.)*, 157(3789):694–697, 1967.

[110] M Sundberg-Kövamees, T Holme and A Sjögren. Interaction of the c-polysaccharide of streptococcus pneumoniae with the receptor asialo-gm1. *Microbial Pathogenesis*, 21(4):223–234, 1996.

[111] EA de Velasco, D Merkus, S Anderton, AF Verheul, EF Lizzio, R van der Zee, W van Eden, T Hoffman, J Verhoef and H Snippe. Synthetic peptides representing t-cell epitopes act as carriers in pneumococcal polysaccharide conjugate vaccines. *Infection and immunity*, 63(3):961–968, 1995.

[112] JR Catterall. Streptococcus pneumoniae. *Thorax*, 54(10):929–937, 1999.

[113] JB Rubins and EN Janoff. Pneumolysin: A multifunctional pneumococcal virulence factor. *Journal of Laboratory and Clinical Medicine*, 131(1):21–27, 1998.

[114] PC Appelbaum. Epidemiology and in vitro susceptibility of drug-resistant streptococcus pneumoniae. *The Pediatric infectious disease journal*, 15(10):932–934, 1996.

[115] J Eskola and M Anttila. Pneumococcal conjugate vaccines. *The Pediatric infectious disease journal*, 18(6):543–551, 1999.

[116] S Hammerschmidt, SR Talay, P Brandtzaeg and GS Chhatwal. Spsa, a novel pneumococcal surface protein with specific binding to secretory immunoglobulin a and secretory component. *Molecular microbiology*, 25(6):1113–1124, 1997.

[117] S Hammerschmidt, MP Tillig, S Wolff, JP Vaerman and GS Chhatwal. Species-specific binding of human secretory component to spsa protein of streptococcus pneumoniae via a hexapeptide motif. *Molecular microbiology*, 36(3):726–736, 2000.

[118] JR Zhang, KE Mostov, ME Lamm, M Nanno, SI Shimida, M Ohwaki and E Tuomanen. The polymeric immunoglobulin receptor translocates pneumococci across human nasopharyngeal epithelial cells. *Cell*, 102(6):827–837, 2000.

[119] SC Brock, PA McGraw, PF Wright and JE Crowe. The human polymeric immunoglobulin receptor facilitates invasion of epithelial cells by streptococcus pneumoniae in a strain-specific and cell type-specific manner. *Infection and immunity*, 70(9):5091–5095, 2002.

[120] G Pulvirenti, GF Parisi, A Giallongo, M Papale, S Manti, S Savasta, A Licari, GL Marseglia and S Leonardi. Lower airway microbiota. *Frontiers in pediatrics*, 7:393, 2019.

[121] L Dethlefsen, M McFall-Ngai and DA Relman. An ecological and evolutionary perspective on human-microbe mutualism and disease. *Nature*, 449(7164):811–818, 2007.

[122] J Durack, HA Boushey and SV Lynch. Airway microbiota and the implications of dysbiosis in asthma. *Current allergy and asthma reports*, 16(8):52, 2016.

[123] K Hasegawa and CA Camargo. Airway microbiota and acute respiratory infection in children. *Expert review of clinical immunology*, 11(7):789–792, 2015.

[124] RP Dickson, JR Erb-Downward, FJ Martinez and GB Huffnagle. The microbiome and the respiratory tract. *Annual review of physiology*, 78:481–504, 2016.

[125] RP Dickson, JR Erb-Downward, CM Freeman, N Walker, BS Scales, JM Beck, FJ Martinez, JL Curtis, VN Lama and GB Huffnagle. Changes in the lung microbiome following lung transplantation include the emergence of two distinct pseudomonas species with distinct clinical associations. *PloS one*, 9(5):e97214, 2014.

[126] LN Segal, AV Alekseyenko, JC Clemente, R Kulkarni, B Wu, Z Gao, H Chen, KI Berger, RM Goldring, WN Rom, MJ Blaser and MD Weiden. Enrichment of lung microbiome with supraglottic taxa is associated with increased pulmonary inflammation. *Microbiome*, 1(1):19, 2013.

[127] A Morris, JM Beck, PD Schloss, TB Campbell, K Crothers, JL Curtis, SC Flores, AP Fontenot, E Ghedin, L Huang, K Jablonski, E Kleerup, SV Lynch, E Sodergren, H Twigg, VB Young, CM Bassis, A Venkataraman, TM Schmidt and GM Weinstock. Comparison of the respiratory microbiome in healthy nonsmokers and smokers. *American journal of respiratory and critical care medicine*, 187(10):1067–1075, 2013.

[128] RP Dickson, JR Erb-Downward, CM Freeman, L McCloskey, JM Beck, GB Huffnagle and JL Curtis. Spatial variation in the healthy human lung microbiome and the adapted island model of lung biogeography. *Annals of the American Thoracic Society*, 12(6):821–830, 2015.

[129] MJ Mammen and S Sethi. Copd and the microbiome. *Respirology (Carlton, Vic.)*, 21(4):590–599, 2016.

[130] P Losol, JP Choi, SH Kim and YS Chang. The role of upper airway microbiome in the development of adult asthma. *Immune network*, 21(3):e19, 2021.

[131] PR Marri, DA Stern, AL Wright, D Billheimer and FD Martinez. Asthma-associated differences in microbial composition of induced sputum. *The Journal of allergy and clinical immunology*, 131(2):346–52.e1–3, 2013.

[132] M Hilty, C Burke, H Pedro, P Cardenas, A Bush, C Bossley, J Davies, A Ervine, L Poulter, L Pachter, MF Moffatt and WOC Cookson. Disordered microbial communities in asthmatic airways. *PloS one*, 5(1):e8578, 2010.

[133] YJ Huang, CE Nelson, EL Brodie, TZ Desantis, MS Baek, J Liu, T Woyke, M Allgaier, J Bristow, JP Wiener-Kronish, ER Sutherland, TS King, N Icitovic, RJ Martin, WJ Calhoun, M Castro, LC Denlinger, E Dimango, M Kraft, SP Peters, SI Wasserman, ME Wechsler, HA Boushey and SV Lynch. Airway microbiota and bronchial hyperresponsiveness in patients with suboptimally controlled asthma. *The Journal of allergy and clinical immunology*, 127(2):372–381.e1–3, 2011.

[134] A Sandgren, B Albiger, CJ Orihuela, E Tuomanen, S Normark and B Henriques-Normark. Virulence in mice of pneumococcal clonal types with known invasive disease potential in humans. *The Journal of infectious diseases*, 192(5):791–800, 2005.

[135] KA Wikenheiser, DK Vorbroker, WR Rice, JC Clark, CJ Bachurski, HK Oie and JA Whitsett. Production of immortalized distal respiratory epithelial cell lines from surfactant protein c/simian virus 40 large tumor antigen transgenic mice. *Proceedings of the National Academy of Sciences of the United States of America*, 90(23):11029–11033, 1993.

[136] X Rao, X Huang, Z Zhou and X Lin. An improvement of the 2^(-delta delta ct) method for quantitative real-time polymerase chain reaction data analysis. *Biostatistics, bioinformatics and biomathematics*, 3(3):71–85, 2013.

[137] RC Edgar. Search and clustering orders of magnitude faster than blast. *Bioinformatics (Oxford, England)*, 26(19):2460–2461, 2010.

[138] C Quast, E Pruesse, P Yilmaz, J Gerken, T Schweer, P Yarza, J Peplies and FO Glöckner. The silva ribosomal rna gene database project: improved data processing and web-based tools. *Nucleic Acids Research*, 41(Database issue):D590–6, 2012.

[139] Q Wang, GM Garrity, JM Tiedje and JR Cole. Naive bayesian classifier for rapid assignment of rrna sequences into the new bacterial taxonomy. *Applied and environmental microbiology*, 73(16):5261–5267, 2007.

[140] PJ McMurdie and S Holmes. phyloseq: an r package for reproducible interactive analysis and graphics of microbiome census data. *PloS one*, 8(4):e61217, 2013.

[141] MZ Ladjemi, B Detry, D Gras, M Lecocq, S Dupasquier, J Mouthuy, C Fregimilicka, C Bouzin, H Bowen, H Gould, P Chanez and C Pilette. Impaired synthesis and transport of immunoglobulin a in severe asthma: Role of il-13. In *3.2 Airway Cell Biology and Immunopathology*, page PA5104. European Respiratory Society, 2015.

[142] K Trzciński, D Bogaert, A Wyllie, MLJN Chu, A van der Ende, JP Bruin, G van den Dobbelsteen, RH Veenhoven and EAM Sanders. Superiority of trans-oral over trans-nasal sampling in detecting streptococcus pneumoniae colonization in adults. *PloS one*, 8(3):e60520, 2013.

[143] K Rubin and S Glazer. The pertussis hypothesis: Bordetella pertussis colonization in the etiology of asthma and diseases of allergic sensitization. *Medical hypotheses*, 120:101–115, 2018.

[144] M Fazlollahi, TD Lee, J Andrade, K Oguntuyo, Y Chun, G Grishina, A Grishin and S Bunyavanich. The nasal microbiome in asthma. *The Journal of allergy and clinical immunology*, 142(3):834–843.e2, 2018.

[145] A Pausder, J Fricke, K Schughart, J Schreiber, T Strowig, D Bruder and JD Boehme. Exogenous and endogenous triggers differentially stimulate pigr expression and antibacterial secretory immunity in the murine respiratory tract. *Lung*, 200(1):119–128, 2022.

[146] AJ Macpherson and T Uhr. Induction of protective iga by intestinal dendritic cells carrying commensal bacteria. *Science (New York, N.Y.)*, 303(5664):1662–1665, 2004.

[147] I Ichimiya, H Kawauchi, T Fujiyoshi, T Tanaka and G Mogi. Distribution of immunocompetent cells in normal nasal mucosa: comparisons among germ-free, specific pathogen-free, and conventional mice. *The Annals of otology, rhinology, and laryngology*, 100(8):638–642, 1991.

[148] LV Hooper, MH Wong, A Thelin, L Hansson, PG Falk and JI Gordon. Molecular analysis of commensal host-microbial relationships in the intestine. *Science (New York, N.Y.)*, 291(5505):881–884, 2001.

[149] R Shimazu, S Akashi, H Ogata, Y Nagai, K Fukudome, K Miyake and M Kimoto. Md-2, a molecule that confers lipopolysaccharide responsiveness on toll-like receptor 4. *The Journal of experimental medicine*, 189(11):1777–1782, 1999.

[150] RR Ingalls, E Lien and DT Golenbock. Differential roles of tlr2 and tlr4 in the host response to gram-negative bacteria: lessons from a lipopolysaccharide-deficient mutant of neisseria meningitidis. *Journal of endotoxin research*, 6(5):411–415, 2000.

[151] EKH Schweda, JC Richards, DW Hood and ER Moxon. Expression and structural diversity of the lipopolysaccharide of haemophilus influenzae: implication in virulence. *International journal of medical microbiology : IJMM*, 297(5):297–306, 2007.

[152] C Moon, KL VanDussen, H Miyoshi and TS Stappenbeck. Development of a primary mouse intestinal epithelial cell monolayer culture system to evaluate factors that modulate iga transcytosis. *Mucosal immunology*, 7(4):818–828, 2014.

[153] Q Lei, F Qiang, C Du, W Di, Z Guoqian, Y Bo and Y Lina. Amelioration of hypoxia and lps-induced intestinal epithelial barrier dysfunction by emodin through the suppression of the nf-κb and hif-1α signaling pathways. *International journal of molecular medicine*, 34(6):1629–1639, 2014.

[154] F Rousset, E Garcia and J Banchereau. Cytokine-induced proliferation and immunoglobulin production of human b lymphocytes triggered through their cd40 antigen. *The Journal of experimental medicine*, 173(3):705–710, 1991.

[155] TB Issekutz, JM Stoltz and P vd Meide. Lymphocyte recruitment in delayed-type hypersensitivity. the role of ifn-gamma. *Journal of immunology (Baltimore, Md. : 1950)*, 140(9):2989–2993, 1988.

[156] JD Boehme, S Stegemann-Koniszewski, A Autengruber, N Peters, J Wissing, L Jänsch, A Jeron and D Bruder. Chronic lung inflammation primes humoral immunity and augments antipneumococcal resistance. *Scientific reports*, 7(1):4972, 2017.

[157] VV Polosukhin, JM Cates, WE Lawson, R Zaynagetdinov, AP Milstone, PP Massion, S Ocak, LB Ware, JW Lee, RP Bowler, AV Kononov, SH Randell and TS Blackwell. Bronchial

secretory immunoglobulin a deficiency correlates with airway inflammation and progression of chronic obstructive pulmonary disease. *American journal of respiratory and critical care medicine*, 184(3):317–327, 2011.

[158] S Bartel, N Schulz, F Alessandrini, AC Schamberger, P Pagel, FJ Theis, K Milger, E Noessner, SM Stick, A Kicic, O Eickelberg, RJ Freishtat and S Krauss-Etschmann. Pulmonary microrna profiles identify involvement of creb1 and sec14l3 in bronchial epithelial changes in allergic asthma. *Scientific reports*, 7:46026, 2017.

[159] B Machiels, M Dourcy, X Xiao, J Javaux, C Mesnil, C Sabatel, D Desmecht, F Lallemand, P Martinive, H Hammad, M Guilliams, B Dewals, A Vanderplasschen, BN Lambrecht, F Bureau and L Gillet. A gammaherpesvirus provides protection against allergic asthma by inducing the replacement of resident alveolar macrophages with regulatory monocytes. *Nature immunology*, 18(12):1310–1320, 2017.

[160] J Bousquet, P Chanez, JY Lacoste, G Barnéon, N Ghavanian, I Enander, P Venge, S Ahlstedt, J Simony-Lafontaine and P Godard. Eosinophilic inflammation in asthma. *The New England journal of medicine*, 323(15):1033–1039, 1990.

[161] PK Jeffery. Remodeling in asthma and chronic obstructive lung disease. *American journal of respiratory and critical care medicine*, 164(10 Pt 2):S28–38, 2001.

[162] RK Kumar. Understanding airway wall remodeling in asthma: a basis for improvements in therapy? *Pharmacology & Therapeutics*, 91(2):93–104, 2001.

[163] B Burrows, FD Martinez, M Halonen, RA Barbee and MG Cline. Association of asthma with serum ige levels and skin-test reactivity to allergens. *The New England journal of medicine*, 320(5):271–277, 1989.

[164] H Yssel and H Groux. Characterization of t cell subpopulations involved in the pathogenesis of asthma and allergic diseases. *International archives of allergy and immunology*, 121(1):10–18, 2000.

[165] O Kaminuma, A Mori, K Ogawa, A Nakata, H Kikkawa, K Ikezawa and H Okudaira. Cloned th cells confer eosinophilic inflammation and bronchial hyperresponsiveness. *International archives of allergy and immunology*, 118(2-4):136–139, 1999.

[166] WA Neveu, JL Allard, DM Raymond, LM Bourassa, SM Burns, JY Bunn, CG Irvin, DA Kaminsky and M Rincon. Elevation of il-6 in the allergic asthmatic airway is independent of inflammation but associates with loss of central airway function. *Respiratory research*, 11:28, 2010.

[167] L Guanghui, Z Rongfei and L Baozhu. Tnf-alpha and il-8 of the patients with allergic asthma. *Journal of Huazhong University of Science and Technology. Medical sciences = Hua zhong ke ji da xue xue bao. Yi xue Ying De wen ban = Huazhong keji daxue xuebao. Yixue Yingdewen ban*, 25(3):274–5, 309, 2005.

[168] DF Rogers. Airway mucus hypersecretion in asthma: an undervalued pathology? *Current opinion in pharmacology*, 4(3):241–250, 2004.

[169] DF Rogers. Airway goblet cells: responsive and adaptable front-line defenders. *The European respiratory journal*, 7(9):1690–1706, 1994.

[170] R Dajani, Y Zhang, PJ Taft, SM Travis, TD Starner, A Olsen, J Zabner, MJ Welsh and JF Engelhardt. Lysozyme secretion by submucosal glands protects the airway from bacterial infection. *American journal of respiratory cell and molecular biology*, 32(6):548–552, 2005.

[171] J Zebrak, T Herman, R Werys, J Pryjma and J Gaweł. Proteins in bronchial secretion of children with chronic pulmonary diseases. ii. relation to bronchoscopic and bronchographic examination. *Scandinavian journal of respiratory diseases*, 60(2):69–75, 1979.

[172] DJ Barrett and EM Ayoub. Igg2 subclass restriction of antibody to pneumococcal polysaccharides. *Clinical and experimental immunology*, 63(1):127–134, 1986.

[173] NH Khattar, SM Lele and CS Kaetzel. Down-regulation of the polymeric immunoglobulin receptor in non-small cell lung carcinoma: correlation with dysregulated expression of the transcription factors usf and ap2. *Journal of biomedical science*, 12(1):65–77, 2005.

[174] S Loman, HM Jansen, TA Out and R Lutter. Interleukin-4 and interferon-gamma synergistically increase secretory component gene expression, but are additive in stimulating secretory immunoglobulin a release by calu-3 airway epithelial cells. *Immunology*, 96(4):537–543, 1999.

[175] C Hupin, P Rombaux, H Bowen, H Gould, M Lecocq and C Pilette. Downregulation of polymeric immunoglobulin receptor and secretory iga antibodies in eosinophilic upper airway diseases. *Allergy*, 68(12):1589–1597, 2013.

[176] Z Jaffar, ME Ferrini, LA Herritt and K Roberts. Cutting edge: lung mucosal th17-mediated responses induce polymeric ig receptor expression by the airway epithelium and elevate secretory iga levels. *Journal of immunology (Baltimore, Md. : 1950)*, 182(8):4507–4511, 2009.

[177] M Carrasco-Yepez, R Campos-Rodriguez, I Lopez-Reyes, P Bonilla-Lemus, AY Rodriguez-Cortes, A Contis-Montes de Oca, A Jarillo-Luna, A Miliar-Garcia and S Rojas-Hernandez. Intranasal coadministration of cholera toxin with amoeba lysates modulates the secretion of iga and igg antibodies, production of cytokines and expression of pigr in the nasal cavity of mice in the model of naegleria fowleri meningoencephalitis. *Experimental parasitology*, 145 Suppl:S84–92, 2014.

[178] Y Ohashi, M Hiraguchi and K Ushida. The composition of intestinal bacteria affects the level of luminal iga. *Bioscience, biotechnology, and biochemistry*, 70(12):3031–3035, 2006.

[179] WAA de Steenhuijsen Piters, EAM Sanders and D Bogaert. The role of the local microbial ecosystem in respiratory health and disease. *Philosophical transactions of the Royal Society of London. Series B, Biological sciences*, 370(1675), 2015.

[180] Y Morinaga, Y Take, D Sasaki, K Ota, N Kaku, N Uno, K Sakamoto, K Kosai, T Miyazaki, H Hasegawa, K Izumikawa, H Mukae and K Yanagihara. Exploring the microbiota of upper respiratory tract during the development of pneumonia in a mouse model. *PloS one*, 14(9):e0222589, 2019.

[181] O Lüderitz, MA Freudenberg, C Galanos, V Lehmann, ET Rietschel and DH Shaw. Lipopolysaccharides of gram-negative bacteria. In *Membrane Lipids of Prokaryotes*, volume 17 of *Current Topics in Membranes and Transport*, pages 79–151. Elsevier, 1982.

[182] R Malley, P Henneke, SC Morse, MJ Cieslewicz, M Lipsitch, CM Thompson, E Kurt-Jones, JC Paton, MR Wessels and DT Golenbock. Recognition of pneumolysin by toll-like receptor 4 confers resistance to pneumococcal infection. *Proceedings of the National Academy of Sciences of the United States of America*, 100(4):1966–1971, 2003.

[183] E Lüllau, S Heyse, H Vogel, I Marison, U von Stockar, JP Kraehenbuhl and B Corthésy. Antigen binding properties of purified immunoglobulin a and reconstituted secretory immunoglobulin a antibodies. *The Journal of biological chemistry*, 271(27):16300–16309, 1996.

[184] M Deleuran, AR Ellingsen, K Paludan, C Schou and K Thestrup-Pedersen. Purified der p1 and p2 patch tests in patients with atopic dermatitis: evidence for both allergenicity and proteolytic irritancy. *ACTA DERMATOVENEREOLOGICA-STOCKHOLM-*, 78:241–244, 1998.

[185] M Humbert, SR Durham, S Ying, P Kimmitt, J Barkans, B Assoufi, R Pfister, G Menz, DS Robinson, AB Kay and CJ Corrigan. Il-4 and il-5 mrna and protein in bronchial biopsies from patients with atopic and nonatopic asthma: evidence against "intrinsic" asthma being a distinct immunopathologic entity. *American journal of respiratory and critical care medicine*, 154(5):1497–1504, 1996.

[186] JF Piskurich, KR Youngman, KM Phillips, PM Hempen, MH Blanchard, JA France and CS Kaetzel. Transcriptional regulation of the human polymeric immunoglobulin receptor gene by interferon-γ. *Molecular Immunology*, 34(1):75–91, 1997.

[187] S McEldowney and R Bush. House dust mite-specific iga and exhaled nitric oxide are elevated in allergic asthma and rhinitis patients with positive methacholine challenges. *Journal of Allergy and Clinical Immunology*, 121(2):S198–S198, 2008.

[188] F Cuypers, A Schäfer, SB Skorka, S Surabhi, LA Tölken, AD Paulikat, TP Kohler, SA Otto, TC Mettenleiter, S Hammerschmidt, U Blohm and N Siemens. Innate immune responses at

the asymptomatic stage of influenza a viral infections of streptococcus pneumoniae colonized and non-colonized mice. *Scientific reports*, 11(1):20609, 2021.

[189] C Cunningham-Rundles. Physiology of iga and iga deficiency. *Journal of clinical immunology*, 21(5):303–309, 2001.

[190] EN Janoff, C Fasching, JM Orenstein, JB Rubins, NL Opstad and AP Dalmasso. Killing of streptococcus pneumoniae by capsular polysaccharide-specific polymeric iga, complement, and phagocytes. *The Journal of clinical investigation*, 104(8):1139–1147, 1999.

[191] M Janzi, I Kull, R Sjöberg, J Wan, E Melén, N Bayat, E Ostblom, Q Pan-Hammarström, P Nilsson and L Hammarström. Selective iga deficiency in early life: association to infections and allergic diseases during childhood. *Clinical immunology (Orlando, Fla.)*, 133(1):78–85, 2009.

[192] WA Jensen, RM Rose, RH Burke, K Anton and HG Remold. Cytokine activation of antibacterial activity in human pulmonary macrophages: Comparison of recombinant interferon-γ and granulocyte-macrophage colony-stimulating factor. *Cellular Immunology*, 117(2):369–377, 1988.

[193] PL Heritage, BJ Underdown, AL Arsenault, DP Snider and MR McDermott. Comparison of murine nasal-associated lymphoid tissue and peyer's patches. *American journal of respiratory and critical care medicine*, 156(4 Pt 1):1256–1262, 1997.

[194] C Albanesi, HR Fairchild, S Madonna, C Scarponi, O de Pità, DYM Leung and MD Howell. Il-4 and il-13 negatively regulate tnf-alpha- and ifn-gamma-induced beta-defensin expression through stat-6, suppressor of cytokine signaling (socs)-1, and socs-3. *Journal of immunology (Baltimore, Md. : 1950)*, 179(2):984–992, 2007.

[195] H Wang, M FitzPatrick, NJ Wilson, D Anthony, PC Reading, C Satzke, EM Dunne, PV Licciardi, HJ Seow, K Nichol, IM Adcock, KF Chung, GP Anderson, R Vlahos, P Wark and S Bozinovski. Csf3r/cd114 mediates infection-dependent transition to severe asthma. *The Journal of allergy and clinical immunology*, 143(2):785–788.e6, 2019.

[196] ND Pugh, CR Jackson and DS Pasco. Total bacterial load within echinacea purpurea, determined using a new pcr-based quantification method, is correlated with lps levels and in vitro macrophage activity. *Planta medica*, 79(1):9–14, 2013.

[197] J Dormans, M Burger, D Aguilar, R Hernandez-Pando, K Kremer, P Roholl, SM Arend and D van Soolingen. Correlation of virulence, lung pathology, bacterial load and delayed type hypersensitivity responses after infection with different mycobacterium tuberculosis genotypes in a balb/c mouse model. *Clinical and experimental immunology*, 137(3):460–468, 2004.

[198] J Zhang. Yin and yang interplay of ifn-gamma in inflammation and autoimmune disease. *The Journal of clinical investigation*, 117(4):871–873, 2007.

[199] CK Kim, J Choi, Z Callaway, K Iijima, G Volcheck and H Kita. Increases in airway eosinophilia and a th1 cytokine during the chronic asymptomatic phase of asthma. *Respiratory Medicine*, 104(10):1436–1443, 2010.

[200] K Samitas, A Carter, HH Kariyawasam and G Xanthou. Upper and lower airway remodelling mechanisms in asthma, allergic rhinitis and chronic rhinosinusitis: The one airway concept revisited. *Allergy*, 73(5):993–1002, 2018.

7.2 Declaration of honor

I hereby declare that I prepared this thesis without impermissible help of third parties and that none other than the indicated tools have been used; all sources of information are clearly marked, including my own publications.

In particular I have not consciously:

• Fabricated data or rejected undesired results

• Misused statistical methods with the aim of drawing other conclusions than those warranted by the available data

• Plagiarized external data or publications

• Presented the results of other researchers in a distorted way

I am aware that violations of copyright may lead to injunction and damage claims of the author and also to prosecution by the law enforcement authorities.

I hereby agree that the thesis may be reviewed for plagiarism by mean of electronic data processing.

This work has not yet been submitted as a doctoral thesis in the same or a similar form in Germany or in any other country. It has not yet been published as a whole.

The acquisition, processing, analysis and interpretation of human sample material was executed in colaboration with Paula Mras. The data generated in this process will be utilized in this doctoral thesis as well as in the medical doctoral thesis of Paula Mras.

Magdeburg, 21.11.2022